ST-3

(NsG-598)

SPACE
TECHNOLOGY
SUMMER
INSTITUTE

Spacecraft Propulsion

by

F. E. Marble

CALIFORNIA INSTITUTE OF TECHNOLOGY

PASADENA, CALIFORNIA

JUNE 1964

SPACE TECHNOLOGY SUMMER INSTITUTE

ST-3

Spacecraft Propulsion

by

F. E. Marble

June 1964

A program sponsored by the
National Aeronautics and Space Administration
under
Grant No. NsG-598
and given by the
California Institute of Technology
in cooperation with the
Jet Propulsion Laboratory

Preface

This is the third of a series of six publications prepared as notes for a six-weeks course in Space Technology, given at the California Institute of Technology (Caltech) from 19 June to 31 July 1964. The program was sponsored by the National Aeronautics and Space Administration and was taught by engineers from industry, from the California Institute, and from the Jet Propulsion Laboratory (JPL). The complete set consists of

ST-1	Spacecraft Systems by L. H. Abraham	(Douglas Aircraft Co., Inc.)
ST-2	Spacecraft Engineering by J. L. Adams	(JPL)
ST-3	Spacecraft Propulsion by F. E. Marble	(Caltech)
ST-4	Space Sciences by C. W. Snyder	(JPL)
ST-5	Spacecraft Guidance and Control by J. R. Scull	(JPL)
ST-6	Telecommunications by J. J. Stiffler	(JPL)

TABLE OF CONTENTS

INTRODUCTION

The first comprehensive series of lectures covering the scientific fundamentals and technology of jet propulsion were given at the Guggenheim Aeronautical Laboratory, California Institute of Technology, under the direction of Professor Theodore von Kármán, during the academic year 1943-44. This course was sponsored by the Air Technical Service Command of the Army Air Force with the enlightened encouragement of General H. H. Arnold. The lectures were a direct outgrowth of the early investigations by Dr. von Kármán and Dr. Frank J. Malina who, together with Mr. J. W. Parsons and Mr. E. Forman, carried out extensive work on solid propellant rockets, leading eventually to the founding of the Jet Propulsion Laboratory.

Through Dr. von Kármán's extensive influence, through the excellent book "Jet Propulsion" edited by Dr. H. S. Tsien, and through the dispersion of the dozen original lecturers throughout the world, these lectures deeply influenced the orientation and content of virtually all subsequent instruction in America and Europe. The depth and accuracy of Dr. von Kármán's insight are borne out by the fact that the ensuing 20 years have not altered the general pattern of the courses although the propulsion technology has advanced so dramatically. The subjects of nuclear propulsion, electrical propulsion, and energy conversion have assumed substantial importance but will influence space exploration only a few years hence.

Instruction of the Jet Propulsion Sciences at the California Institute of Technology was given additional impetus by the establishment of the Daniel and Florence Guggenheim Jet Propulsion Center in

1949 and the appointment of Dr. H. S. Tsien as the Goddard Professor of Jet Propulsion, a chair which he held until 1955. During this period the instruction was expanded in scope and extensive research activity was undertaken. Professor W. D. Rannie, successor to the Goddard Professorship, has subsequently amplified and changed emphasis of the instruction in rocket flight mechanics, propulsion technology, and propulsion chemistry until it has taken the present form of three courses, each covering a complete academic year.

The present lectures cover a few topics from the courses currently given at the California Institute of Technology. The notes consist in a small selection of information from certain areas that are more easily presented in written form than in lectures. Nuclear propulsion, electrical propulsion, and power conversion will be covered only in the lectures.

The notes themselves have been collected from material usually employed in the Cal Tech courses. Chapter I, Mechanics of Rocket Propulsion, was taken from unpublished notes of Professor W. D. Rannie which he employs as introductory material in his lectures on rocket propulsion technology. Chapter II, Elementary Theory of the Rocket Nozzle, was adapted from some early notes by Professor H. S. Tsien and augmented by recent material by the author on heterogeneous flow in nozzles. Chapter III, Combustion Thermodynamics and Chemical Propellants contains material from the excellent little book, "Elements of Chemical Thermodynamics," by L. K. Nash (Addison-Wesley Publishing Co.) and detailed material on chemical equilibrium calculations in nozzle flow (including tables) borrowed from the well known book by

my colleague, Professor S. S. Penner, "Chemistry Problems in Jet Propulsion" (Pergamon Press). The course in propulsion chemistry has been given from this book at Cal Tech for many years by Professor Penner.

Chapter IV, Solid Propellant Rocket Motors, and Chapter V, Liquid Propellant Rocket Motors, are based on material from "Jet Propulsion," edited by H. S. Tsien and a considerable amount of material (including figures) from the extensive book, "Rocket Propulsion," by Barrere, Jaumotte, de Veubeke, and Vandenkerckhove (Elsevier Publishing Co.). This book is an appropriate source for the present notes, inasmuch as that book was deeply influenced not only by Professor von Kármán himself but through the training in jet propulsion that Mr. Vandenkerckhove received at Cal Tech.

1. MECHANICS OF ROCKET PROPULSION

The Rocket in Gravity-Free Space

Let m be the mass of a rocket at any instant t, and v the velocity at that instant. The mass m includes unexpended propellant. Relative to a stationary coordinate system, the momentum of the rocket is mv. Let a mass of propellant Δm_p be ejected opposite to the direction of velocity of the rocket.

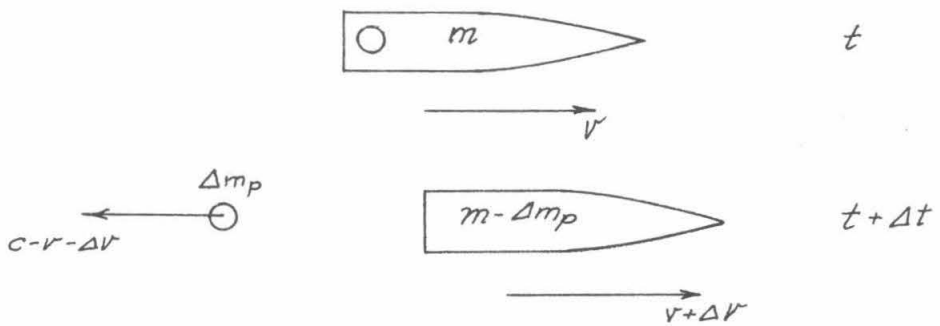

There are no external forces acting on the system, since gravity and drag are neglected; hence, the total momentum of rocket and propellant is the same after ejection as before. At time $t + \Delta t$, the rocket of mass $m - \Delta m_p$ has velocity $v + \Delta v$, and the ejected mass Δm_p has velocity $c - v - \Delta v$ in the opposite direction, as shown in the figure.

The equation of conservation of momentum is

$$(m-\Delta m_p)(v+\Delta v) - \Delta m_p(c-v-\Delta v) = mv ,$$

which can be simplified to

$$m\Delta v = c\Delta m_p .$$

This equation is exact; that is, does not require that Δm_p or Δv be small. However, in conventional rockets, the ejection of propellant is continuous, so Δv is replaced by $\frac{dv}{dt}dt$ and Δm_p by $-\frac{dm}{dt}dt$ in the finite difference equation above, which becomes

$$m\frac{dv}{dt} = -c\frac{dm}{dt} = F \ . \qquad (1.1)$$

Here, F is defined as the rocket thrust, since $m\frac{dv}{dt}$ is the force required to give an acceleration dv/dt to the mass m.

This equation is of fundamental importance, and it is worth while to derive it in a different way. Suppose that a force F acts on the mass Δm_p between times t and $t+\Delta t$ separating the mass of propellant and accelerating it relative to the rocket. The total impulse applied to Δm_p is $\int_t^{t+\Delta t} F dt = \overline{F}\Delta t$, say, where $\overline{F}$ is the average force. The propellant, initially with velocity v, is ejected backward with velocity $c-\Delta v$ relative to the rocket, so the change of

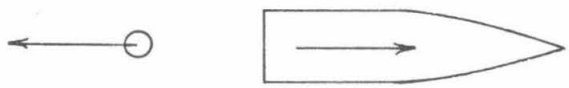

momentum is $\Delta m_p(c-\Delta v)$, and equating to the total impulse

$$\Delta m_p(c-\Delta v) = \overline{F}\Delta t \ .$$

From Newton's Law, the force on the rocket is an equal and opposite reaction, and equating the momentum gain of the rocket of mass $m - \Delta m_p$ to the total impulse

$$(m-\Delta m_p)\Delta v = \overline{F}\Delta t$$

and hence

$$m\Delta v = c\Delta m_p = \overline{F}\Delta t + \Delta m_p \Delta v \ .$$

The equality on the left is the same as that derived previously; the

force $\bar{F}$ reduces to the thrust F defined in Eq. (1.1) when the increments are infinitesimal so that the second order term $\Delta m_p \cdot \Delta v$ can be neglected in comparison with the other terms.

Equation (1.1) can be written in the form

$$dv = -c\frac{dm}{m}$$

and integrated to give the velocity increment

$$v - v_o = \int_{m}^{m_o} c\frac{dm}{m}, \tag{1.2}$$

where m_o is the initial mass and v_o the initial velocity. If the rocket starts from rest ($v_o = 0$) and the mass at burnout is m_b, the velocity at burnout, v_b, is given by

$$v_b = \int_{m}^{m_o} c\frac{dm}{m}. \tag{1.3}$$

For a fixed propellant mass $m_o - m_b$, the burnout velocity is clearly a maximum when c is as large as possible. Generally, the exhaust velocity of a given rocket and propellant combination cannot exceed some maximum value because of limitations of the propellant and motor. Equation (1.3) shows that v_b will decrease if the motor is run so c is at any time less than this maximum value. Hence, c can be considered a constant throughout the burning period for any particular rocket, since this represents the operation that gives the largest value of v_b.

With the simplification that c is constant, the integral in Eq. (1.3) can be evaluated to give

$$v_b = c\,\ell n \frac{m_o}{m_b} = c\,\ell n \frac{W_o}{W_b} \tag{1.4}$$

where W_o/W_b is the "weight ratio" replacing the mass ratio. It is convenient to introduce a weight breakdown for discussion of Eq. (1.4). Define

$$\left.\begin{aligned} W_o &= \text{initial gross weight} \\ W_p &= \text{propellant weight} \\ W_s &= \text{structural weight} \\ W_l &= \text{payload weight} \end{aligned}\right\} \tag{1.5}$$

The structural weight W_s includes the rocket motor, propellant tanks, controls, and all supporting structure; that is, everything required for the rocket operation except propellant and payload. In a two-stage rocket, the payload W_l includes the second rocket, with associated tanks and propellant, and the second-stage payload. The relations $W_o = W_p + W_s + W_l$ and $W_b = W_s + W_l$ must hold with the definitions above. Two dimensionless weight ratios are useful; these are defined as

$$\begin{aligned} \alpha &= W_l/W_o\,, \text{ the payload weight ratio,} \\ \beta &= W_s/(W_p+W_s)\,, \text{ the structural weight ratio.} \end{aligned} \tag{1.6}$$

From the definitions

$$W_b = W_s + W_l = \beta(W_o - W_l) = [\beta + (1-\beta)\alpha]\,W_o\,,$$

and substituting into Eq. (1.4),

$$v_b = c\,\ell n \frac{1}{\beta + (1-\beta)} \quad . \tag{1.7}$$

The magnitude of the thrust does not enter into this expression for

burnout velocity.

The Sounding Rocket

The findings in the previous section show that neither the time of burning nor the magnitude of the thrust influences the burnout velocity. It is clear that this cannot be true for a rocket in the gravity field of the Earth, for instance, and it is of considerable important to determine the deterioration of burnout velocity resulting from gravity. The simplest quantitative demonstration of these effects can be shown for a sounding rocket, that is, a rocket in vertical flight from the Earth's surface. Air resistance, the decrease of acceleration of gravity with height, and the effect of the Earth's rotation are neglected in the first analysis.

The equation of motion of a rocket in vertical flight in a constant gravity field g is

$$\ddot{y} = -c\frac{\dot{m}}{m} - g, \tag{1.8}$$

where m is the mass of the rocket at any time, and y is the height above the Earth's surface. If the exhaust velocity c is constant, this equation can be integrated once

$$y = c\,\ell n\frac{m_o}{m} - gt, \tag{1.9}$$

where the constant of integration is evaluated from the conditions $\dot{y} = 0$ and $m = m_o$ at $t = 0$. Integrating again with respect to t,

$$y = c\int_0^t \ell n\frac{m_o}{m}\,dt - \tfrac{1}{2}gt^2, \tag{1.10}$$

where $y = 0$ when $t = 0$. If t_b is the time at burnout, the burnout

velocity and height are

$$y_b = c\,\ell n \frac{m_o}{m_b} - gt_b$$
$$y_b = c \int_0^{t_b} \ell n \frac{m_o}{m}\,dt - \tfrac{1}{2}gt_b^2 \qquad (1.11)$$

Since part of the work done on the rocket appears as potential energy in the Earth's gravity field, it seems most appropriate to compare total burnout energies rather than burnout velocities as in gravity-free flight. The total burnout energy in the constant gravity field is made up of the potential energy gy_b and the kinetic energy $\frac{1}{2}\dot{y}_b^2$, each per unit mass. Denoting by v_o the velocity at $y = 0$ that corresponds to the same total energy, and by H_m the maximum height that the rocket would reach in the flight following burnout, we have

$$\tfrac{1}{2}v_o^2 = gH_m = \tfrac{1}{2}\dot{y}_b^2 + gy_b\,. \qquad (1.12)$$

Substituting from Eqs. (1.11) and rearranging,

$$v_o^2 = c^2\left(\ell n \frac{m_o}{m_b}\right)^2 - 2gc \int_0^{t_b} \ell n \frac{m}{m_b}\,dt$$

and replacing dt by $dm/\dot{m}$,

$$v_o^2 = c^2\left(\ell n \frac{m_o}{m_b}\right)^2 - 2gc \int_{m_b}^{m_o} \ell n \frac{m}{m_b} \cdot \frac{dm}{(-\dot{m})}\,. \qquad (1.13)$$

The first term on the right-hand side of Eq. (1.13) is the same as would result from gravity-free flight; the second term is the gravity correction. The latter term decreases as $(-\dot{m})$ increases and approaches zero as $(-\dot{m})$ becomes very large, i.e., as the thrust be-

comes large. In actual practice, the magnitude of $(-\dot{m})$ is limited by size of the rocket motor and by acceleration loads on the vehicle. Clearly, any decrease of $(-\dot{m})$ below its maximum allowable value tends to increase the integral on the right of Eq. (1.13) and hence to decrease v_o. For best performance, $(-\dot{m})$ is a constant.

With $(-\dot{m})$ a constant (i.e., thrust constant, since c has already been assumed constant), the height reached at any time t is obtained from Eq. (1.10) in the form

$$y = \frac{c}{(-\dot{m})} \int_{m}^{m_o} \ell n \frac{m_o}{m} \, dm - \tfrac{1}{2} g t^2 ,$$

and the integral can be evaluated to give

$$y = \frac{cm_o}{(-\dot{m})} \left[1 - \frac{m}{m_o} - \frac{m}{m_o} \ell n \frac{m_o}{m} \right] - \tfrac{1}{2} g t^2 . \qquad (1.14)$$

It is convenient to introduce a dimensionless time variable τ defined as

$$\tau = t/t_b \qquad (1.15)$$

and a dimensionless constant γ combining the effects of structural and payload weight ratios defined as

$$\gamma = (1-\alpha)(1-\beta) = 1 - (m_b/m_o) . \qquad (1.16)$$

Then the mass ratio m/m_o can be given in the form

$$m/m_o = 1 - \gamma\tau , \qquad (1.17)$$

and since $m_o - m_b = (-\dot{m})t_b$,

$$\frac{gt_b}{c} = \frac{g(m_o - m_b)}{(-\dot{m})c} = \gamma \frac{W_o}{F} , \qquad (1.18)$$

where W_o/F is the initial thrust/weight ratio. Substituting these new

parameters into Eqs. (1.9) and (1.14), and dividing by c and c^2/g, respectively, the velocity and height at any time are

$$\frac{\dot{y}}{c} = \ell n \frac{1}{1-\gamma\tau} - \frac{W_o}{F} \gamma\tau$$

$$\frac{gy}{c^2} = \frac{W_o}{F}\left[\gamma\tau - (1-\gamma\tau)\ell n \frac{1}{1-\gamma\tau}\right] - \frac{1}{2}\frac{W_o}{F}(\gamma\tau)^2 \qquad (1.19)$$

The expressions for $\dot{y}/c$ and gy/c^2 in Eqs. (1.19) are functions of $\gamma\tau$ and W_o/F only. The parameter W_o/F is, of course, always less than unity. For W_o/F close to unity, the terms on the right of Eq. (119) tend to cancel each other for $\gamma\tau$ small; hence, it is convenient to have a table of the functions multiplying the factors W_o/F with sufficient significant figures so cancellation errors do not become large. Table 1.1 below gives the four required functions of $\gamma\tau$. This table is useful in the approximate calculation of the effect of aerodynamic drag.

TABLE 1.1

$\gamma\tau$	$\ell n \frac{1}{1-\gamma\tau}$	$\gamma\tau - (1-\gamma\tau)\ell n \frac{1}{1-\gamma\tau}$	$\frac{1}{2}(\gamma\tau)^2$
0	0	0	
.05	.05129	.001271	.001250
.10	.10535	.005175	.005000
.15	.1626	.01186	.01125
.20	.2231	.02149	.02000
.25	.2876	.03425	.03125
.30	.3567	.05033	.04500
.35	.4308	.07000	.06125
.40	.5108	.09350	.08000
.45	.5978	.12120	.1012
.50	.6931	.1534	.1250

$\gamma\tau$	$\ell n \frac{1}{1-\gamma\tau}$	$\gamma\tau - (1-\gamma\tau)\ell n \frac{1}{1-\gamma\tau}$	$\frac{1}{2}(\gamma\tau)^2$
.55	.7895	.1907	.1512
.60	.9163	.2335	.1800
.65	1.050	.2828	.2112
.70	1.204	.3388	.2450
.75	1.386	.4034	.2812
.80	1.609	.4781	.3200
.85	1.897	.5654	.3612
.90	2.303	.6697	.4050
.95	2.996	.8002	.4512

At burnout, $\tau = 1$ in Eq. (1.19), and hence

$$\frac{\dot{y}_b}{c} = \ell n \frac{1}{1-\gamma} - \frac{W_o}{F}\gamma \quad ,$$

$$\frac{g y_b}{c^2} = \frac{W_o}{F}\left[\gamma - (1-\gamma)\ell n \frac{1}{1-\gamma}\right] - \frac{1}{2}\left(\frac{W_o}{F}\right)^2 \gamma^2 \quad . \tag{1.20}$$

The velocity v_o corresponding to total burnout energy is given by

$$v_o^2 = 2gH_m = c^2\left(\ell n \frac{1}{1-\gamma}\right)^2 - 2c^2 \frac{W_o}{F}\left(\ell n \frac{1}{1-\gamma} - \gamma\right), \tag{1.21}$$

and this can be expressed in the more convenient form

$$v_o = c\left[\ell n \frac{1}{1-\gamma}\right]\left[1 - \frac{W_o}{F} f(\gamma)\right]^{\frac{1}{2}}, \tag{1.22}$$

where

$$f(\gamma) = \frac{2\left(\ell n \frac{1}{1-\gamma} - \gamma\right)}{\left(\ell n \frac{1}{1-\gamma}\right)^2} \quad . \tag{1.23}$$

The variation of $f(\gamma)$ with γ is given in Table 1.2.

TABLE 1.2

γ	0.4	0.5	0.6	0.7	0.75	0.80	0.85	0.90	0.95
$f(\gamma)$	.848	.805	.753	.695	.664	.625	.582	.529	.456

It is important to remember that the results above are based on the assumptions that c and F are constants.

Values of Parameters for Rocket Equations

The equation for the burnout velocity in gravity-free space, Eq. (1.7), shows that v_b increases as c increases and as β decreases for a fixed payload radio α. In order to increase the burnout velocity for a fixed payload weight, one may employ a larger rocket (i.e., decrease α), employ a higher performance propellant (i.e., increase c), or construct a lighter and more efficient structure (i.e., decrease β). Further, Eq. (1.22) shows that v_o increases as the initial thrust/weight ratio F/W_o increases. The values of the three parameters c, B, and F/W_o are not independent, and the optimum choice to give the highest value of v_o is not a simple procedure. However, some general statements can be made concerning the values of the parameters without detailed discussion of rocket design.

The value of the exhaust velocity c increases as the combustion chamber temperature increases and as the molecular weight of the exhaust products decreases, as will be shown later. Systematic studies of the chemical properties of elements and compounds demonstrate that a fuel of low molecular weight should be combined with an oxidizer such as oxygen, or better, fluorine, for the highest value of c. Therefore, hydrogen is the best fuel, and when combined with oxygen or fluorine, can produce a value of c of about 12,000 ft/sec. Our knowledge of theoretical chemistry leaves no doubt that this is very close to the highest value of c attainable from stable chemical species. The

light metals have very high heats of reaction but form exhaust products with high molecular weights, and worse, liquid or solid rather than gaseous form. Chemical compounds for fuels generally give smaller values of c as the percentage of hydrogen is decreased.

The first liquid propellant rocket to reach an operational status was the V-2, with alcohol and liquid oxygen as the propellant combination. This rocket motor developed an exhaust velocity of about 6500 ft/sec. Current large liquid-propellant rockets employ kerosene and liquid oxygen, and have increased the value of c to about 9000 ft/sec, the increment resulting more from better motor design and higher chamber pressure than from inherent characteristics of the propellant. Storable liquid propellants such as hydrazine and nitrogen tetroxide have obvious operational advantages over the cryogenics hydrogen and oxygen, but because they are more complicated compounds, the exhaust velocity is not quite as high as with kerosene and liquid oxygen.

Solid propellants for rockets must have satisfactory structural characteristics, and are therefore rather complex chemical compounds (e.g. nitroglycerine and nitrocellulose). As a result, the solid propellants usually produce values of the exhaust velocity of 8500 ft/sec or less. Recently, light metals have been incorporated into the solid propellants, and the value of c has been increased toward 9000 ft/sec. Very much higher values of c in solid propellants seem unlikely.

The values of the exhaust velocities quoted above are representative of the propellants alone, although the precise values will depend on nozzle design and ambient pressure. Strictly, comparison

should be made only for specified conditions of operation. The value of c for a given propellant combination can vary by 10 per cent to 15 per cent, depending on chamber pressure, nozzle exit pressure, and ambient pressure.

Although the exhaust velocity c is the most natural index of propellant performance, another quantity called the specific impulse, I or I_{sp}, is widely used. The specific impulse is defined as thrust divided by mass flow rate of the propellant in the units (pounds thrust)/(lb. mass flow per sec.), and hence $I_{sp} = c/g_o$, where $g_o = 32.1740$ is the numerical value of the standard gravitational acceleration. The specific impulse is usually quoted as so many seconds, although a glance at the definition shows that it is really a velocity with g_o a numerical conversion factor. In applications, one converts to $c = 32.1740\ I_{sp}$ ft/sec, so the confusion in dimensions is not very important.

The second important parameter is the structural weight ratio $\beta = W_s/(W_p+W_s)$. This parameter is inseparable from the mechanical design details of the rocket, in contrast with the exhaust velocity c, which is determined more by intrinsic chemical properties of the propellant than by specific rocket design. Hence, it is not possible to predict a minimum value of β in the way that a maximum value of c can be predicted. Estimates of weights of components will be made later in the course; for the moment, representative values taken from recent journals will be quoted. The value of β for each stage of the present Titan liquid propellant rocket is stated to be 0.06 ('Missiles and Rockets,' Sept. 5, 1960), with the implication that this will be

improved in later modifications. The very marked improvement since the V-2 with $\beta \cong 0.25$ is more striking than the gain in exhaust velocity. The value of β for the Titan is appropriate for "conventional" fuels. No figure for a hydrogen-fueled rocket (e. g. Centaur) is easily available, but it is certainly higher than 0.06 because of the large tanks required for low-density hydrogen. Hence, the gain in burnout velocity resulting from higher c for hydrogen is partially balanced by the larger value for β. The value of β for current large, solid-propellant rockets is stated to be 0.07 with expectation that it can be decreased to 0.04 ('Missiles and Rockets,' July 27, 1959, p. 32).

The value of β also depends on the ratio F/W_o. As F is increased, the size of the rocket nozzle increases, and hence β increases; further, as F is increased, the acceleration of the vehicle increases, and a heavier structure may be required. For current large liquid-propellant rockets, the value of F/W_o seems to be about 1.4 or 1.5; and for large solid-propellant rockets, F/W_o is in the range of 2.5 to 3.5. This difference is not surprising; much of the structural weight of liquid-propellant rockets consists of propellant tanks which become heavy if the acceleration loads are high, whereas the cases of solid-propellant rockets are already rather heavy to withstand the chamber pressure, and can take appreciable acceleration loads with no increase in weight.

The minimum velocities at the Earth's surface required for certain trajectories and orbits are listed in Table 1.3. Although the correspondence is not quite exact, the combination of burnout velocity in gravity-free space, Eq. (1.7), and the gravity correction for a

TABLE 1.3

Trajectory or Orbit	v_o (ft./sec.)
Maximum range, 100 miles	4,100
Maximum range, 500 miles	8,900
Maximum range, 1000 miles	12,200
Maximum range, 3000 miles	19,000
Maximum range, 6000 miles	24,000
Orbit at the Earth's surface	26,000
Escape from the Earth	36,700
Escape from the solar system	77,500

sounding rocket, Eq. (1.22), in the form

$$v_o = c\left[\ell n \frac{1}{1-\gamma}\right]\left[1 - \frac{W_o}{F} f(\gamma)\right]^{\frac{1}{2}}$$

with

$$\gamma = (1-\alpha)(1-\beta)$$

gives an approximation to the values of v_o as listed in Table 1.3. Substitution of appropriate combinations of c, β, and W_o/F shows that only the first few of the trajectories in the table can be accomplished with a single-stage rocket, even with very low payload.

Staged Rockets

The maximum burnout velocity that can be attained with a single-stage rocket in gravity-free space is $c\,\ell n \frac{1}{\beta}$ with a negligible payload. The structural weight ratio can be reduced, in effect, by the use of step rockets or staging. Suppose that a part of the propellant of a rocket is put in a second, smaller rocket carried along as the payload of the first rocket. After burnout of the first rocket, the structure is disengaged and the second rocket is fired. The propellant

of the second rocket accelerates a smaller structural mass than it would if part of the propellant of the first stage, so that a higher terminal velocity for the actual payload is achieved.

For a first quantitative examination of the effect of staging, let us neglect the effect of gravity and assume that each of the rockets in the several stages has the same exhaust velocity c and the same structural weight ratio β. Let $\alpha_1 = W_1/W_o$ be the payload weight ratio of the first rocket, where W_o is the initial gross weight, and W_1 includes all subsequent rockets beyond the first, as well as the actual payload. According to Eq. (1.7), the burnout velocity of the first stage is v_1, say, where

$$v_1 = c \ln \frac{1}{\beta + (1-\beta)\alpha_1} , \tag{1.24}$$

assuming that the motion starts from rest. Let W_2 be the payload for the second rocket; W_2 includes all subsequent rockets beyond the second rocket and the actual payload. Define $\alpha_2 = W_2/W_1$ as the payload ratio of the second rocket. Since the second rocket has velocity v_1 initially, the burnout velocity v_2 is given by

$$\frac{v_2}{c} - \frac{v_1}{c} = \ln \frac{1}{\beta + (1-\beta)\alpha_2} . \tag{1.25}$$

Continuing the process, we have for the last stage, if n is the number of stages,

$$\frac{v_n}{c} - \frac{v_{n-1}}{c} = \ln \frac{1}{\beta + (1-\beta)\alpha_n} . \tag{1.26}$$

Adding up the n equations,

$$\frac{v_n}{c} = \sum_{i=1} \ln \frac{1}{\beta + (1-\beta)\alpha_i} . \tag{1.27}$$

The payload ratios $\alpha_1, \alpha_2, \ldots, \alpha_n$ are connected by the relation

$$\alpha_1, \alpha_2, \ldots, \alpha_n = \frac{W_1}{W_o} \cdot \frac{W_2}{W_1} \cdots \frac{W_n}{W_{n-1}} = \alpha ,$$

or

$$\sum \ell n \, \alpha_i = \ell n \, \alpha , \tag{1.28}$$

where W_n is the actual payload of the entire system, and α is the overall payload weight ratio.

If α is given, the final burnout velocity v_n varies with the choice of α_i's as given by Eq. (1.27). These α_i's are not completely arbitrary, however, since they must satisfy the condition of Eq. (1.28). The values of α_i that give the maximum v_n and this maximum are most easily found by the method of Lagrange multipliers. The condition that v_n in Eq. (1.27) be an extremum is that

$$\frac{\delta v_n}{c} = - \sum_{i=1}^{n} \frac{1-\beta}{\beta + (1-\beta)\alpha_i} \delta\alpha_i = 0 \tag{1.29}$$

for all <u>possible</u> variations $\delta\alpha_i$. However, the variations $\delta\alpha_i$ must satisfy the condition (from Eq. 1.28) that

$$\sum_{i=1}^{n} \frac{1}{\alpha_i} \delta\alpha_i = 0 , \tag{1.30}$$

since α = constant. This last condition is unchanged if an arbitrary multiplier λ is introduced, i.e., the condition to be satisfied by the variations $\delta\alpha_i$ is

$$\lambda \sum_{i=1}^{n} \frac{1}{\alpha_i} \delta\alpha_i = 0 . \tag{1.31}$$

Adding Eq. (1.31) to Eq. (1.29), we have, for the condition for an extremum of v_n,

$$\sum_{i=1}^{n} \left[- \frac{1-\beta}{\beta + (1-\beta)\alpha_i} + \frac{\lambda}{\alpha_i} \right] \delta\alpha_i = 0 \qquad (1.32)$$

again for all possible variations $\delta\alpha_i$.

Only (n-1) of the n variations $\delta\alpha_1$, $\delta\alpha_2$, . . . , $\delta\alpha_n$ are arbitrary in Eq. (1.32) because of the relation (1.30) that they must satisfy. Let $\delta\alpha_1, \ldots, \delta\alpha_{n-1}$ be chosen arbitrarily; then the coefficients of these in Eq. (1.32) must all be zero to satisfy the condition for an extremum. The coefficient of $\delta\alpha_n$ will not be zero in general because $\delta\alpha_n$ can be expressed in terms of the other $\delta\alpha_i$'s. However, λ is still an arbitrary multiplier and is now chosen so the coefficient of $\delta\alpha_n$ is zero; hence, coefficients of all $\delta\alpha_i$'s in Eq. (1.32) are zero, or

$$\frac{1-\beta}{\beta + (1-\beta)\alpha_i} = \frac{\lambda}{\alpha_i} \qquad i = 1, \ldots, n \qquad (1.33)$$

and these n equations along with Eq. (1.28) are sufficient to determine the n+1 unknowns, $\alpha_1, \alpha_2, \ldots, \alpha_n$ and λ . In this particular example, solving for α_i from Eq. (1.33)

$$\alpha_i = \frac{\lambda\beta}{(1-\lambda)(1-\beta)} \quad ,$$

and clearly all α_i's are equal; hence, from Eq. (1.28),

$$\alpha_i = \alpha^{1/n} \qquad i = 1, 2, \ldots, n \qquad (1.34)$$

and the maximum value of v_n, which we will denote by V_n , is

$$V_n = nc\,\ell n \frac{1}{\beta + (1-\beta)\alpha^{1/n}} \quad . \qquad (1.35)$$

When the Lagrange multipliers are introduced in a problem such as this, the simplest method of demonstrating that V_n is a maximum is to choose any other set of α_i's for which v_n is easily calculated and

show that $v_n \to V_n$.

For $n \to \infty$, one can put $\alpha = 1-\epsilon$ where ϵ is a very small number; substituting for n in terms of ϵ in Eq. (1.35) and letting $\epsilon \to 0$, the limiting value of V_n is

$$\lim_{n\to 0} V_n = c(1-\beta)\ell n \frac{1}{\alpha} . \qquad (1.36)$$

This mathematical limit of course is not attainable in practice, because it is scarcely possible to construct a rocket with an infinite number of stages, but it does give a useful index of the maximum advantage of staging. For instance, it can be seen immediately that high burnout velocities cannot be achieved unless α is very small.

The ratio of the maximum burnout velocity V_n to the exhaust velocity c is shown in Table 1.4 for various values of α and β. The table demonstrates clearly that staging is effective only for small payload ratios. With small payload ratios, however, high burnout velocities are attainable with quite modest values of c and β .

The conditions (1.33) or (1.34) for v_n to be a maximum for fixed α are also the conditions that α be a maximum for fixed v_n . To show this, one simply interchanges the roles of Eqs. (1.29) and (1.30), that is, let Eq. (1.30) be the condition that α be an extremum and Eq. (1.29) be the auxiliary condition that v_n is given.

The solution of the staging problem above is particularly simple because c and β are the same for each stage. In the more general problem, with exhaust velocity c_i and structural weight ratio β_i for the i^{th} stage, the procedure is the same. The burnout velocity of the n^{th} stage in gravity-free space is

TABLE 1.4

V_n/c for n-Stages in Gravity-Free Space

		α								
β	n	0.2	0.1	0.05	0.02	0.01	0.005	0.002	0.001	0
0.25	1	0.92	1.12	1.24	1.33	1.36	1.37	1.38	1.38	1.39
	∞	1.21	1.83	2.25	2.93	3.45	3.98	4.66	5.18	∞
0.10	1	1.27	1.66	1.93	2.14	2.22	2.26	2.28	2.29	2.30
	2	1.38	1.91	2.40	2.96	3.32	3.62	3.93	4.10	4.60
	3	1.40	1.97	2.52	3.20	3.67	4.11	4.62	4.98	6.91
	4	1.42	2.00	2.57	3.30	3.82	4.32	4.95	5.38	9.21
	∞	1.45	2.07	2.70	3.32	4.14	4.77	5.59	6.22	∞
0.05	1	1.43	1.93	2.33	2.67	2.82	2.90	2.96	2.98	3.00
	2	1.49	2.10	2.68	3.38	3.79	4.29	4.76	5.05	5.99
	3	1.50	2.13	2.75	3.54	4.10	4.65	5.32	5.79	8.99
	4	1.51	2.15	2.78	3.60	4.20	4.78	5.57	6.09	11.98
	∞	1.53	2.18	2.84	3.72	4.38	5.03	5.90	6.56	∞

$$v_n = \sum_{i=1}^{n} c_i \ln \frac{1}{\beta_i + (1-\beta_i)\alpha_i} \tag{1.37}$$

where the α_i's satisfy Eq. (1.28) as before. The conditions for v_n to be an extremum, corresponding to Eqs. (1.33), are readily found to be

$$c_i \frac{1-\beta_i}{\beta_i + (1-\beta_i)\alpha_i} = \frac{\lambda}{\alpha_i} \qquad i = 1, \ldots, n \tag{1.37}$$

and solving for α_i ,

$$\alpha_i = \frac{\lambda \beta_i}{(c_i - \lambda)(1-\beta_i)} \qquad i = 1, \ldots, n \quad . \tag{1.38}$$

Substituting for α_i into $\alpha_1, \alpha_2, \ldots, \alpha_n = \alpha$, one obtains a relation for λ in terms of the prescribed parameters c_i and β_i .

$$\frac{\lambda^n}{(c_1-\lambda)(c_2-\lambda)\ldots(c_n-\lambda)} = \frac{(1-\beta_1(1-\beta_2)\ldots(1-\beta_n)}{\beta_1, \beta_2, \ldots, \beta_n} \quad . \tag{1.39}$$

This last equation is polynomial of the n^{th} degree in λ and must be solved numerically. Usually, only one root represents a practical solution; having found this root, the α_i's are determined from Eqs. (1.38).

The problem of the optimum distribution of payload wieght ratios in a multi-stage sounding rocket operating in a constant gravity field is important, but unfortunately, it is one of considerable difficulty. Suppose that any particular stage has as its initial condition $\dot{y} = v_1$ and $y = y_1$ where v_1 and y_1 are given. For constant c and constant thrust, Eqs. (1.20) can be extended readily to the new initial conditions, giving

$$\dot{y}_b = c\left[\ln \frac{1}{1-\gamma} - \frac{W_1}{F_1}\gamma\right] + v_1 \tag{1.40}$$

$$y_b = \frac{c^2}{g}\left[\frac{W_1}{F_1}\{\gamma - (1-\gamma)\ln \frac{1}{1-\gamma}\} - \frac{1}{2}\left(\frac{W_1}{F_1}\right)^2 \gamma^2\right] + \frac{cv_1}{g}\frac{W_1}{F_1}\gamma + y_1 \tag{1.41}$$

where $\gamma = (1-\alpha)(1-\beta)$ and F_1/W_1 is the initial thrust-weight ratio. The initial energy per unit mass is $E_1 = \frac{1}{2}v_1^2 + gy_1$, and the burnout energy per unit mass is $E = \frac{1}{2}\dot{y}_b^2 + gy_b$. The increment of energy of this particular stage is then

$$E - E_1 = \tfrac{1}{2}c^2\left[\left(\ell n \frac{1}{1-\gamma}\right)^2 - \frac{W_1}{F_1}\,2\left(\ell n \frac{1}{1-\gamma} - \gamma\right)\right] + cv_1 \ell n \frac{1}{1-\gamma} \qquad (1.42)$$

To find the burnout energy of a two-stage rocket with the first stage fired at $y = 0$ with zero velocity and the second stage fired immediately upon burnout of the first stage, let $c_1, \gamma_1, W_o/F_o$ refer to the first stage and put $c = c_2$, $\gamma = \gamma_2$ in Eq. (1.42) representing the second stage. Then

$$v_1 = c_1\left(\ell n \frac{1}{1-\gamma_1} - \frac{W_o}{F_o}\gamma_1\right)$$

and

$$E_1 = \tfrac{1}{2}c_1^2\left[\left(\ell n \frac{1}{1-\gamma_1}\right)^2 - \frac{W_o}{F_o}\,2\left(\ell n \frac{1}{1-\gamma_1} - \gamma_1\right)\right]$$

and substituting into Eq. (1.25) above,

$$\begin{aligned} E_2 = {} & \tfrac{1}{2}c_1^2\left[\left(\ell n \frac{1}{1-\gamma_1}\right)^2 - \frac{W_o}{F_o}\,2\left(\ell n \frac{1}{1-\gamma_1} - \gamma_1\right)\right] \\ & + \tfrac{1}{2}c_2^2\left[\left(\ell n \frac{1}{1-\gamma_1}\right)^2 - \frac{W_1}{F_1}\,2\left(\ell n \frac{1}{1-\gamma_1} - \gamma_2\right)\right] \\ & + c_2c_1\left(\ell n \frac{1}{1-\gamma_2}\right)\left(\ell n \frac{1}{1-\gamma_1} - \frac{W_o}{F_o}\gamma_1\right) \end{aligned} \qquad (1.43)$$

where

$$\alpha_1\alpha_2 = \left(1 - \frac{\gamma_1}{1-\beta_1}\right)\left(1 - \frac{\gamma_2}{1-\beta_2}\right) = \alpha\ . \qquad (1.44)$$

In these expressions, γ_1 and γ_2 replace α_1 and α_2 as independent variables to simplify the form of the expression for E_2.

When gravity is neglected, i.e., $W_o/F_o = W_1/F_1 = 0$ in Eq. (1.43), the expression for E_2 is a perfect square. Then it is clear that the order of firing of the rockets designated by 1 and 2 does not matter. With gravity, the expression for E_2 is not a perfect square, and the maximum burnout energy depends on which rocket is used as the first stage. Frequently one finds in the literature the following statement --- if a two-stage rocket is made up of one "low performance" stage and one "high performance" stage, the "high performance" rocket should be in the second stage for maximum burnout energy. If in the high-performance stage, c is higher and both β and W/F lower than in the low-performance stage, a numerical example will convince one of the validity of the statement above. However, one type of rocket is generally superior to another with respect to one or two of the parameters c, β, and W/F, rather than all three, and the choice of optimum arrangement becomes more subtle. The simplest procedure in a specific example is to solve Eq. (1.44) for γ_2 and use this result to plot E_2 as a function of γ_1 from Eq. (1.43) for the two possible orders of type of rocket.

Rockets with Energy Sources Other than Chemical

The chemical rockets discussed in the previous sections combine energy source and propellant as a unit. The release of the stored chemical energy is used through the action of guiding surfaces of chamber and nozzle to accelerate the propellant, consisting of the products of the chemical reaction. The characteristics of the products of reaction (specifically low molecular weight) are as important

in choosing a propellant combination as the magnitude of the energy stored in the combination (i. e., the chemical heat release).

Mechanical and electrical means of storing energy give very much smaller energy per unit mass than chemical; but nuclear energy sources have enormously greater energy per unit mass, and it is only natural that their applicability to rocket propulsion should be the object of intensive study. The energy per unit mass of fissionable nuclear fuel is of the order of 10^7 times that of chemical compounds, so great that the weight of the energy source itself is quite negligible compared with the weight of the device that converts the energy in a practical manner into thrust. Because the energy has negligible weight, the coupling between energy and propellant that is a characteristic of the chemical system is removed, and the propellant for the nuclear energy source can be chosen quite independently.

If one considers the possibility of using a fissionable fuel in a rocket chamber similar to the way in which a chemical fuel is used, a serious difficulty presents itself. A chemical reaction will proceed rapidly to completion as soon as the temperature becomes moderately high, independeltly of external conditions. A nuclear fission reaction, on the other hand, continues only as long as the unreacted fuel concentration stays above a certain value, the critical concentration. As the chamber mixture flows out the nozzle, the nuclear reaction is quenched immediately, although the unreacted fuel concentration is high. In fact, the rate of discharge of unreacted fuel is so high that such a rocket would be completely unacceptable.

Clearly, the nuclear rocket must have some means of retain-

ing the nuclear fuel and allowing only propellant to escape. One method is to retain the fuel in a solid matrix and let the heat generated by the fission reaction be transferred to the propellant flowing through the matrix. The maximum temperature is limited by the allowable temperature in the solid, and hence is 2000°F or more lower than the maximum temperature in chemical reactions where walls can be cooled and are cooler than the propellant rather than hotter. The effect of the relatively low temperature of the propellant in a nuclear rocket is more than balanced by the possibility of using a propellant with a low molecular weight (hydrogen). Apparently exhaust velocities of 20,000 to 25,000 ft/sec can be realized. Such exhaust velocities are sufficiently attractive that an active program for development of the nuclear rocket has begun.

Other means of containing the nuclear fuel and at the same time relieving the temperature limitation of the heat-transfer nuclear rocket have been considered. One possibility is to establish a strong vortex or vortices in the rocket chamber to separate heavy fuel from light propellant by the centrifugal pressure field. Propellant with a very low concentration of fuel might be discharged, leaving the fuel-rich mixture in the rocket chamber. Much more basic investigation is required before such an arrangement could be considered seriously.

One method of carrying a nuclear reaction reasonably close to completion is by an explosion. A series of nuclear explosions in some form of chamber has been suggested as a rocket device. A large mass of propellant, preferably of low molecular weight, could be heated and then discharged. The difficulty here is that with the high-

est densities attainable for fissionable fuel the critical mass corresponds to the explosive energy of perhaps several kilotons of TNT. Obviously, the rocket required to fit explosions of this magnitude would be of enormous size and presents engineering problems of an entirely different scale than met heretofore in propulsion. The possibility of a controlled thermonuclear device as a rocket cannot be dismissed, although it can scarcely be discussed intelligently before a controlled reaction is achieved.

All of the propulsion devices mentioned above accelerate the propellant in the same manner as a chemical rocket, that is, by the action of pressure transmitted through the fluid propellant by the walls of the rocket chamber and nozzle. If very high propellant temperatures are required, the walls transmitting the force to the propellant must be cooled. The problem of wall heating could be alleviated or even eliminated if the accelerating process could be carried out by means of body forces acting directly on the propellant, so that no walls are in contact with the propellant. The only body forces that are of practical use are electric and magnetic forces. These can be effective, of course, only if the propellant molecules are electrically charged. Two principal types of electric propulsion devices are being investigated extensively.

One of these is the "ion rocket", in which the propellant is completely ionized and the positive ions are accelerated by an electric field to give a high-velocity beam. This positively-charged beam must be neutralized after acceleration by adding electrons; otherwise, the behicle would accumulate a negative charge, and the discharged

ion beam would return to the vehicle.

Another type of accelerator is based on the body force that arises when a magnetic field H is impressed at right angles to an electric current flow j , giving rise to a force proportional to jH and at right angles to both. To make use of this effect, the propellant must be electrically conducting, i. e., must be ionized, although electrically neutral, and flow between electrodes that pass a current through the propellant. A magnetic field at right angles to the current and to the direction of flow of the propellant produces the required acceleration. Problems may arise in cooling the electrode surfaces that are in contact with the propellant. It is not possible at the present time to predict which of the devices above, or of others based on similar principles, will prove most suitable for propulsion.

Any of the propulsion systems based on electric and magnetic body forces require electric generating equipment. The total weight of the system for conversion of nuclear energy to electrical energy will be approximately proportional to the electrical power output. The best systems available now or in the very near future have a weight of 100 lb/h. p. or so; a weight of 10 lb/h. p. can be expected in a few years from systems under development; and a weight of 1 lb/h. p. is estimated, rather hopefully, as a possibility in the future. With electric power systems of such high weight/power ratio, the thrust that can be produced is a small fraction of the weight of the system, and take-off from the surface of the Earth is not possible. The usefulness of the electric power systems for propulsion appears to be limited to acceleration from a satellite orbit. In a satellite orbit,

centrifugal force balances gravity, and a small thrust acting over a long period of time can produce a large impulse as in gravity-free space.

The optimum proportioning of propellant and power conversion system masses in a rocket of this type can be determined relatively easily. The basic rocket equation for gravity-free space is still applicable, i.e.,

$$\Delta v_b = c \ell n \frac{1}{\beta + (1-\beta)\alpha} , \tag{1.45}$$

where Δv_b is the increment of velocity resulting from discharge of the propellant. If m_p is the total propellant mass and t_b the "burning" time, the power output of the rocket motor is

$$P = \frac{m_p}{t_b} \cdot \tfrac{1}{2} c^2 = W_p \frac{c^2}{2gt_b} , \tag{1.46}$$

since this simply represents the rate at which kinetic energy is discharged in the jet. We assume that initially the rocket weight is made up of structural weight W_s, propellant weight W_p, and payload weight W_l. As in the earlier definitions,

$$\beta = \frac{W_s}{W_p + W_s} , \qquad \alpha = \frac{W_l}{W_s + W_p + W_l} ,$$

and we assume that the structural weight consists principally of the power conversion system, including the propellant accelerator. Then if the weight of the power conversion system is proportional to the power output, we can put

$$W_s = KP = W_p \frac{K}{2} \frac{c^2}{gt_b} , \tag{1.47}$$

and, from the definition of β,

$$\beta = x^2/(1 + x^2) , \tag{1.48}$$

where

$$x^2 = \frac{K}{2}\frac{c^2}{gt_b} \quad . \tag{1.49}$$

Solving for c and substituting into Eq. (1.45),

$$\sqrt{\frac{K}{2gt_b}}\,\Delta v_b = x\,\ell n\,\frac{1+x^2}{\alpha+x^2} \quad . \tag{1.50}$$

The expression on the left of Eq. (1.50) is positive for all positive values of x ; since it approaches zero as x approaches zero and also as x approaches infinity, it must have a maximum for some positive value of x. Hence, for fixed K, α, and t_b , there is some value of x that gives the maximum velocity increment. The condition for Δv_b to be a maximum as a function of x is readily found by differentiating the right hand side of Eq. (1.50). However, the resulting transcendental equation is not easy to solve, and it is more convenient to choose a new variable y , defined as

$$y = (1+x^2)/(\alpha+x^2) \quad , \tag{1.51}$$

then

$$x = \sqrt{\frac{1-\alpha}{y-1} - \alpha}$$

and

$$\sqrt{\frac{K}{2gt_b}}\,\Delta v_b = \sqrt{\frac{1-\alpha}{y-1} - \alpha}\;\ell n\, y \, . \tag{1.52}$$

Differentiating with respect to y and equating the result to zero, the condition for maximum Δv_b is

$$2(y-1)^2\left(\frac{1-\alpha}{y-1} - \alpha\right) = (1-\alpha)y\,\ell n\, y \, , \tag{1.53}$$

and solving for α as a function of y , the condition becomes

$$\alpha = \frac{2(y-1) - y\,\ell n\, y}{y[2(y-1)-\ell n\, y]} \quad . \tag{1.54}$$

One can readily show that this is also the condition that α be a maximum for $K/2gt_b \Delta v_b$ prescribed. The table below lists the parameters resulting from various choices for y.

y	1.2	1.3	1.4	1.5	1.75	2.0	2.5	3.0
α	.735	.590	.506	.439	.318	.235	.136	.081
$x = \sqrt{\frac{K}{2gt_b}} c$	.774	.880	.853	.827	.763	.727	.662	.613
$\sqrt{\frac{K}{2gt_b}} \Delta v_b$	.141	.230	.288	.336	.428	.503	.606	.673

As an example, suppose that K = 0.02 lb./ft. pound $\cong$ 10 lb/h.p. and that Δv_b = 20,000 ft./sec. is required. With a payload weight ratio α = 0.506, $t_b = 1.5 \times 10^6$ sec. $\cong$ 17 days, c = 57.500 ft./sec., and the average acceleration is 1.3×10^{-2} ft. sec^2. The effect of changing α, Δv_b, and K can be found with the help of the table.

Several types of power conversion systems for electric propulsion are being considered. Some consist of a closed-cycle heat engine with a nuclear reactor as a heat source and a radiator as a heat sink to produce mechanical power for a light-weight electric generator. Others are based on direct conversion devices, again with the reactor as a heat source and a radiator. So far, the direct conversion schemes have lower efficiency than the heat engines, and hence require a larger radiator for the same power, but the predicted overall weights are comparable. The propellant accelerator, particularly for the electrostatic type, will weigh much less than the remainder of the power conversion system. Solar power, with direct conversion devices, is much more convenient for production of small electric

power than the nuclear energy sources, but it does not appear competitive for the relatively large power required for propulsion of large vehicles.

At first sight, the very small acceleration of a vehicle with an electric propulsion device makes it appear quite inferior to the chemical rocket, even though the payload ratio can be much higher, as shown in the example above. However, if very great distances are involved, as for interplanetary flight, the time of flight will be of the order of several months, or even years, and there will be little difference in travel time between a chemical rocket that produces the velocity increment from satellite speed in a few minutes and the electric propulsion device that requires a few weeks to produce the velocity increment.

2. ELEMENTARY THEORY OF THE ROCKET NOZZLE

In its simplest form, the theory of gas flow through a rocket nozzle may be carried out completely utilizing only the most elementary mathematical means. In carrying out the analysis, several explicit assumptions will be made which limit the accuracy and applicability of the results. In spite of these, the results are usually quite close to physical reality. The assumptions are:

1. The combustion process is complete before the gas encounters the nozzle; the flow consists of a homogeneous non-reacting ideal gas.

2. The process is reversible; dissipation arising from shear within the wall boundary layer and from volume dilatation in the main stream is neglected.

3. The flow is locally adiabatic; no heat is transferred from the gas to its surroundings or between adjacent portions of the gas.

4. The flow is one dimensional; all gradients of temperature, velocity, and pressure normal to the principal direction of flow are neglected.

The First Law of Thermodynamics, in a form appropriate for use here, states that the internal energy of the gas is increased by the addition of heat and by doing work on the gas. This law may be written

$$\delta e = \delta q + \delta w , \qquad (2.1)$$

where δq, δe, and δw are the heat transferred to the gas, the internal energy of the gas, and the work done on the gas, respectively. The symbol δ is used, in agreement with the usual convention, to denote the change in a thermodynamic quantity, the magnitude of which may

depend upon the details of the process and not just upon the end points. Under the assumption of a reversible process, the work done on the gas is $-pd(1/\rho)$, where p and ρ are, respectively, the pressure and density of the gas. Therefore, equation (2.1) becomes

$$\delta q = de + pd(1/\rho) \tag{2.2}$$

where $d(1/\rho)$ is exact and de may be shown to be so. If the gas temperature and density (or its reciprocal $V = 1/\rho$) are chosen as the independent variables, various important partial derivatives may be computed from equation (2.2). If the temperature T is allowed to vary while the specific volume V (or density) is held constant, it is found that

$$\left.\frac{\partial q}{\partial T}\right|_V = \left.\frac{\partial e}{\partial T}\right|_V + 0 \equiv C_v . \tag{2.3}$$

The specific heat at constant volume, C_v, is defined as the heat required to raise the gas temperature one degree while the gas volume is held constant. The deduction above shows that this heat goes entirely toward increasing the internal energy of the gas.

The enthalpy of a gas is defined to be

$$h = e + p/\rho , \tag{2.4}$$

and the First Law of Thermodynamics expressed in terms of the enthalpy becomes

$$dq = dh - \frac{1}{\rho} dp . \tag{2.5}$$

Consider the temperature and the pressure as the independent variables expressing the state of the gas. This is clearly possible because the pressure and density are related through the equation of state for a perfect gas

$$p/\rho = RT \tag{2.6}$$

where R is the gas constant. If the variations in equations (2.5) are carried out holding the pressure constant,

$$\left.\frac{\partial q}{\partial T}\right|_p = \left.\frac{\partial h}{\partial T}\right|_p + 0 \equiv C_p . \tag{2.7}$$

The quantity C_p is the specific heat at constant pressure, that is, the quantity of heat required to raise the temperature of the gas one degree while the pressure is held fixed. According to the above, the specific heat at constant pressure is equal to increase of enthalpy at constant pressure. Because the pressure is positive and the density decreases as heat is added, the specific heat at constant pressure exceeds the specific heat at constant volume.

If the definition of the enthalpy is utilized in equation (2.7),

$$C_p = \left.\frac{\partial h}{\partial T}\right|_p = \left.\frac{\partial}{\partial T}(e + \frac{p}{\rho})\right|_p + \left.\frac{\partial (RT)}{\partial T}\right|_p \tag{2.8}$$

where the equation of state has been used in the last step. The term $\left.\frac{\partial e}{\partial T}\right|_p$ of equation (2.8) may be evaluated by considering the temperature and specific volume as the independent variables. Therefore

$$\left.\frac{\partial e}{\partial T}\right|_p = \left.\frac{\partial e}{\partial T}\right|_v \left.\frac{\partial T}{\partial T}\right|_p + \left.\frac{\partial e}{\partial V}\right|_T \left.\frac{\partial V}{\partial T}\right|_p = C_v + \left.\frac{\partial e}{\partial V}\right|_T \left.\frac{\partial V}{\partial T}\right|_p . \tag{2.9}$$

The partial derivative $\left.\frac{\partial e}{\partial T}\right|_T$ is the one involved in the famous Joule-Thomson investigation. Although the value of this derivative is not zero, it becomes smaller as the gas becomes more nearly perfect, that is, as the state of the gas is removed farther from condensation. For a perfect gas, that is, one satisfying the equation of state (2.6) rigorously, $\left.\frac{\partial e}{\partial V}\right|_T = 0$. Substituting this result back into equation (2.8) it follows that

$$C_p = C_v + R$$

or, in another form, the gas constant R may be expressed as the difference between the two values of specific heats

$$R = C_p - C_v \quad . \tag{2.10}$$

According to the assumptions which have been placed on the nozzle flow, no heat is transferred to or from each element of the gas during the expansion process. Therefore, the nozzle flow is a continuous adiabatic process, and the appropriate form of the First Law of Thermodynamics is

$$de + pd(1/\rho) = 0 \quad . \tag{2.11}$$

However, since it has been shown that $\partial e/\partial T\big|_v = C_v$ and that $\partial e/\partial V\big|_T \approx 0$, the last equation may be expressed in the form

$$C_v dT + pd(1/\rho) = 0 \quad . \tag{2.12}$$

This relation may be rewritten in terms of the pressure and density alone, using the equation of state. For writing

$$dT = d\left(\frac{p}{\rho R}\right) = \frac{1}{R}\left[pd(1/\rho) + \frac{1}{\rho}\,dp\right] \tag{2.13}$$

where R is treated as a constant independent of the gas state, equation (2.12) becomes

$$\frac{C_v}{R}\left[pd\left(\frac{1}{\rho}\right) + \frac{1}{\rho}\,dp\right] + pd\,\frac{1}{\rho} = \frac{C_p}{R}\,pd\left(\frac{1}{\rho}\right) + \frac{C_v}{R}\,\frac{1}{\rho}\,dp = 0 \quad . \tag{2.14}$$

This is a differential equation in which the variables may be separated

$$\frac{C_p}{C_v}\,\frac{d\rho}{\rho} = \frac{dp}{p} \quad . \tag{2.15}$$

In all real gases, the values of the specific heats as well as their ratio C_p/C_v, vary with the state of the gas. In many instances, how-

ever, it is possible to achieve a good approximation by assuming the specific heats to be constant at appropriate average values. A gas for which C_v is constant (and hence C_p is constant because of their relation through the constant R) is said to be thermally perfect. Then, calling the ratio of specific heats, $\gamma \equiv C_p/C_v$, equation (2. 15) may be integrated directly to give

$$\gamma \log \rho = \log p + \text{constant},$$

or

$$p\rho^{-\gamma} = \text{constant}. \tag{2. 16}$$

The result is the well-known law for the reversible adiabatic or isentropic process, and will apply to each element of the gas as it flows through the nozzle. By use of the equation of state, the result may be expressed in terms of the temperature and density

$$T/(\rho)^{\gamma-1} = \text{constant}, \tag{2. 17}$$

or, in terms of the temperature and pressure,

$$\frac{T^{\gamma/(\gamma-1)}}{p} = \text{constant}. \tag{2. 18}$$

From the First Law of Thermodynamics and momentum equation for the gas, there follows a general integral for adiabatic one-dimensional flow usually known as the energy equation. Under the present assumptions, the energy equation may be written

$$e + \frac{p}{\rho} + \tfrac{1}{2}v^2 = C_p T + \frac{v^2}{2} = C_p T_c = \text{constant} \ , \tag{2. 19}$$

where T and v are the values of gas temperature and velocity, respectively, at any point of the nozzle. The stagnation temperature and pressure of the gas are denoted T_c and p_c and are the values that would exist within the combustion chamber of the rocket if the gas ve-

locity vanished identically. The gas temperature depends primarily upon the nature of the propellant and slightly upon the combustion chamber pressure, p_c. If the state of the gas at the nozzle outlet is denoted by the subscript e, then the gas states at the nozzle outlet and the combustion chamber are related as

$$C_p T_e + \tfrac{1}{2} v_e^2 = C_p T_c . \tag{2.20}$$

Solving for the discharge velocity, which will be important in determining the thrust,

$$v_e^2 = 2C_p T_c \left(1 - \frac{T_e}{T_c}\right) . \tag{2.21}$$

Because the gas follows an isentropic process between the combustion chamber and the nozzle exit, equation (2.18) may be employed to express the discharge velocity in terms of the corresponding pressure ratio. This is appropriate, inasmuch as it is the ambient pressure at the nozzle exit, which is known in advance. Therefore,

$$v_e = \sqrt{2C_p T_c \left[1 - \left(\frac{p_e}{p_c}\right)^{(\gamma-1)/\gamma}\right]} = \sqrt{\frac{2\gamma}{\gamma-1} RT_c \left[1 - \left(\frac{p_e}{p_c}\right)^{(\gamma-1)/\gamma}\right]} \tag{2.22}$$

The form of the last result may be modified somewhat by putting in evidence the molecular weight of the gas. Let M be the molecular weight of the gas which is flowing through the nozzle, and V^* is the volume corresponding to this weight. Then if R^* is the gas constant for the equation

$$PV^* = R^* T , \tag{2.23}$$

it is found that R^* is a universal constant, which is not only independent of the state, but also of the gas. Clearly $V^* = MV$, and consequently

$$p/\rho = (R^*/M)T . \tag{2.24}$$

Using this relation in the expression for the nozzle discharge velocity, it follows that

$$v_e = \sqrt{\frac{2\gamma}{\gamma-1}\,\frac{R^*}{M}\,T_c\left[1 - \left(\frac{p_e}{p_c}\right)^{(\gamma-1)/\gamma}\right]} \,. \qquad (2.25)$$

It is evident, therefore, that the nozzle discharge velocity is increased not only by increasing the chamber temperature and increasing the nozzle pressure ratio, but also by decreasing the molecular weight of the propellant combustion products.

To proceed further in the calculation of rocket nozzle performance it is necessary to express the mass of gas flowing through the nozzle in terms of the rocket chamber conditions, the atmospheric pressure, and the rocket nozzle geometry. In the course of this calculation it will be necessary to employ the value of the propagation velocity of a small disturbance in the gas whose state is prescribed in advance. This value is the so-called velocity of sound propagation.

Consider a plane disturbance in a fluid body which propagates with a velocity v. By imposing an equal and opposite velocity to the fluid, the disturbance may be brought to rest, thereby reducing the problem to one of steady state. Then, the velocity of the fluid to the left of the wave is v, while that on the right is $v + dv$. If p and ρ are corresponding values of the pressure and density to the left of the wave, the values to the right of the wave are $p + dp$ and $\rho + d\rho$, respectively. Then, across the wave, the continuity equation reads

$$d(\rho v) = 0 \qquad (2.26)$$

and the momentum equation is

$$d(\rho v^2) = -\,dp \,. \qquad (2.27)$$

Carrying out the indicated differentiation on the left side of (2. 27) and taking account of (2. 26), it is seen that

$$\rho v\, dv = - dp \ . \tag{2.28}$$

Furthermore, the continuity equation states that $\rho dv = - v d\rho$ so that substituting into equation (2. 28),

$$v^2 d\rho = dp \ . \tag{2.29}$$

The differentials appearing in equation (2. 29) are taken in the direction of flow, and consequently their quotient may be considered the derivative taken under conditions prevailing along the direction of flow. Then if the propagation velocity for small disturbances is given the special notation a,

$$a^2 = dp/d\rho \ . \tag{2.30}$$

For the nozzle, the relation becomes particularly simple, inasmuch as the flow is isentropic, the pressure and density are connected by equation (2. 16). Then, carrying out the indicated differentiation,

$$a^2 = \gamma \frac{p}{\rho} = \gamma RT \ . \tag{2.31}$$

Thus the local sonic velocity depends only upon the temperature of the gas. The energy equation is conveniently expressed in terms of the local velocity of sound, for equation (2. 19) is just

$$a^2 + \frac{\gamma - 1}{2} v^2 = a_c^2 \ , \tag{2.32}$$

where a_c is the velocity of sound in the combustion chamber.

Now the general geometry of the rocket nozzle as well as the conditions at the nozzle throat may be ascertained from the logarithmic differential of the continuity equation ρva = constant. This gives

$$\frac{dA}{A} + \frac{d\rho}{\rho} + \frac{dv}{v} = 0 \ . \tag{2.33}$$

But the momentum relation may be written, for one-dimensional flow, in the form

$$\rho v dv = - dp = - \frac{dp}{d\rho} d\rho = - a^2 d\rho \ . \qquad (2.33)$$

This equation may be solved for $d\rho/\rho$:

$$d\rho/\rho = - (vdv)/a^2$$

and used to eliminate this quantity in equation (2.33). Thus

$$\frac{dA}{A} = \left(\frac{v^2}{a^2} - 1\right) \frac{dv}{v} \qquad (2.34)$$

which may be used to investigate the manner in which the nozzle area must change along its length in order to insure accelerating flow. There are three cases to be considered: $v < a$, $v > a$, and $v = a$.

I. $v < a$. When $v < a$, that is, when the local velocity of the gas is subsonic, and when the flow is accelerating, i.e., $dv/v > 0$, the right side of equation (2.34) is negative to that $dA/A < 0$. This is the familiar circumstance from hydraulics, namely, that the area of the nozzle must decrease to accelerate the fluid.

II. $v > a$. When $v > a$, that is, when the local velocity of the gas is supersonic, and when $dv/v > 0$, the right side of equation (2.34) is positive so that $dA/A > 0$. Thus, when the nozzle flow has become supersonic, it is necessary to diverge the passage in order to accelerate the gas.

The fact that the initial portion of the nozzle must converge and the final supersonic portion must diverge leads to the existence of a throat, that is, a section of smallest cross-sectional area. This circumstance is covered by case III.

III. $\underline{v = a}$. When $v = a$ and when the local acceleration is finite, the variation of area vanishes, that is, $dA/A = 0$. However, the condition $dA = 0$ implies the throat, that is, the section where the nozzle changes from converging to diverging. Hence, it may be concluded that, within the approximation of one-dimensional gas dynamics, the gas is moving at the sonic velocity at the throat.

In summarizing it may be said that to insure accelerating flow in the nozzle, the following conditions must exist:

$$\begin{array}{lll} dA/A < 0 & \text{when} & v < a \\ dA/A > 0 & \text{when} & v > a \\ dA/A = 0 & \text{when} & v = a \text{ (throat)} \end{array} \qquad (2.35)$$

In all rocket applications, the pressure ratio across the nozzle exceeds that necessary to produce sonic velocity, and consequently the appropriate nozzles are of the convergent (divergent) type with sonic velocity at the throat. Because of the existence of a sonic throat, it is particularly convenient to calculate the mass flowing through the nozzle by working at the throat section. If the subscript t is used to denote quantities at the throat section, the mass of gas flowing per unit time, m, is

$$m = \rho_t a_t A_t = \rho_c a_c A_t \left(\frac{\rho_t}{\rho_c}\right)\left(\frac{a_t}{a_c}\right) \qquad (2.36)$$

where ρ_c and a_c depend upon chamber conditions and are known. The velocity and density ratios may be calculated from the energy equation in the form given by equation (2.32). At the throat the sonic velocity and the gas velocity both become a_t, so that

$$a_t^2 + \frac{\gamma-1}{2} a_t^2 = a_c^2$$

or

$$a_t^2/a_c^2 = \frac{2}{\gamma-1}. \tag{2.37}$$

Furthermore, because the gas temperature is proportional to the square of the sonic velocity, it is clear that

$$T_t/T_c = 2/(\gamma+1) . \tag{2.38}$$

Because the flow is isentropic, the corresponding density ratio follows from the temperature - density relation, equation (2.17).

$$\frac{\rho_t}{\rho_c} = \left(\frac{T_t}{T_c}\right)^{1/(\gamma-1)} = \left(\frac{2}{\gamma+1}\right)^{1/(\gamma-1)} . \tag{2.39}$$

Now by means of equations (2.37) and (2.39), the mass flow may be written in terms of known quantities.

$$m = \rho_c a_c A_t \left(\frac{2}{\gamma+1}\right)^{1/(\gamma-1)} \left(\frac{2}{\gamma+1}\right)^{\frac{1}{2}} = \rho_c a_c A_t \left(\frac{2}{\gamma+1}\right)^{(\gamma+1)/2(\gamma-1)} . \tag{2.40}$$

Because the pressure and temperature in the combustion chamber are known either by direct calculation or measurement, there is a certain advantage to expressing equation (2.40) in the form

$$m = \gamma\left(\frac{2}{\gamma+1}\right)^{(\gamma+1)/2(\gamma-1)} \frac{p_c}{a_c} A_t = \Gamma' \frac{p_c}{a_c} A_t \tag{2.41}$$

where the quantity Γ' is

$$\Gamma' = \gamma \left(\frac{2}{\gamma+1}\right)^{(\gamma+1)/2(\gamma-1)} . \tag{2.42}$$

The thrust of a nozzle under conditions of ideal expansion may be computed from the known values of exit velocity. Because the discharge velocity is supersonic, the discharge pressure is fixed by the

chamber conditions and the area ratio and is not necessarily equal to the surrounding atmospheric pressure. By ideal expansion, it is implied that the nozzle area ratio is chosen so that the expansion does take place close to the ambient pressure.

Now the thrust for ideal expansion is just

$$F = mv_e = \Gamma' \frac{p_c}{a_c} A_t \sqrt{\frac{2\gamma}{\gamma-1} RT_c \left[1 - \left(\frac{p_e}{p_c}\right)^{(\gamma-1)/\gamma}\right]}$$

but since $a_c = \sqrt{\gamma R T_c}$, it follows directly that

$$F = p_c a_t \Gamma' \sqrt{\frac{2}{\gamma-1} \left[1 - \left(\frac{p_e}{p_c}\right)^{(\gamma-1)/\gamma}\right]}. \qquad (2.43)$$

The thrust coefficient, defined as $C_F = F/(p_c A_t)$, may be written as

$$CF \equiv \frac{F}{p_c A_t} = \Gamma' \sqrt{\frac{2}{\gamma-1} \left[1 - \left(\frac{p_e}{p_c}\right)^{(\gamma-1)/\gamma}\right]} \qquad (2.44)$$

and is seen to depend only on the nozzle pressure ratio and the properties of the propellant gas. For the ideally expanded nozzle, the specific impulse is proportional to the discharge velocity and consequently may be found from equation (2.25). Therefore, to obtain a given thrust, mass of gas required is decreased as the chamber temperature increases and the molecular weight decreases.

In order to obtain the value of thrust calculated above, it is necessary to construct the nozzle with a certain outlet area A_e. For the conditions of ideal expansion the outlet area is determined by the chamber conditions and the ambient atmospheric pressure or "back pressure" against which the gas is discharged. Therefore, there is no difficulty in calculating the ratio $\epsilon \equiv A_e/A_t$, the so-called expansion ratio. From continuity considerations it is clear that

$$\varepsilon = A_e/A_t = (\rho_t/\rho_e)(a_t/v_e) . \tag{2.45}$$

The density ratio may be written down directly

$$\frac{\rho_t}{\rho_e} = \frac{\rho_t}{\rho_c}\frac{\rho_c}{\rho_e} = \left(\frac{2}{\gamma+1}\right)^{1/(\gamma-1)}\left(\frac{p_c}{p_e}\right)^{1/\gamma} \tag{2.46}$$

where the results of equation (2.39) have been used. Now using the discharge velocity as calculated in equation (2.22), the expansion ratio may be written as

$$\varepsilon = \left(\frac{2}{\gamma+1}\right)^{1/(\gamma-1)} \frac{a_t}{a_c\left(\frac{p_e}{p_c}\right)^{1/\gamma}\sqrt{\frac{2}{\gamma-1}\left[1-\left(\frac{p_e}{p_c}\right)^{(\gamma-1)/\gamma}\right]}} . \tag{2.47}$$

The value of a_t/a_c follows from equation (2.37) to give

$$\varepsilon = \left(\frac{2}{\gamma+1}\right)^{(\gamma+1)/2(\gamma-1)} \frac{1}{\left(\frac{p_e}{p_c}\right)^{1/\gamma}\sqrt{\frac{2}{\gamma-1}\left[1-\left(\frac{p_e}{p_c}\right)^{(\gamma-1)/\gamma}\right]}} .$$

Now if the parameter Γ is defined as

$$\Gamma = \sqrt{\gamma}\left(\frac{2}{\gamma+1}\right)^{(\gamma+1)/2(\gamma-1)} = \Gamma'/\sqrt{\gamma} , \tag{2.48}$$

then the formulas for both the thrust coefficient and the expansion ratio may be written

$$C_F = \Gamma\sqrt{\frac{2\gamma}{\gamma-1}\left[1-\left(\frac{p_e}{p_c}\right)^{(\gamma-1)/\gamma}\right]} , \tag{2.49}$$

$$\varepsilon = \frac{\Gamma}{\left(\frac{p_e}{p_c}\right)^{1/\gamma}\sqrt{\frac{2\gamma}{\gamma-1}\left[1-\left(\frac{p_e}{p_c}\right)^{(\gamma-1)/\gamma}\right]}} . \tag{2.50}$$

It should be borne in mind that these expressions have been derived for ideal expansion, and therefore, the exit pressure p_e is identical with

the atmospheric pressure p_o. When the expansion is non-ideal, the relation between the expansion ratio and the pressure ratio is not modified. However, the thrust coefficient is changed due to the difference between atmospheric pressure and nozzle discharge pressure.

In addition to those mentioned thus far, two additional parameters are used in designating the nozzle or propellant performance. These are the effective exhaust velocity,

$$C \equiv F/m , \tag{2.51}$$

and the characteristic velocity, defined as

$$C^* = (p_c A_t)/m . \tag{2.52}$$

When the nozzle is expanded ideally, the effective exhaust velocity is exactly the actual exhaust velocity v_e. However, when the nozzle is not ideally expanded, and the atmospheric pressure contributes to the rocket thrust, the effective exhaust velocity is equal to the true exhaust velocity of an ideally expanded nozzle using the same gas mass and giving the same thrust. The characteristic velocity may be expressed in a somewhat different manner by recalling the mass flow relation, equation (2.41). Then

$$C^* = a_c/\Gamma' = 1/\Gamma \sqrt{RT_c} , \tag{2.53}$$

and hence is a multiple of the chamber sonic velocity, independent of the nozzle and dependent only upon the propellant used.

There is a simple relation between the characteristic velocity and the effective exhaust velocity which may be found by expressing the thrust coefficient

$$C_F = F/(p_c A_t) .$$

Now substituting for the thrust in terms of the effective exhaust velocity,

$$C_F = \frac{C}{(p_c A_t)/m} ,$$

and the denominator is clearly the characteristic velocity. Therefore, the thrust coefficient is related to the effective exhaust velocity and the characteristic velocity simply as

$$C_F = C/C^* . \qquad (2.54)$$

The following table gives the usual range of values for the various parameters which have been introduced to describe nozzle and propellant performance.

Parameter	Definition	Dimension	Range of Values
Specific Impulse, I_{sp}	F/mg	sec	185 - 425
Effective Exhaust Velocity, C	F/m	ft/sec	5900 - 12,000
Characteristic Velocity, C*	$\frac{p_c A_t}{m}$	ft/sec	4500 - 8000
Thrust Coefficient, C_F	$\frac{F}{p_c A_t}$	---	1.1 - 1.6

Nozzle with Non-Ideal Expansion

The discussion of nozzle flow so far has dealt only with ideally expanded nozzles, that is, those having the ideal nozzle exit pressure equal to the atmospheric pressure. Actually, a rocket nozzle spends most of its useful life operating under conditions of non-ideal expansion, and consequently performance calculation under these conditions

is of importance. A nozzle for which the ideal exit pressure is less than the ambient atmospheric pressure is referred to as being over-expanded. When the ideal exit pressure exceeds the atmospheric pressure, it is said to be under-expanded. The thrust for the over- and under-expanded rocket nozzles will be developed, and an approximate calculation of thrust slightly off the ideal operating condition will be carried out.

When the nozzle is not ideally expanded, the thrust relation has an additional term accounting for the difference between nozzle outlet and ambient pressure. By placing the control plane for the momentum calculation directly at the nozzle outlet the thrust may be computed without considering the expansion or shock wave mechanism by which nozzle outlet pressure is finally transformed into the ambient pressure.

If p_e is the ideal nozzle exit pressure, p_o the atmospheric pressure, and A_e the nozzle exit area, the thrust (or drag) contributed by this pressure variation is

$$A_e (p_e - p_o) \ . \tag{2.55}$$

The entire thrust is then simply

$$F = p_c A_t \Gamma' \sqrt{\frac{2}{\gamma-1}\left[1 - \left(\frac{p_e}{p_c}\right)^{(\gamma-1)/\gamma}\right]} + A_e(p_e - p_o) \ , \tag{2.56}$$

and the thrust coefficient is

$$C_F \equiv \frac{F}{p_c A_t} = \Gamma' \sqrt{\frac{2}{\gamma-1}\left[1 - \left(\frac{p_e}{p_c}\right)^{(\gamma-1)/\gamma}\right]} + \frac{A_e}{A_t}\left(\frac{p_e}{p_c} - \frac{p_o}{p_c}\right) . \tag{2.57}$$

Inasmuch as the area ratio of a nozzle, rather than the pressure ratio, p_e/p_c, is usually fixed, it is convenient to express the thrust coeffi-

cient C_F as a function of the area ratio A_e/A_t and the ratio of chamber pressure to the atmospheric pressure. Then for any nozzle geometry, chamber pressure, and operating altitude, the rocket thrust coefficient may be determined. It is not convenient to express the thrust coefficient explicitly in these variables; however, the computations are readily carried out. The only additional development required is that of expressing the pressure ratio p_e/p_c in terms of the area ratio A_e/A_t. This is easily done by employing the continuity relation

$$\rho_t a_t A_t = \rho_e v_e A_e , \tag{2.58}$$

so that

$$\frac{A_e}{A_t} = \left(\frac{\rho_t}{\rho_e}\right)\left(\frac{a_t}{v_e}\right), \tag{2.59}$$

and only the density and velocity ratios must be determined. From the isentropic relation

$$\frac{\rho_t}{\rho_e} = \left(\frac{p_t}{p_e}\right)^{1/\gamma} , \tag{2.60}$$

while the ratio of throat pressure to chamber pressure is simply

$$\frac{p_t}{p_c} = \left(\frac{2}{\gamma+1}\right)^{\gamma/(\gamma-1)} .$$

Therefore, the density ratio may be written in the form

$$\frac{\rho_t}{\rho_e} = \left(\frac{p_t}{p_e}\right)^{1/\gamma} \cdot \left(\frac{p_c}{p_t}\right)^{1/\gamma} \left(\frac{2}{\gamma+1}\right)^{1/(\gamma-1)} = \left(\frac{2}{\gamma+1}\right)^{1/(\gamma-1)} \left(\frac{p_c}{p_e}\right)^{1/\gamma} . \tag{2.61}$$

The velocity at the nozzle exit is, as shown previously

$$v_e = \sqrt{\frac{2}{\gamma-1}(\gamma R T_c)\left[1 - \left(\frac{p_e}{p_c}\right)^{(\gamma-1)/\gamma}\right]} \tag{2.62}$$

and the required velocity ratio is

$$\frac{v_e}{a_t} = \frac{a_c}{a_t}\sqrt{\frac{2}{\gamma-1}\left[1 - \left(\frac{p_e}{p_c}\right)^{(\gamma-1)/\gamma}\right]} = \sqrt{\frac{\gamma+1}{2}}\sqrt{\frac{2}{\gamma-1}\left[1 - \left(\frac{p_e}{p_c}\right)^{(\gamma-1)/\gamma}\right]} \tag{2.63}$$

The ratio of the nozzle exit area to the nozzle throat area may now be written using relations (2.61) and (2.63) in equation (2.59). This gives

$$\frac{A_e}{A_t} = \left(\frac{2}{\gamma+1}\right)^{\frac{1}{\gamma-1}+\frac{1}{2}} \frac{(p_c/p_e)^{1/\gamma}}{\sqrt{\frac{2}{\gamma-1}\left[1 - \left(\frac{p_e}{p_c}\right)^{(\gamma-1)/\gamma}\right]}}$$

$$= \frac{\left(\frac{2}{\gamma+1}\right)^{(\gamma+1)/2(\gamma-1)}}{\left(\frac{p_e}{p_c}\right)^{1/\gamma}\sqrt{\frac{2}{\gamma-1}\left[1 - \left(\frac{p_e}{p_c}\right)^{(\gamma-1)/\gamma}\right]}} . \tag{2.64}$$

With this relation, the thrust coefficient of equation (2.57) may be expressed in terms of either the pressure ratio p_e/p_c or the nozzle area ratio $A_e/A_t \equiv \varepsilon$, and the atmospheric pressure ratio p_o/p_c. For a given pressure ratio p_o/p_c, the values of thrust coefficient have a maximum with respect to the area ratio A_e/A_t. Thus, an optimum nozzle expansion ratio exists for given chamber and atmospheric pressures.

The condition for the optimum expansion ratio may be obtained from the relation of the pressure ratio p_e/p_c to the nozzle area ratio A_e/A_t, for if the change of thrust coefficient with p_e/p_c is calculated, it follows that

$$\frac{\partial C_F}{\partial (p_e/p_c)} = \frac{\partial}{\partial (p_e/p_c)} \Gamma' \sqrt{\frac{2}{\gamma-1}\left[1 - \left(\frac{p_e}{p_c}\right)^{(\gamma-1)/\gamma}\right]} + \frac{A_e}{A_t} +$$

$$+ \left(\frac{p_e - p_o}{p_c}\right) \frac{\partial \varepsilon}{\partial (p_e/p_c)} \quad . \tag{2.65}$$

Computing the derivative of the first term on the right side,

$$\frac{\Gamma' \frac{2}{\gamma-1} \cdot \frac{1}{2} \cdot \left(-\frac{\gamma-1}{\gamma}\right)\left(\frac{p_e}{p_c}\right)^{-1/\gamma}}{\sqrt{\frac{2}{\gamma-1}\left[1 - \left(\frac{p_e}{p_c}\right)^{(\gamma-1)/\gamma}\right]}} = \frac{-\left(\frac{2}{\gamma+1}\right)^{(\gamma+1)/2(\gamma-1)}}{\left(\frac{p_e}{p_c}\right)^{1/\gamma} \sqrt{\frac{2}{\gamma-1}\left[1 - \left(\frac{p_e}{p_c}\right)^{(\gamma-1)/\gamma}\right]}} \quad .$$

Comparing this with the results of equation (2.64), it is seen that the first two terms on the right side of equation (2.65) cancel each other so that, in general,

$$\partial C_F / \partial \varepsilon = \left(\frac{p_e - p_o}{p_c}\right) \quad . \tag{2.66}$$

It follows obviously that the thrust coefficient has a stationary value at $p_e = p_c$. Furthermore, it is a maximum, since the derivative is positive for values of ε below the value satisfying equation (2.66) and is negative for greater values of ε. The optimum value of the thrust coefficient then occurs when the theoretical nozzle outlet pressure is equal to the back pressure.

Suppose now that the values of the chamber pressure and the ambient pressure are known, and are such that $(p_e - p_o)/p_o \ll 1$. By development about the point of ideal expansion, $p_e = p_o$, an approximation for performance with slightly non-ideal expansion may be obtained. If the small parameter $(p_e - p_o)/p_o$ is denoted by δ, the development will be made in terms of this dimensionless quantity.

Consider the first term on the right side of equation (2.57). This may be written as

$$\Gamma' \sqrt{\frac{2}{\gamma-1}\left[1 - \left(\frac{p_o}{p_c} + \frac{p_e - p_o}{p_c}\right)^{(\gamma-1)/\gamma}\right]}$$

$$= \Gamma' \sqrt{\frac{2}{\gamma-1}\left[1 - \left(\frac{p_o}{p_c}\right)^{(\gamma-1)/\gamma} (1+\delta)^{(\gamma-1)/\gamma}\right]} .$$

Expanding in powers of δ, this term may be rewritten in the approximate form

$$\Gamma' \sqrt{\frac{2}{\gamma-1}\, 1 - \left(\frac{p_o}{p_c}\right)^{(\gamma-1)/\gamma} \left(1 + \frac{\gamma-1}{\gamma}\,\delta - \frac{1}{2}\,\frac{\gamma-1}{\gamma}\,\frac{1}{\gamma}\,\delta^2\right)}$$

$$\approx \Gamma' \sqrt{\frac{2}{\gamma-1}\, 1 - \left(\frac{p_o}{p_c}\right)^{(\gamma-1)/\gamma}} \sqrt{1 - \frac{\left(p_o/p_c\right)^{(\gamma-1)/\gamma}}{1 - \left(\frac{p_o}{p_c}\right)^{(\gamma-1)/\gamma}}\,\frac{\gamma-1}{\gamma}\left[\delta - \frac{1}{2\gamma}\,\delta^2\right]}$$

$$\approx \Gamma' \sqrt{\frac{2}{\gamma-1}\, 1 - \left(\frac{p_o}{p_c}\right)^{(\gamma-1)/\gamma}} \left\{1 - \frac{\gamma-1}{2\gamma}\,\frac{1}{\left(\frac{p_c}{p_o}\right)^{(\gamma-1)/\gamma} - 1}\,\delta \right.$$

$$\left. + \frac{\gamma-1}{2\gamma}\,\frac{1}{\left(\frac{p_c}{p_o}\right)^{(\gamma-1)/\gamma} - 1}\left[\frac{1}{\gamma} - \frac{\gamma-1}{4\gamma}\,\frac{1}{\left(\frac{p_c}{p_o}\right)^{(\gamma-1)/\gamma} - 1}\right]\delta^2 \right\} . \qquad (2.67)$$

It will be noted that this approximation has been computed to the second order in δ; the reason for this will become clear presently. The second term may also be calculated approximately. For

$$\frac{A_e}{A_t}\left(\frac{p_e - p_o}{p}\right) = \frac{\left(\frac{2}{\gamma+1}\right)^{(\gamma+1)/2(\gamma-1)}}{\sqrt{\frac{2}{\gamma-1}\left[1 - \left(\frac{p_e}{p_c}\right)^{(\gamma-1)/\gamma}\right]}} \left(\frac{p_e}{p_c}\right)^{-1/\gamma} \left(\frac{p_o}{p_c}\right) \delta .$$

In terms of the parameter δ, this term becomes

$$\left(\frac{2}{\gamma+1}\right)^{\frac{\gamma+1}{2(\gamma-1)}} \frac{(p_o/p_c)^{(\gamma-1)/\gamma}}{\sqrt{\frac{2}{\gamma-1}\left[1-\left(\frac{p_o}{p_c}\right)^{(\gamma-1)/\gamma}(1+\delta)^{(\gamma-1)/\gamma}\right]}}\,\delta(1+\delta)^{-1/\gamma} .$$

In a manner similar to that employed above, this term may be written to the second order,

$$\left(\frac{2}{\gamma+1}\right)^{\frac{\gamma+1}{2(\gamma-1)}} \frac{(p_o/p_c)^{(\gamma-1)/\gamma}}{\sqrt{\frac{2}{\gamma-1}\left[1-\left(\frac{p_o}{p_c}\right)^{(\gamma-1)/\gamma}\right]}}\left\{\delta-\frac{1}{\gamma}\left[1-\frac{\gamma-1}{2}\,\frac{1}{\left(\frac{p_c}{p_o}\right)^{(\gamma-1)/\gamma}-1}\right]\delta^2\right\} \tag{2.68}$$

Now, finally substituting the approximate results of equations (2.67) and (2.68) into the expression for the thrust coefficient, it follows that

$$C_F' - C_F = \frac{\Gamma'}{2\gamma^2}\,\frac{1}{\sqrt{\frac{2}{\gamma-1}\left[1-\left(\frac{p_o}{p_c}\right)^{(\gamma-1)/\gamma}\right]}}\left\{1-\frac{\gamma-1}{2}\,\frac{1}{\left(\frac{p_c}{p_o}\right)^{(\gamma-1)/\gamma}-1}\right\}\delta^2 \tag{2.69}$$

where

$$C_F' = \Gamma'\sqrt{\frac{2}{\gamma-1}\left[1-\left(\frac{p_o}{p_c}\right)^{(\gamma-1)/\gamma}\right]} . \tag{2.70}$$

Now equation (2.69) shows several interesting features. First, it is noted that the first order terms in δ cancel so that the deviation from the C_F', the thrust coefficient with ideal expansion ratio, is a quantity of the second order. This result was obvious from the outset inasmuch as the point about which the expansion was made has a maximum value. Furthermore, the sign of the second order variation is such that C_F never exceeds C_F', likewise following from the fact that C_F'

is the maximum value of C_F for a given chamber pressure and atmospheric pressure. It is actually more convenient to express equation (2.69) in terms of the ideal thrust coefficient C_F', as

$$C_F' - C_F = \tfrac{1}{2}\left(\frac{\Gamma'}{\gamma}\right)^2 \frac{1}{C_F'} \left\{ 1 - \frac{\gamma-1}{2} \frac{1}{\left(\frac{P_c}{P_o}\right)^{(\gamma-1)/\gamma} - 1} \delta^2 \approx \frac{1}{2C_F'} \left(\frac{\Gamma'}{\gamma}\right)^2 \delta^2 \right. . \quad (2.71)$$

Heterogeneous Flow in Nozzles

The presence of small solid particles occurring in the exhaust of rocket motors causes losses of specific impulse up to about 5 per cent of the value which would obtain if the same material were exhausted as a vapor. The magnitude of the loss depends, of course, upon the size of the solid particles and the fraction of exhaust mass flow that occurs as solid. The loss in rocket motor impulse is due to the facts that (i) the particle velocity lags behind the velocity of the gas, since the particles are accelerated by drag forces arising from relative motion of the gas and particles; (ii) heat is stored in the solid particles, since they do not cool as rapidly as the gas during the expansion process. As a consequence of this heat storage and the particle drag forces exerted upon the gas, the gas exit velocity is reduced below that which would occur without particles. (iii) The relative motion of gas and particles results in a dissipation that reduces the gas stagnation pressure below the chamber value.

It is possible to calculate the losses to be expected in any nozzle flow of a heterogeneous mixture to a reasonable degree of accuracy. The error in the calculation is determined largely by the accuracy of particle drag and heat transfer information and by some uncertainties

in the transport properties of the gas. For small particles in nozzles that do not incorporate too abrupt gas acceleration, the problem may be linearized, assuming the lag to be a small fraction of the gas velocity. Such calculations may be carried out quite directly.

Formulation of the two-phase gas - particle flow problem is most easily carried out as if the particle cloud behaved as a sort of fluid with appropriate properties. Then the conservation equations may be written for each phase or "fluid" which include coupling terms describing the exchange of momentum and heat between phases and the dissipation caused by the passage of particles through the viscous gas. It will simplify further considerations if it is assumed that particles of only a single size are present in the gas. Thus, if we denote velocity parallel to the nozzle axis by u, the mass density by ρ, and designate quantities associated with the particulate phase by a subscript p, then the equations of continuity for each phase may be written

$$\rho u A = \dot{m} , \tag{2.72}$$

$$\rho_p u_p A = \varkappa \dot{m} , \tag{2.73}$$

where $\dot{m}$ is the mass flow rate of gas through a cross section A, and $\varkappa\dot{m}$ is the mass flow rate of solid particles. The momentum equation for each phase may also be written as

$$\rho u \frac{du}{dx} + \frac{dp}{dx} = F_p , \tag{2.74}$$

$$\rho_p u_p \frac{du_p}{dx} = - F_p , \tag{2.75}$$

where p is the local gas pressure, and the quantity F_p is the force exerted upon a unit volume of gas by the particles contained within that

volume. In particular, it is to be noted that there exists no partial pressure of the solid phase; in other words, the particles interact with the fluid and not with each other. If it is assumed that the particles obey the first-order Stokes drag law, then the force F_p exerted by the particles upon a unit volume of the gas is

$$F_p = n_p \cdot 6\pi\sigma\mu (u_p - u) = \rho_p a \frac{u_p - u}{\lambda_v} , \qquad (2.76)$$

where n_p is the number of particles of radius σ in a unit volume, and consequently the effective mass density ρ_p of the solid phase is mn_p, where m is the mass of a single particle. The gas viscosity μ will be assumed to vary as the square root of gas temperature, $T^{\frac{1}{2}}$, so that the ratio μ/a is constant where a denotes the gaseous velocity of sound. The quantity λ_v is a characteristic length associated with the velocity equilibration rate of a single particle, and is defined as

$$\lambda_v \equiv ma/(6\pi\sigma\mu) . \qquad (2.77)$$

Physically, λ_v is the distance traversed while a particle of mass m and radius σ reduces its relative velocity to e^{-1} of its initial value after being injected into a gas stream of viscosity μ moving at its sonic velocity. We denote λ_v the velocity equilibration range and note that since a/μ is constant, λ_v is also constant. For rocket motor atmospheres and particle radii of one micron, the values of λ_v are of the magnitude of one centimeter. Since the particle mass m varies as the particle radius cubed, it follows that λ_v varies as the square of the particle radius.

The First Law of thermodynamics may be written for the gas as

$$\rho u c_p \frac{dT}{dx} = u \frac{dp}{dx} + (u_p - u) F_p + Q_p \qquad (2.78)$$

where Q_p is the heat transferred per unit volume per second from the particles to gas, and the term $(u_p-u)F_p$ is the work done on the gas by the passage of particles through the gas. It is to be noted that $(u_p-u)F_p \sim (u_p-u)^2$, and consequently represents a dissipative interaction; the sign remains unchanged regardless of whether the particles or gas are moving the faster. The value of c_p, specific heat of the gas at constant pressure, is assumed constant in the analysis, largely as a matter of analytical convenience. The heat transfer rate Q_p from particles to gas is approximately calculated as if the Nusselt number were unity, inasmuch as the particles were assumed to follow the Stokes drag law. Thus, Q_p may be written

$$Q_p = n_p\left(\frac{k}{\sigma}\right)4\pi\sigma^2(T_p-T) \equiv \rho_p c_p a\,\frac{T_p-T}{\lambda_T} \qquad (2.79)$$

where k is the thermal conductivity of the gas and T_p is the local temperature of solid particles. The characteristic length λ_T has a physical significance similar to its counterpart λ_v, except that in this case, it is the temperature difference rather than the velocity difference that is decaying with distance. Specifically, λ_T is defined as

$$\lambda_T \equiv (c_p m a)/(4\pi\sigma k) = 3/2\ \mathrm{Pr}\ \lambda_v \qquad (2.80)$$

and is designated the temperature equilibration range. It is to be noted that λ_T is directly proportional to λ_v, the factor of proportionality being 3/2 Pr, where $\mathrm{Pr} \equiv c_p\mu/k$ is the Prandtl number of the gas, assumed to be a constant in the present analysis. Because of this proportionality between λ_v and λ_T, the presence of particles in the gasdynamic flow field adds only one characteristic length to the problem; in many cases, 3/2 Pr is near enough to unity that λ_v and λ_T

may be considered equal.

Returning now to the basic equations, the First Law of thermodynamics for the solid phase may be written

$$\rho_p u_p c \frac{dT_p}{dx} = - Q_p , \tag{2.81}$$

where c is the constant specific heat of the solid material, and the individual solid particles are assumed undeformed by stresses imposed upon them by the gas. The fact that the particles are not deformed by the flow accounts for the absence of terms in equation (2.81) corresponding to volumetric dilatation or dissipation within the solid.

Together with the gaseous equation of state, the preceding relations give a complet analytical description of the one-dimensional heterogeneous flow. Because it is the intention here to consider the special circumstances where the differences $u-u_p$ and $T-T_p$ may be considered small in comparison with u and T respectively, there is an advantage of introducing the variables

$$\begin{aligned} u - u_p &\equiv u_s \\ T - T_p &\equiv T_s \\ 1 - (\rho_p/\varkappa\rho) &\equiv \rho_s \end{aligned} \tag{2.82}$$

in preference to the particle quantities u_p, T_p, and ρ_p. A comparable transformation in the equations of continuity, momentum, and energy may be effected to emphasize the fact that u_s, T_s, and ρ_s are essentially of much smaller numerical magnitude than u, T, and unity, respectively. By adding the equations of motion for gaseous and solid phase, equations (2.74) and (2.75), the force F_p acting between the two phases disappears and, after some rearrangement,

$$(1+\varkappa)\rho u \frac{du}{dx} + \frac{dp}{dx} = \varkappa\rho u \frac{du_s}{dx} \quad . \tag{2.83}$$

In much the same manner, addition of statements of the First Law for gaseous and solid phase, equations (2.78) and (2.79), eliminates the heat exchange between the two phases. Moreover, the two momentum relations, equations (2.74) and (2.75), may be employed to eliminate the pressure and inter-phase force. This operation yields a relation that may be integrated from the rocket chamber to an arbitrary position of the nozzle and gives:

$$\left(\frac{c_p+\varkappa c}{1+\varkappa}\right)(T-T_c) + \tfrac{1}{2}u^2 = \frac{\varkappa}{1+\varkappa}\left[cT_s + uu_s - \tfrac{1}{2}u_s^2\right], \tag{2.84}$$

where it has been taken into account that u, u_s, and T_s vanish in the rocket chamber, and that T_c is the common temperature of the gas and solid phases in the chamber.

Now consider the limiting circumstance where the velocities and temperatures of the two phases remain exactly equal throughout the nozzle; this condition will be designated the "equilibrium" flow. Then, since $u_s = T_s = 0$, equation (2.83) becomes

$$(1+\varkappa)\rho u \frac{du}{dx} + \frac{dp}{dx} = 0 , \tag{2.85}$$

and equation (2.84) reads

$$\left(\frac{c_p+\varkappa c}{1+\varkappa}\right)(T-T_c) + \tfrac{1}{2}u^2 = 0 . \tag{2.86}$$

If appropriate forms of the equations of continuity are used,

$$(1+\varkappa)\rho u A = (1+\varkappa)\dot{m} , \tag{2.87}$$

and the equation of state may be rewritten

$$p = (1+\varkappa)\rho\left(\frac{R}{1+\varkappa}\right)T . \tag{2.88}$$

Equations (2.85) through (2.88) are recognized as those describing the isentropic flow of a gas through a nozzle of mass flow $(1+\varkappa)\dot{m}$ and cross-sectional area A, where the gas has an effective density

$$\overline{\rho} = (1+\varkappa)\rho , \tag{2.89}$$

and effective gas properties

$$\begin{aligned} \overline{c}_p &\equiv (c_p+\varkappa c)/(1+\varkappa) \\ \overline{c}_v &= (c_v+\varkappa c)/(1+\varkappa) \\ \overline{R} &= (c_p-c_v)/(1+\varkappa) \\ \overline{\gamma} &= (c_p+\varkappa c)/(c_v+\varkappa c) \end{aligned} \tag{2.90}$$

Then clearly the expansion process takes place according to the law

$$T/T_c = (p/p_c)^{(\overline{\gamma}-1)/\overline{\gamma}} = (\overline{\rho}/\overline{\rho}_c)^{\overline{\gamma}-1} , \tag{2.91}$$

where p_c and $\overline{\rho}_c$ are the pressure and effective density in the rocket chamber. All familiar relationships for isentropic nozzle flow hold, then, provided they are written in terms of the effective quantities given above. Although this condition of "equilibrium" flow is an artificial one, so far as actual rocket nozzles are concerned, it does form a suitable starting place for an approximate performance calculation, since it is quite nearly correct for any nozzle of reasonable performance.

Returning now to the problem of heterogeneous nozzle flow under non-equilibrium conditions, it is worth noting that the equilibrium nozzle flow problem is a simple one, because the isentropic integral, equation (2.91), renders the momentum equation (2.85) redundant. With the aim of utilizing any simplification to the present problem that may ac-

crue from this, the corresponding manipulations of equations (2.85) and (2.84), together with appropriate equations of state and continuity, lead to the relationship

$$\left(\frac{T}{T_c}\right)\left(\frac{p_c}{p}\right)^{(\bar{\gamma}-1)/\bar{\gamma}} = \exp\left\{\frac{\varkappa}{1+\varkappa}\int_0^x \frac{1}{\bar{c}_p T}\left[c\frac{dT_s}{dx} + u_s\frac{d}{dx}(u-u_s)\right]dx\right\} \quad (2.92)$$

In the analysis of non-equilibrium heterogeneous flow, it will be convenient to work with equations (2.84) and (2.92). They do not suffice to complete the problem, and additional linear combinations of the original equations are required. From equations (2.72) and (2.73), it follows directly that

$$\rho_s u + u_s = \rho_s u_s \,, \quad (2.93)$$

while from equations (2.75) and (2.72) it is not difficult to show that

$$u\frac{du}{dp} - \frac{au_s}{\bar{\lambda}_v}\frac{1}{dp/dx} = -\rho_s\frac{au_s}{\bar{\lambda}_v}\frac{1}{dp/dx} + u\frac{du_s}{dp} \,, \quad (2.94)$$

where a is the equilibrium speed of sound; that is,

$$a^2 = \bar{\gamma}\bar{R}T \,,$$

and $\bar{\lambda}_v$ is the velocity equilibrium length (equation 2.77) based upon the equilibrium speed of sound. Similarly, from equations (2.81) and (2.72), it follows that

$$u\frac{dT}{dp} - \frac{\bar{c}_p}{c}\frac{aT_s}{\bar{\lambda}_T}\frac{1}{dp/dx} = -\rho_s\frac{\bar{c}_p}{c}\frac{aT_s}{\bar{\lambda}_T}\frac{1}{dp/dx} + u\frac{dT_s}{dp} \quad (2.95)$$

where $\bar{\lambda}_T$ is based upon the equilibrium speed of sound and the effective specific heat $\bar{c}_p$. The set of equations (2.84), (2.87), (2.88), and (2.92) through (2.94) are completely equivalent to the original equations and they are written explicitly in terms of the quantities u_s, T_s, and ρ_s. Moreover, the independent variable has been changed to the gas

pressure p, and the distribution of pressure along the nozzle axis, $p(x)$ or its inverse, is assumed to be prescribed.

When the three dependent variables ρ_s, u_s, and T_s are small, a perturbation solution naturally suggests itself, and the appropriate small quantity in terms of which the solutions should be expanded is $\bar{\lambda}_v/L$ where L is the fixed nozzle length. The state of the gas may then be written

$$\begin{aligned} \rho &= \rho^{(0)} + (\bar{\lambda}_v/L)\,\rho^{(1)} + (\bar{\lambda}_v/L)^2\rho^{(2)} + \dots \\ u &= u^{(0)} + (\bar{\lambda}_v/L)\,u^{(1)} + (\bar{\lambda}_v/L)^2 u^{(2)} + \dots \\ T &= T^{(0)} + (\bar{\lambda}_v/L)\,T^{(1)} + (\bar{\lambda}_v/L)^2 T^{(2)} + \dots \end{aligned} \tag{2.96}$$

where each coefficient is a function of the local pressure p. Each of these variables has a non-vanishing zeroth degree part, and all coefficients in the expansions are of order unity. The variations of the particle state from that of the gas, ρ_s, u_s, and T_s, have leading terms of the first degree

$$\begin{aligned} \rho_s &= (\bar{\lambda}_v/L)\rho_s^{(1)} + (\bar{\lambda}_v/L)^2\rho_s^{(2)} + \dots \\ u_s &= (\bar{\lambda}_v/L)u_s^{(1)} + (\bar{\lambda}_v/L)^2 u_s^{(2)} + \dots \\ T_s &= (\bar{\lambda}_v/L)T_s^{(1)} + (\bar{\lambda}_v/L)^2 T_s^{(2)} + \dots \end{aligned} \tag{2.97}$$

The functions giving terms of various order in each variable may be determined by substituting expressions (2.96) and (2.97) into the equations (2.84), (2.87), (2.88), and (2.92) through (2.95) and separating each equation according to the powers of the small parameter $\bar{\lambda}_v/L$. In the present analyses, there will be no need to consider more than the zeroth and first degree terms.

The functions $\rho^{(0)}$, $u^{(0)}$, and $T^{(0)}$ are described by the zeroth order parts of equations (2.84), (2.88), and (2.92). Inspection of these shows immediately that this solution corresponds exactly to the so-called equilibrium solution described previously by equations (2.86), (2.88), and (2.91); to this order of approximation, then, the gas and particles have the same velocity and temperature. Clearly then, the solution being employed consists in a perturbation expansion about the equilibrium flow. Physically, this implies that as $\overline{\lambda}_v/L$ becomes very small, the actual flow approaches more and more closely to the equilibrium flow. That is equivalent to saying that when the equilibration range $\overline{\lambda}_v$ is negligible compared with the nozzle length, the gas and particles achieve an equilibrium state before a significant fraction of the nozzle length has been traversed. These quantities are readily written down in terms of the prescribed pressure distribution along the nozzle.

$$\rho^{(0)}/\rho_c = (p/p_c)^{1/\overline{\gamma}} \tag{2.98}$$

$$T^{(0)}/T_c = (p/p_c)^{(\overline{\gamma}-1)/\overline{\gamma}} \tag{2.99}$$

$$u^{(0)} = \sqrt{2\overline{c}_p T_c \left(1 - (p/p_c)^{(\overline{\gamma}-1)/\overline{\gamma}}\right)} \tag{2.100}$$

Calculation of the first order terms $\rho_s^{(1)}$, $u_s^{(1)}$, and $T_s^{(1)}$ follows quite directly from equations (2.93), (2.94), and (2.95). In equations (2.94) and (2.95), the presence of the small quantity λ_v in the denominator of their right hand sides reduces the order of these terms by one. Consequently, it follows from the zeroth order part of equation (2.94) that

$$u_s^{(1)} = \frac{u^{(0)}}{a^{(0)}} \frac{du^{(0)}}{dp} \left(\frac{dp}{d\xi}\right),$$

where the new length variable $\xi = x/L$ has been introduced. Utilizing the relationships between the pressure and zeroth order quantities in the above equation gives the somewhat simpler form

$$u_s^{(1)} = -\frac{a^{(0)}}{\bar{\gamma}} \left(\frac{1}{p} \frac{dp}{d\xi}\right). \tag{2.101}$$

Similarly, from the form of the energy relation given by equation (2.95) it follows, after some reduction, that

$$T_s^{(1)} = \frac{1}{\bar{c}_p} \frac{c}{\bar{c}_p} \left(\frac{\lambda_T}{\bar{\lambda}_v}\right) \frac{a^{(0)}}{\bar{\gamma}} u^{(0)} \left(\frac{1}{p} \frac{dp}{d\xi}\right), \tag{2.102}$$

and from equation (2.93),

$$\rho_s^{(1)} = \frac{1}{\bar{\gamma}} \frac{1}{M^{(0)}} \left(\frac{1}{p} \frac{dp}{d\xi}\right). \tag{2.103}$$

From equations (2.101) and (2.102), in which $u_s^{(1)}$ and $T_c^{(1)}$ are determined algebraicly, it is apparent that the order of differential equations has been reduced by one in each case; that is, the perturbation employed is a singular one, and hence some "boundary layer" regions will be ignored. The physical effect of this fact may be illustrated by considering a situation where, due to a change in nozzle slope, the pressure gradient $dp/d\xi$ is discontinuous. Then, according to equation (2.101), the particle slip velocity is discontinuous, a circumstance which is clearly impossible. The exact solution, or the local boundary layer solution, would smooth this discontinuity into the physically correct one.

Evaluation of the remaining first order terms may be carried out from equations (2.84), (2.88), and (2.92), noting particularly the

fact that the right hand sides of both equations (2.84) and (2.92) are of the first order and are known to that order. These two perturbation relations may be written explicitly as

$$\frac{T^{(1)}}{T^{(0)}} + (\bar{\gamma}-1)\,M^{(0)^2}\left(\frac{u^{(1)}}{u^{(0)}}\right) = \frac{\varkappa}{1+\varkappa}\,F\left(\frac{p}{p_c}\right) \tag{2.104}$$

and

$$\frac{T^{(1)}}{T^{(0)}} = \frac{\varkappa}{1+\varkappa}\,G\left(\frac{p}{p_c}\right) \tag{2.105}$$

where the functions on the right hand sides of equations (2.104) and (2.105) are the known functions of the prescribed pressure ratio

$$F(p/p_c) = (\eta-1)(\bar{\gamma}-1/\bar{\gamma})M^{(0)}\,\frac{1}{p}\,\frac{dp}{d\xi} \tag{2.106}$$

and

$$G(p/p_c) = \int_{p_c}^{p} \frac{1}{\bar{c}_p\,T^{(0)}}\left\{(1-\eta)u_s^{(1)}\,\frac{du^{(0)}}{dp} - \eta u^{(0)}\,\frac{du_s^{(1)}}{dp}\right\} dp \tag{2.107}$$

where the possible simplification of the last integral will be postponed. Here, we have denoted the quantity $(\bar{\lambda}_T/\bar{\lambda}_v)(c/\bar{c}_p)^2 \equiv \eta$. The first order perturbation to the equation of state, equation (2.88), gives

$$\rho^{(1)}/\rho^{(0)} = -\,T^{(1)}/T^{(0)}\,. \tag{2.108}$$

Now equation (2.105) gives directly the first-order gas temperature perturbation, and equations (2.104) and (2.108) may be solved for velocity and density perturbations directly as

$$\frac{u^{(1)}}{u^{(0)}} = \frac{\varkappa}{1+\varkappa}\,\frac{1}{(\bar{\gamma}-1)M^{(0)^2}}\,F\left(\frac{p}{p_c}\right) - G\left(\frac{p}{p_c}\right) \tag{2.109}$$

and

$$\rho^{(1)}/\rho^{(0)} = -(\varkappa/1+\varkappa)\, G(p/p_c) . \qquad (2.110)$$

The first order modifications to equilibrium nozzle flow, due to the effects of solid particles transported by the gas, is then given by equations (2.105), (2.109), (2.110) for the gas flow, and equations (2.101), (2.102), and (2.103) for the particle flow where the gas pressure is a prescribed function of x or of ξ .

The required cross-sectional area of a nozzle carrying mass flow $\dot{m}$ and providing the required pressure distribution must also be expressed as a series in powers of λ_v/L . That is,

$$A(p/p_c) = A^{(0)}(p/p_c) + (\lambda_v/L)A^{(1)}(p/p_c) + \ldots \qquad (2.111)$$

where the coefficients $A^{(0)}$, $A^{(1)}$, etc., are readily determined from the equation of continuity, equation (2.72). It will prove most convenient to express the zeroth area in the form $\rho_c a_c A^{(0)}/\dot{m}$, since the chamber conditions are assumed constant and the area may be scaled up or down depending upon the desired mass flow. This gives, according to the well-known relations,

$$\frac{\rho_c a_c A^{(0)}}{\dot{m}} \left(\frac{p}{p_c}\right) = \left(\frac{p}{p_c}\right)^{1/\bar{\gamma}} \left\{ \frac{2}{\bar{\gamma}-1} \left(1 - \left(\frac{p}{p_c}\right)^{(\bar{\gamma}-1)/\bar{\gamma}} \right) \right\}^{\frac{1}{2}} . \qquad (2.112)$$

The ratio of the first area perturbation to the zeroth order area may be written as

$$\frac{A^{(1)}}{A^{(0)}} = -\left(\frac{\rho^{(1)}}{\rho^{(0)}} + \frac{u^{(1)}}{u^{(0)}} \right) ,$$

and consequently, is given in terms of the F and G functions, equations (2.106) and (2.107). Through partial integration of (2.107) and ensuing simplification, the expression for $A^{(1)}/A^{(0)}$ may be written

$$\frac{A^{(1)}}{A^{(0)}} = \frac{\varkappa}{1+\varkappa}\frac{1}{\bar{\gamma}M^{(0)}}\left\{\left(1+\eta(\bar{\gamma}-1)M^{(0)^2}\right)\frac{1}{p}\frac{dp}{d\xi}\right.$$

$$\left. + \frac{1+(\bar{\gamma}-1)M^{(0)^2}}{\bar{\gamma}^2\bar{M}^{(0)^2}}\int_1^{p/p_c}\frac{1+\eta(\bar{\gamma}-1)M^{(0)^2}}{M^{(0)}}\frac{1}{\alpha^2}\frac{d\alpha}{d\xi}\,d\alpha\right\} \qquad (2.113)$$

None of the calculations involved encounter any difficulties in the neighborhood of the nozzle throat.

The particle velocity lag and particle temperature deviation cause a general reduction in the specific impulse of a rocket motor. To calculate this loss to the first order in λ_v/L, consider a nozzle of fixed length L expanding the gas from a given chamber state p_c, T_c, to a prescribed exhaust pressure p_e. If the specific impulse

$$I^{(0)} \equiv u_e^{(0)}/g, \qquad (2.114)$$

that occurring under conditions of equilibrium flow, is taken as the reference value, then the fractional loss of impulse caused by the presence of the particles is

$$\frac{I^{(0)}-I}{I^{(0)}} = -\frac{\varkappa}{1+\varkappa}\frac{\lambda_v}{L}\frac{u^{(1)}}{u^{(0)}}\Big|_{p_e} \frac{\varkappa}{1+\varkappa}\left(\frac{u^{(1)}}{u^{(0)}} - \frac{u_s^{(1)}}{u^{(0)}}\right)_{p_e}$$

$$= -\frac{\lambda_v}{L}\left(\frac{u^{(1)}}{u^{(0)}} - \frac{\varkappa}{1+\varkappa}\frac{u_s^{(1)}}{u^{(0)}}\right)_{p_e} \qquad (2.115)$$

The term associated with the pressure at the nozzle discharge is absent because nozzles carrying both equilibrium and non-equilibrium flow are expanded to the local atmosphere pressure. This loss may be written down explicitly utilizing the values for $u^{(1)}/u^{(0)}$ and $u_s^{(1)}/u^{(0)}$ from equations (2.109) and (2.111), respectively. With

this substitution,

$$\frac{I^{(0)}-I}{I^{(0)}} = -\frac{\bar{\lambda}_v}{L}\left(\frac{\varkappa}{1+\varkappa}\right)\left\{\frac{1}{(\bar{\gamma}-1)M_e^{(0)2}}\left(F\left(\frac{p_e}{p_c}\right)-G\left(\frac{p_e}{p_c}\right)\right)+\frac{1}{\bar{\gamma}M_e^{(0)}}\frac{1}{p_e}\frac{dp}{d\xi}\Big|_e\right\},$$

$$\frac{I^{(0)}-I}{I^{(0)}} = \frac{\lambda_v}{L}\frac{\varkappa}{1+\varkappa}\left\{-\frac{\eta}{\bar{\gamma}M^{(0)}}\frac{1}{p_e}\frac{dp}{d\xi}(p_e)+\frac{1-\eta}{\bar{\gamma}^2M_e^{(0)2}}\int_{p_c}^{p_e}\frac{1}{M^{(0)}}\frac{1}{p^2}\frac{dp}{d\xi}\,d\xi\right.$$

$$\left.+\frac{\eta}{(\bar{\gamma}-1)M_e^{(0)2}}\int_{p_c}^{p_e}\frac{u^{(0)}}{\bar{c}_p T^{(0)}}\frac{d}{dp}\left(\frac{a^{(0)}}{\bar{\gamma}p}\frac{dp}{d\xi}\right)dp\right\} \qquad (2.116)$$

where the subscript e has been used to denote the value of the variables at the nozzle exit; that is, when $p = p_e$. Partial integration of the second integral in equation (2.116) and some subsequent simplification yield a final convenient form for the fractional impulse loss:

$$\frac{I^{(0)}-I}{I^{(0)}} = -\frac{\bar{\lambda}_v}{L}\left(\frac{\varkappa}{1+\varkappa}\right)\frac{1}{\bar{\gamma}^2M_e^{(0)2}}\int_{p_e}^{p_c}\frac{1+\eta(\bar{\gamma}-1)M^{(0)2}}{M^{(0)}}\frac{1}{p^2}\frac{dp}{d\xi}\,dp\ . \qquad (2.117)$$

It should be noted that for most cases of practical interest $\eta \approx 1$, and the error introduced into equation (2.117) by setting $\eta = 1$ is correspondingly small.

Evaluation of the impulse loss from equation (2.117) presents no difficulty so long as the pressure distribution along the axis $p(\xi)$, or its inverse $\xi(p)$, is prescribed. Then, writing the Mach number in terms of the pressure

$$M^{(0)2} = 2/(\bar{\gamma}-1)\left[(p_c/p)^{(\bar{\gamma}-1)/\bar{\gamma}}-1\right], \qquad (2.118)$$

evaluation of equation (2.117) is, at worst, an elementary numerical

integration.

The analysis which has been carried out for a fixed exhaust pressure can be extended to a nozzle of fixed outlet area rather easily. The discharge area A_e and the pressure at the nozzle exit are coupled through the continuity relation. If there were no particle slip, the pressure $p_e^{(0)}$ at the outlet of the nozzle satisfies the equation

$$\frac{\rho \bar{a}_c A_e}{\dot{m}} = (p_c/p_e^{(0)})^{1/\bar{\gamma}} \left\{ 2/(\bar{\gamma}-1) \left[1 - (p_e^{(0)}/p_c)^{(\bar{\gamma}-1)/\bar{\gamma}} \right] \right\}^{\frac{1}{2}} . \quad (2.119)$$

Since the outlet area is fixed, particle slip and the attending non-equilibrium effects cause the pressure at the outlet to be modified by an amount proportional to $\bar{\lambda}_v/L$, with the nozzle outlet pressure in the form

$$\frac{p_e}{p_c} = \frac{p_e^{(0)}}{p_c} + \frac{\bar{\lambda}_v}{L} \frac{p_e^{(1)}}{p_c} + \ldots \quad . \quad (2.120)$$

Now utilizing equations (2.111), (2.112), and (2.113), the nozzle outlet area parameter may be written to the first order of $\bar{\lambda}_v/L$ as

$$\frac{\rho \bar{a}_c A_e}{\dot{m}} = (p_c/p_e)^{1/\bar{\gamma}} \left\{ 2/(\bar{\gamma}-1) \; 1 - (p_e/p_c)^{(\bar{\gamma}-1)/\bar{\gamma}} \right\}^{\frac{1}{2}}$$

$$\times \left\{ 1 + (\bar{\lambda}_v/L) \frac{\varkappa}{1+\varkappa} \left[\left(1 + \frac{1}{(\bar{\gamma}-1)M^{(0)2}} \right) G(p_e/p_c) - \frac{1}{(\bar{\gamma}-1)M^{(0)2}} F(p_e/p_c) \right] \right\}$$

(2.121)

But p_e/p_c is expressed by equation (2.120) so that retaining only the zeroth and first order parts,

$$\frac{\rho \bar{a}_c A_e}{\dot{m}} = \left(\frac{p_c}{p_e^{(0)}}\right)^{1/\bar{\gamma}} \left\{ \frac{2}{\bar{\gamma}-1} \left[1 - \left(\frac{p_e^{(0)}}{p_c} \right)^{(\bar{\gamma}-1)/\bar{\gamma}} \right] \right\}^{-\frac{1}{2}}$$

$$+ \frac{\bar{\lambda}_v}{L} \left(\frac{p_c}{p_e^{(0)}}\right)^{1/\bar{\gamma}} \left[\frac{2}{\bar{\gamma}-1} \left(1 - \left(\frac{p_e^{(0)}}{p_c} \right)^{(\bar{\gamma}-1)/\bar{\gamma}} \right) \right]^{-\frac{1}{2}}$$

$$\times \left\{ - \frac{1}{\bar{\gamma}} \left(\frac{p_c}{p_e^{(0)}}\right) \left[\frac{\bar{\gamma}+1}{2} - \frac{\bar{\gamma}-1}{2} \left(1 - \left(\frac{p_e^{(0)}}{p_c} \right)^{(\bar{\gamma}-1)/\bar{\gamma}} \right)^{-1} \right] \left(\frac{p_e^{(1)}}{p_c} \right) \right.$$

$$\left. + \frac{\varkappa}{1+\varkappa} \left[\left(1 + \frac{1}{(\bar{\gamma}-1) M_e^{(0)2}} \right) G\left(\frac{p_e^{(0)}}{p_c} \right) - \frac{1}{(\bar{\gamma}-1) M_e^{(0)2}} F\left(\frac{p_e^{(0)}}{p_c} \right) \right] \right\} \cdot \quad (2.122)$$

The condition that the outlet area parameter be unchanged by the flow perturbation is simply that the nozzle outlet pressure be modified by an amount $\frac{\bar{\lambda}_v}{L} p_e^{(1)}/p_c$ such that the coefficient of $\bar{\lambda}_v/L$ in equation (2.122) vanish. This then states that for a nozzle of fixed mass flow, the outlet area is not modified by the flow perturbation. Explicitly, this gives the outlet pressure perturbation $p_e^{(1)}/p_c$ as

$$\frac{p_e^{(1)}}{p_c} = \frac{\varkappa}{1+\varkappa} \left(\frac{\bar{\gamma} p_e^{(0)}}{p_c} \right) \frac{1 + \frac{1}{(\bar{\gamma}-1) M_e^{(0)2}} G\left(\frac{p_e^{(0)}}{p_c} \right) - \frac{1}{(\bar{\gamma}-1) M_e^{(0)2}} F\left(\frac{p_e^{(0)}}{p_c} \right)}{\frac{\bar{\gamma}+1}{2} - \frac{\bar{\gamma}-1}{2} \left(1 - \left(\frac{p_e^{(0)}}{p_c} \right)^{(\gamma-1)/\gamma} \right)^{-1}} \quad (2.123)$$

which may then be computed when the functions F and G are known.

Now the thrust of the motor may also be expanded in a perturbation series

$$\frac{\mathcal{F}^{(0)} + \frac{\bar{\lambda}_v}{L}\mathcal{F}^{(1)}}{(1+\varkappa)\dot{m}} = u^{(0)}\left(\frac{p_e^{(0)}}{p_c}\right) + \left.\frac{du^{(0)}}{d(p/p_c)}\right|_{p_e^{(0)}/p_c} \frac{\bar{\lambda}_v}{L}\frac{p_e^{(1)}}{p_c}$$

$$+ \frac{\lambda_v}{L}\left[\frac{1}{1+\varkappa}u^{(1)}\left(\frac{p_e^{(0)}}{p_c}\right) + \frac{\varkappa}{1+\varkappa}u_p^{(1)}\left(\frac{p_e^{(0)}}{p_c}\right)\right] + \frac{\bar{\lambda}_v}{L}\frac{A_e p_c}{(1+\varkappa)\dot{m}}\frac{p_e^{(1)}}{p_c} \quad . \quad (2.124)$$

The straightforward calculation of the derivative shows that

$$\left.\frac{du^{(0)}}{d(p/p_c)}\right|_{p_e^{(0)}/p_c} = -\frac{A_e p_c}{(1+\varkappa)\dot{m}} \quad , \quad (2.125)$$

so that the remaining perturbation terms are

$$-\frac{\frac{\bar{\lambda}_v}{L}\mathcal{F}^{(1)}}{(1+\varkappa)\dot{m}} \equiv \left(\frac{I^{(0)}-I}{I^{(0)}}\right) =$$

$$= -\frac{\bar{\lambda}_v}{L}\left\{\frac{\varkappa}{1+\varkappa}\frac{u^{(1)}}{u^{(0)}}\left(\frac{p_e^{(0)}}{p_c}\right) + \frac{\varkappa}{1+\varkappa}\frac{u_p^{(1)}}{u^{(0)}}\left(\frac{p_e^{(0)}}{p_c}\right)\right\} . \quad (2.126)$$

Comparison with equation (2.115) shows this to be identical with the result obtained for a fixed outlet pressure. The two are the same, therefore, up to the first order terms in $\bar{\lambda}_v/L$, the accuracy of our calculation.

3. COMBUSTION THERMODYNAMICS AND CHEMICAL PROPELLANTS

Free Energy and Equilibrium

The Helmholtz free energy, or work function, is defined by the equation

$$A = E - TS \tag{3.1}$$

Defined entirely in terms of functions of state, A is also a function of state. Compare two states of a system held at constant temperature:

$$A_2 = E_2 - T_2 S_2$$

$$A_1 = E_1 - T_1 S_1$$

Subtracting, we find that for any change at constant temperature

$$\Delta A = \Delta E - T\Delta S \tag{3.2}$$

Substituting from the First Law for a reversible change, we have

$$\Delta A = q_{rev} - w_{max} - T\Delta S$$

But since $\Delta S = q_{rev}/T$, it follows that

$$\Delta A = T\Delta S - w_{max} - T\Delta S = -w_{max}$$

from which

$$-\Delta A = w_{max} \tag{3.3}$$

For any given change at constant temperature, there is a maximum extractable work, expressible as the difference of a function of state, $-\Delta A$.

To find, in terms of A , criteria for determining the direction of spontaneous reaction, and the situation at equilibrium, we again set out from equation (3.2) for any isothermal change. Now, however, we do <u>not</u> stipulate a reversible change, but substitute for ΔE the general

case expressed in the First Principle of Thermodynamics:

$$\Delta A = \Delta E - T\Delta S = (q - w) - T\Delta S$$

Stipulating that only P dV work is possible, and that the system is maintained at constant volume, we reduce w to zero. Hence,

$$\Delta A = q - T\Delta S$$

For any observable change, $T\Delta S > q$. Therefore, for every observable change at constant temperature and volume, there is a decrease of the Helmholtz free energy. The criterion of a spontaneous change at constant T and V is thus

$$\Delta A < 0 \qquad (3.4)$$

At equilibrium, $T\Delta S = q$, and the criterion of equilibrium in a system at constant T and V is

$$\Delta A = 0 \qquad (3.5)$$

In the special circumstances indicated, spontaneous change always reduces the capacity of the system to do work, and equilibrium is reached only when that capacity has been reduced to a minimum. Here then, we have a function that can represent the changes and equilibria of chemical systems in much the way that the concept of mechanical potential energy represents change and equilibrium in purely mechanical systems. Consider a reaction of the following type: G + H = L + M. We construct the curve showing on one side the total value of A for the reactants G and H; on the other side, the total value of A for the products L and M; and in between, the values of A for the various mixtures of G, H, L, and M corresponding to different degrees of completion of the reaction. The equilibrium com- is that represented by x, where, in the trough of the curve, the equi-

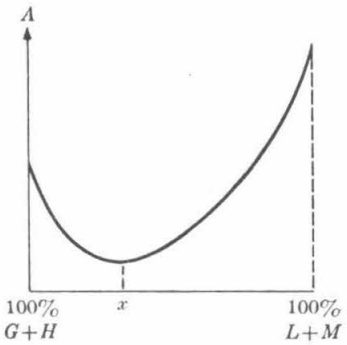

Fig. 3.1. Variation of free energy with composition of reaction mixture.

librium defined by the condition $\Delta A = 0$ is established where A assumes its minimum value. If the reaction proceeds at a finite rate in either direction, its progress from any initial condition to equilibrium is then a matter of "sliding down to the bottom."

Every system not at equilibrium is potentially capable of delivering work, but no system at equilibrium is capable of furnishing any work whatsoever. The maximum work output recoverable from the change represented above is given by the vertical drop -- that is, by $A_{initial} - A_{equil}$, and this same quantity of work is the minimum input required for the non-spontaneous change in which the initial state of the system is restored after it has reached equilibrium. In practice, of course, no change is ever strictly reversible, so that the maximum work is never recovered in any actual process. But since A is a function of state, the value $-\Delta A$ for a given change is always the same. Although the total energy of system and surroundings remains constant, every spontaneous change must result in a degradation of energy, an irrecoverable decrease in the amount of ("free") energy available to do work.

Substituting from equation (3.3) into (3.2),

$$W_{max} = -\Delta E + T\Delta S$$

we obtain the relation of the maximum work output to the decrease in internal energy. If ΔS is positive for the given change, the maximum work output is greater than the reduction in internal energy by the margin of $T\Delta S = q_{rev}$, where q_{rev} is heat absorbed by the system. Thus, in the reversible isothermal expansion of an ideal gas, there is no reduction in internal energy, and the work output is simply equal to the heat input. On the other hand, if ΔS is negative for the given change, the maximum work output is less than the reduction in internal energy by the margin of $T\Delta S = q_{rev}$, where q_{rev} is now heat released by the system. The heat so rejected corresponds to the heat rejected at exhaust temperature by a Carnot engine, and $T\Delta S$ is there the measure of the unavailable energy. Thus, for example, if an isothermal reaction at constant volume involves the formation of product molecules with structures having a degree of organized complexity greater than that of the reactant molecules, then that reaction has negative ΔS and, of any drop in internal energy, only the difference $(-\Delta E + T\Delta S)$ is extractable as useful work, i.e., recoverable "free energy."

Equilibrium criteria in terms of ΔA do not fully meet the requirements of calculations carried out under conditions of constant temperature and constant pressure. For these conditions, the essential criterial are better expressed in terms of the Gibbs free energy, F, defined by the equation

$$F = H - TS \qquad (3.6)$$

A development paralleling that which yielded equation (3.2) yields here, for a change at constant temperature,

$$\Delta F = \Delta H - T\Delta S \tag{3.7}$$

Assuming constant pressure, we can substitute for ΔH to give

$$\Delta F = \Delta E + p\Delta V - T\Delta S$$

whence, in view of equation (3.3), we can conclude that

$$-\Delta F = w_{max} - p\Delta V = w_{net} \tag{3.8}$$

Dismissing the work done against the atmosphere, the maximum "net work" obtainable from an isothermal change is then represented by $-\Delta F$. In any actual change, the net work recovered will be less than $-\Delta F$, but, since F is a function of state, $-\Delta F$ for a given change remains the same however much work is or is not recovered.

Let us now express in terms of F the criteria for direction of spontaneous reaction and position of equilibrium. At constant temperature and pressure,

$$\Delta F = \Delta E + p\Delta V - T\Delta S$$

Substituting from the First Principle of Thermodynamics for any change, reversible or irreversible,

$$\Delta F = (q - w) + p\Delta V - T\Delta S$$

When only $p\Delta V$ work is possible, the last equation reduces to

$$\Delta F = q - T\Delta S$$

It is now clear that the equilibrium criteria can be re-expressed in terms of F. The criterion of a spontaneous change at constant T and p is

$$\Delta F < 0 \tag{3.9}$$

The criterion of equilibrium in a system at constant T and p is

$$\Delta F = 0 \tag{3.10}$$

No system is at equilibrium if it can undergo a change that reduces its capacity to do work. Only when a minimum free energy has been attained (dF = 0) is the system at equilibrium.

Returning to equation (3.7), we see how the direction of the spontaneous chemical reaction is controlled. Clearly, loss of heat content ($-\Delta H$) and increase in entropy ($+\Delta S$) both tend to produce ($-\Delta F$) spontaneous reaction. Four possible situations are indicated in the table. At sufficiently low temperatures (minimizing the $T\Delta S$ term), exothermic reactions ($-\Delta H$) will be spontaneous ($-\Delta F$); at sufficiently high temperatures, the $T\Delta S$ term must become dominant. A complex compound formed from its elements in an exothermic reaction will be stable at low temperatures even though, since it is a comparatively

ΔH	ΔS	ΔF
-	+	- reaction always spontaneous
+	-	+ reaction never spontaneous
-	-	? direction depends on the conditions
+	+	? direction depends on the conditions

highly-ordered structure, the ΔS term is negative. But, assuming constant pressure, at high temperatures this compound, like complex compounds generally, will become unstable as the $T\Delta S$ term assumes control.

As in the case of E and H, only changes in F are thermodynamically significant, and for convenience, we may arbitrarily assign zero free energy to the elements in their standard states at 25°C. For these we say $F^0_{298} = 0$, and we can then calculate ΔF^0_f, the free en-

ergy of formation of one mole of any compound.

Equilibrium State and Equilibrium Constant

It is easily shown that, at constant temperature, the variation with pressure of the free energy of a mole of the substance j is given by the equation $d\tilde{F}_j = \tilde{V}_j dp_j$. If the substance is a perfect gas,

$$d\tilde{F}_j = RT \frac{dp_j}{p_j}$$

For integration, take the lower limit to be a pressure of one atmosphere, for which the gas has its standard free energy, F_j^0. As the upper limit, take the free energy F_j corresponding to any other pressure, p_j. Then

$$\int_{F_j^\circ}^{F_j} d\tilde{F}_j = RT \int_1^{p_j} \frac{dp_j}{p_j}$$

$$\tilde{F}_j - \tilde{F}_j^\circ = RT \ln p_j \qquad (3.11)$$

For any number of moles, n_j, of the ideal gas,

$$F_j = n_j \tilde{F}_j = n_j \tilde{F}_j^\circ + n_j RT \ln p_j$$

For the general case of a reaction involving ideal gases, we represent by n_j the number of moles of j consumed, and by n_k the number of moles of k formed. For the reaction, we have

$$\Delta F = \sum n_k \tilde{F}_k - \sum n_j \tilde{F}_j$$

For a reaction of the form $gG + hH + lL + mM$, we write

$$\Delta F = l\tilde{F}_L + m\tilde{F}_M - g\tilde{F}_G - h\tilde{F}_H$$

The free energy of a mixture of ideal gases is simply the sum of the

free energies of the component gases, each exerting its own partial pressure p_j. For ideal gases in a reaction mixture, we can then substitute as follows:

$$\Delta F = [l\tilde{F}_L^\circ + m\tilde{F}_M^\circ - g\tilde{F}_G^\circ - h\tilde{F}_N] + RT[l \ln p_L + m \ln p_M - g \ln p_G - h \ln p_N]$$

$$= \Delta F^\circ + RT \ln \left(\frac{p_L^{\,l}\, p_M^{\,m}}{p_G^{\,g}\, p_N^{\,h}} \right)$$

The pressure function has precisely the form of the equilibrium constant for the reaction. Now let us suppose that the reaction has proceeded to equilibrium. At this point $\Delta F = 0$, and the pressures of the gases will be such that the pressure function takes on the value of the equilibrium constant, with partial pressures expressed in atmospheres. Thus:

$$0 = \Delta F^\circ + RT \ln K_p \qquad \text{or} \qquad \ln K_p = -\frac{\Delta F^\circ}{RT}$$

This simple relation has so far been obtained only for the case of reactions involving strictly hypothetical ideal gases. In general we find that a relation of the form of equation (3.11) can be written for any substance j in terms of the "activity," a_j, of that substance. Thus,

$$\tilde{F}_j = \tilde{F}_j^\circ + RT \ln a_j \qquad (3.12)$$

We can now set out from equation (3.12), as formerly we did from (3.11), and obtain a general relation just like the above, except that the equilibrium constant, K_a, is now expressed in terms of activities. The activity of a substance is a function of its concentration; by dealing only with ideal gases, it is possible to overlook a complicated function of concentration which arises from strong molecular interactions. By

and large, however, with change in concentration, the activity will at least change in the same direction. Often we can, with no major loss of accuracy, replace activities by more familiar partial pressure and mole fraction terms.

Provided that we take care to select the appropriate terms and units, we find that for any reaction we can write

$$\Delta F = \Delta F^\circ + RT \ln Z \tag{3.13}$$

where Z is some concentration function having the form of the equilibrium constant for the reaction concerned. Then, for any reaction at equilibrium, one has

$$-\Delta F^\circ = RT \ln K \tag{3.14}$$

Temperature Dependence of the Equilibrium Constant

Although invariant at constant temperature, the equilibrium constant K does change with changing temperature. By equation (3.7)

$$\Delta F^\circ = \Delta H^\circ - T\Delta S^\circ$$

from which it is evident that ΔF^0 is a function of temperature. This being so, it follows necessarily that K is also a function of temperature. Combining the last equation with (3.14), we have

$$\ln K = \frac{-\Delta F^\circ}{RT} = \frac{-\Delta H^\circ + T\Delta S^\circ}{RT} = \frac{-\Delta H^\circ}{RT} + \frac{\Delta S^\circ}{R}$$

Suppose that we compare values of K over a temperature span in which ΔH^0 is constant. The constancy of ΔH^0 requires that ΔC_P be negligibly small. Under this condition, ΔS^0 must also be constant. We then write

$$\ln K_2 = -\frac{\Delta H^\circ}{RT_2} + \frac{\Delta S^\circ}{R} \; ; \; \ln K_1 = -\frac{\Delta H^\circ}{RT_1} + \frac{\Delta S^\circ}{R}$$

Subtracting the second equation from the first, it follows that

$$\ln\left(\frac{K_2}{K_1}\right) = -\frac{\Delta H^\circ}{R}\left(\frac{1}{T_2} - \frac{1}{T_1}\right) \tag{3.15}$$

This is van't Hoff's law, and it applies excellently to a great many systems.

Observe that deductions drawn from equation (3.15) are in agreement with Le Chatelier's principle. Consider that $T_2 > T_1$. For an endothermic reaction $\Delta H > 0$, $-\Delta H/R < 0$, the right side of the last equation is positive, and $K_2 > K_1$. That is, the rise of temperature favors the endothermic reaction, which has a greater equilibrium constant at the lower temperature. But beyond such qualitative predictions, (3.15) provides the means to calculate the change of equilibrium constant with temperature.

We can then no longer depend on equation (3.15) for our calculation of the change in equilibrium constant over great ranges of temperature. However, we can easily derive an equation on which we can rely even in these circumstances.

Observe that, of the terms appearing in equation (3.14), three vary with temperature: K, ΔF^0, and T itself. Differentiating with respect to T, we have then

$$-\frac{d}{dT}(\Delta F^\circ) = R \ln K + RT \frac{d}{dT} \ln K$$

But now we can substitute for $d\Delta F^0/dT$ from the Gibbs-Helmholtz relation, and so obtain

$$\frac{1}{T}(\Delta H^\circ - \Delta F^\circ) = R \ln K + RT \frac{d}{dT} \ln K$$

Substituting now for ΔF^0, again from equation (3.14), we find

$$\frac{1}{T}(\Delta H^\circ + RT \ln K) = R \ln K + RT \frac{d}{dT} \ln K$$

$$\frac{\Delta H^\circ}{T} + R \ln K = R \ln K + RT \frac{d}{dT} \ln K$$

so that, finally, we have

$$\frac{d}{dT} \ln K = \frac{\Delta H^\circ}{RT^2} \qquad (3.16)$$

When ΔH^0 is constant, this expression integrates to equation (3.15). When ΔH^0 varies, we may express it as a function of temperature and substitute that function in equation (3.16).

Given data on ΔS^0_{298} and ΔH^0_{298}, we can calculate ΔF^0_{298} for any reaction. We see now that, given such a value for ΔF^0_{298}, (3.14) permits us to calculate the equilibrium constant of the reaction at 25°C. We see further that -- given these data, the value of K, and data on the heat capacities of the materials concerned -- equation (3.15) or (3.16) will permit the calculation of the equilibrium constant at any temperature. Given purely thermal data, we can calculate the equilibrium constant of any reaction at any temperature.

Free Energy of Mixing

The internal energy change and the enthalpy change associated with the mixing of ideal gases at constant temperature and pressure are zero,

$$\Delta E_{mixing} = \Delta H_{mixing} = 0 \qquad (3.17)$$

so that the change in free energy due to mixing follows from the definitions for the free energies

$$\Delta F_{mixing} = \Delta A_{mixing} = -T\Delta S_{mixing} = RT\sum_i n_i \ln X_i \qquad (3.18)$$

where X_i represents the mole fraction of species i. Equation (3.18) gives the change in free energy when different gases (n_i moles of component i) are mixed at a given temperature and pressure.

Application of Equilibrium Criteria

Consider the general chemical reaction

$$\sum_1^n \nu_j' M_j \rightleftharpoons \sum_1^n \nu_j'' M_j \qquad (3.19)$$

where ν_j' and ν_j'' represent, respectively, the stoichiometric coefficients of reactants and products for the chemical species M_j, and n is now the total number of chemical species involved. Let

$$K_p = \prod^n (p_{j,e})^{\nu_j'' - \nu_j'} \qquad (3.20)$$

$$K_p' = \prod^n (p_j)^{\nu_j'' - \nu_j'} \qquad (3.21)$$

$$K_c = \prod^n (M_{j,e})^{\nu_j'' - \nu_j'} \qquad (3.22)$$

$$K_c' = \prod^n (M_j)^{\nu_j'' - \nu_j'} \qquad (3.23)$$

$$K_n = \prod^{n} (n_{j,e})^{\nu_j'' - \nu_j'} \tag{3.24}$$

$$K_n' = \prod^{n} (n_j)^{\nu_j'' - \nu_j'} \tag{3.25}$$

$$K_x = \prod^{n} (X_{j,e})^{\nu_j'' - \nu_j'} \tag{3.26}$$

$$K_x' = \prod^{n} (X_j)^{\nu_j'' - \nu_j'} \tag{3.27}$$

$$K_Y = \prod^{n} (Y_{j,e})^{\nu_j'' - \nu_j'} \tag{3.28}$$

and

$$K_Y' = \prod (Y_j)^{\nu_j'' - \nu_j'} \tag{3.29}$$

Here, $p_{j,e}$ = equilibrium partial pressure, p_j = actual partial pressure, $(M_{j,e})$ = equilibrium concentration, (M_j) = actual concentration, $n_{j,e}$ = equilibrium number of moles, n_j = actual number of moles, $X_{j,e}$ = equilibrium mole fraction, X_j = actual mole fraction, $Y_{j,e}$ = equilibrium weight fraction, Y_j = actual weight fraction of the chemical species identified by the symbol M_j. We shall refer to K_ν, K_c, K_n, K_X, and K_Y as equilibrium constants expressed in terms of ratios of pressures, concentrations, moles, mole fractions, and weight fractions, respectively; the primed quantities will be termed quotients.

The equilibrium constants and quotients defined in equations (3.20) to (3.29) are related. For ideal gases,

$$M_{j,e} = \frac{p_{j,e}}{RT} \tag{3.30}$$

$$n_{j,e} = \frac{V p_{j,e}}{RT} = \frac{p_{j,e}}{p_{T,e}} n_{T,e} \tag{3.31}$$

$$X_{j,e} = \frac{p_{j,e}}{p_{T,e}} = \frac{n_{j,e}}{n_{T,e}} \tag{3.32}$$

and

$$Y_{j,e} = \frac{W_j p_{j,e}}{\rho RT} \tag{3.33}$$

where V is the total volume of the system which is at the total pressure $p_{T,e}$ and contains $n_{T,e}$ moles of gas, W_j is the molecular weight of species j, and ρ represents the density of the gas mixture. Combining equations (3.30) to (3.33) with equations (3.20) to (3.29),

$$K_p = K_c (RT)^{\Delta n} = K_n \left(\frac{RT}{V}\right)^{\Delta n} = K_n \left(\frac{p_{T,e}}{n_{T,e}}\right)^{\Delta n}$$
$$= K_X (p_{T,e})^{\Delta n} = K_Y (\rho RT)^{\Delta n} \prod^{n} (W_j)^{\nu_j' - \nu_j''} \tag{3.34}$$

and

$$K_p' = K_c' (RT)^{\Delta n} = K_n' \left(\frac{RT}{V}\right)^{\Delta n} = K_n' \left(\frac{p_T}{n_T}\right)^{\Delta n}$$
$$= K_X' (p_T)^{\Delta n} = K_Y' (\rho RT)^{\Delta n} \prod^{n} (W_j)^{\nu_j' - \nu_j''} \tag{3.34a}$$

where

$$\Delta n = \sum_1^n (\nu_j'' - \nu_j')$$

A most useful relation is obtained by relating the standard (Gibbs) free-energy change to the equilibrium constants. For ideal gases,

$$\Delta F = \sum_1^n (\nu_j'' - \nu_j') F_{Mj}$$

$$= \sum_1^n (\nu_j'' - \nu_j') F_{Mj}^0 + RT \sum_1^n \ln (p_j)^{\nu_j'' - \nu_j'} \tag{3.35}$$

The difference between the standard free energies of products and reactants will be denoted by the symbol ΔF^0, i.e.,

$$\Delta F^0 = \sum_1^n (\nu_j'' - \nu_j') F_{Mj}^{(0)} \tag{3.36}$$

from which equation (3.35) can be written

$$\Delta F - \Delta F^0 = RT \ln K_p' \tag{3.37}$$

For thermodynamic equilibrium at fixed pressure and temperature, $K_p' = K_p$ and $\Delta F = 0$. Hence

$$\Delta F^0 = -RT \ln K_p \tag{3.38}$$

Equation (3.38) shows the relation between the standard free energy change (i.e., the free energy change at 1 atm) and the equilibrium constant at an arbitrary pressure and temperature. The practical importance of the equilibrium constant K_p is the result of the fact that it is independent of total pressure and can therefore be listed as a unique function of temperature.

Equilibrium constants with respect to the elements in their standard states[1]

T, °K	$K_{p,1}$	$K_{p,2}$	$K_{p,3}$	$K_{p,4}$	$K_{p,5}$
298.16	4.8978×10^{-41}	2.4831×10^{-36}	2.8340×10^{-7}	1.1143×10^{40}	1.9187×10^{-60}
300	9.0157×10^{-41}	4.2560×10^{-36}	3.1311×10^{-7}	6.1235×10^{39}	4.6559×10^{-60}
400	5.5335×10^{-30}	1.3459×10^{-26}	2.1419×10^{-5}	1.7418×10^{29}	1.8323×10^{-44}
500	1.7140×10^{-23}	6.9984×10^{-21}	2.6984×10^{-4}	7.6913×10^{22}	4.3351×10^{-35}
600	3.7239×10^{-19}	4.6452×10^{-17}	1.4555×10^{-3}	4.2954×10^{18}	7.8886×10^{-29}
700	4.7315×10^{-16}	2.5351×10^{-14}	4.8362×10^{-3}	3.8282×10^{15}	2.3768×10^{-24}
800	1.0162×10^{-13}	2.9040×10^{-12}	1.1869×10^{-2}	1.9454×10^{13}	5.4828×10^{-21}
900	6.6681×10^{-12}	1.1700×10^{-10}	2.3757×10^{-2}	3.1405×10^{11}	2.2856×10^{-18}
1000	1.9055×10^{-10}	2.2693×10^{-9}	4.1295×10^{-2}	1.1482×10^{10}	2.8708×10^{-16}
1100	2.9703×10^{-9}	2.5852×10^{-8}	6.4834×10^{-2}	7.6015×10^{8}	1.5066×10^{-14}
1200	2.9390×10^{-8}	1.9715×10^{-7}	9.4287×10^{-2}	7.8759×10^{7}	4.0926×10^{-13}
1300	2.0469×10^{-7}	1.1052×10^{-6}	1.2900×10^{-1}	1.1497×10^{7}	6.7143×10^{-12}
1400	1.0824×10^{-6}	4.8596×10^{-6}	1.6899×10^{-1}	2.2060×10^{6}	7.4131×10^{-11}
1500	4.5973×10^{-6}	1.7575×10^{-5}	2.1324×10^{-1}	5.2541×10^{5}	5.9402×10^{-10}
1600	1.6315×10^{-5}	5.4300×10^{-5}	2.6104×10^{-1}	1.4955×10^{5}	3.6787×10^{-9}
1700	4.9911×10^{-5}	1.4710×10^{-4}	3.1180×10^{-1}	4.9204×10^{4}	1.8420×10^{-8}
1800	1.3493×10^{-4}	3.5752×10^{-4}	3.6495×10^{-1}	1.8302×10^{4}	7.7215×10^{-8}
1900	3.2885×10^{-4}	7.9232×10^{-4}	4.2004×10^{-1}	7.5422×10^{3}	2.7861×10^{-7}
2000	7.3350×10^{-4}	1.6233×10^{-3}	4.7664×10^{-1}	3.3931×10^{3}	8.8491×10^{-7}
2100	1.5174×10^{-3}	3.1110×10^{-3}	5.3394×10^{-1}	1.6458×10^{3}	2.5194×10^{-6}
2200	2.9383×10^{-3}	5.6247×10^{-3}	5.9208×10^{-1}	8.5212×10^{2}	6.5283×10^{-6}
2300	5.3753×10^{-3}	9.6627×10^{-3}	6.5041×10^{-1}	4.6677×10^{2}	1.5585×10^{-5}
2400	9.3821×10^{-3}	1.5874×10^{-2}	7.0871×10^{-1}	2.6847×10^{2}	3.4610×10^{-5}
2500	1.5574×10^{-2}	2.5090×10^{-2}	7.6648×10^{-1}	1.6127×10^{2}	7.2161×10^{-5}
2750	4.7424×10^{-2}	6.8250×10^{-2}	9.0910×10^{-1}	5.3272×10^{1}	3.5917×10^{-4}
3000	1.2010×10^{-1}	1.5762×10^{-1}	1.0478	2.0999×10^{1}	1.3515×10^{-3}
3250	2.6381×10^{-1}	3.2048×10^{-1}	1.1788	9.5786	4.2678×10^{-3}
3500	5.1807×10^{-1}	5.8993×10^{-1}	1.3046	4.9295	1.1311×10^{-2}
3750	9.3022×10^{-1}	1.0000	1.4218	2.7498	2.6363×10^{-2}
4000	1.5528	1.5933	1.5315	1.6623	5.5361×10^{-2}
4250	2.4416	2.4010	1.6351	1.0568	1.0668×10^{-1}
4500	3.6521	3.4602	1.7322	7.0307×10^{-1}	1.9134×10^{-1}
4750	5.2349	4.8029	1.8229	4.9181×10^{-1}	3.2321×10^{-1}
5000	7.2395	6.4506	1.9067	3.5465×10^{-1}	5.1874×10^{-1}

[1] By permission, from NBS Circular 500, *Selected Values of Chemical Thermodynamic Properties*, 1 February 1952. The equilibrium constants are defined as follows: $K_{p,1} = p_O/p_{O_2}^{\frac{1}{2}}$, $K_{p,2} = p_H/p_{H_2}^{\frac{1}{2}}$, $K_{p,3} = p_{OH}/p_{O_2}^{\frac{1}{2}} p_{H_2}^{\frac{1}{2}}$, $K_{p,4} = p_{H_2O}/p_{H_2} \cdot p_{O_2}^{\frac{1}{2}}$, $K_{p,5} = p_N/p_{N_2}^{\frac{1}{2}}$. The partial pressures are those of the (ideal) gas, unless the contrary is indicated explicitly.

Equilibrium constants with respect to the elements in their standard states[1]

T, °K	$K_{f,6}$	$K_{p,7}$	$K_{p,8}$	$K_{p,9}$	$K_{p,10}$
298.16	6.5013×10^{-16}	3.1470×10^{-1}	1.2677×10^{-118}	1.0169×10^{24}	1.2331×10^{69}
300	8.1283×10^{-16}	3.1605×10^{-1}	7.4989×10^{-118}	8.4723×10^{23}	4.6559×10^{68}
400	6.9823×10^{-12}	3.7766×10^{-1}	1.4723×10^{-86}	1.3397×10^{19}	3.4356×10^{51}
500	1.6055×10^{-9}	4.1534×10^{-1}	9.2683×10^{-68}	1.7865×10^{16}	1.8113×10^{41}
600	6.0353×10^{-8}	4.4035×10^{-1}	3.2509×10^{-55}	2.1677×10^{14}	2.5177×10^{34}
700	8.0612×10^{-7}	4.5709×10^{-1}	2.9992×10^{-46}	9.2257×10^{12}	3.1842×10^{29}
800	5.6234×10^{-6}	4.6979×10^{-1}	1.5959×10^{-39}	8.5507×10^{11}	6.7143×10^{25}
900	2.5486×10^{-5}	4.7962×10^{-1}	2.7227×10^{-34}	1.3366×10^{11}	9.2470×10^{22}
1000	8.5487×10^{-5}	4.8742×10^{-1}	4.1687×10^{-30}	3.0061×10^{10}	4.7534×10^{20}
1100	2.3020×10^{-4}	4.9363×10^{-1}	1.1092×10^{-26}	8.8004×10^{9}	6.3387×10^{18}
1200	5.2590×10^{-4}	4.9785×10^{-1}	7.9068×10^{-24}	3.1499×10^{9}	1.7378×10^{17}
1300	1.0554×10^{-3}		2.0464×10^{-21}	1.3110×10^{9}	8.2414×10^{15}
1400	1.9178×10^{-3}		2.3988×10^{-19}	6.1660×10^{8}	6.0534×10^{14}
1500	3.2255×10^{-3}		1.4825×10^{-17}	3.1945×10^{8}	6.2951×10^{13}
1600	5.0781×10^{-3}		5.4828×10^{-16}	1.7960×10^{8}	8.6896×10^{12}
1700	7.5770×10^{-3}		1.3183×10^{-14}	1.0708×10^{8}	1.5031×10^{12}
1800	1.0817×10^{-2}		2.2803×10^{-13}	6.7422×10^{7}	3.1623×10^{11}
1900	1.4873×10^{-2}		2.7861×10^{-12}	4.4586×10^{7}	7.8524×10^{10}
2000	1.9815×10^{-2}		2.7102×10^{-11}	3.0641×10^{7}	2.2387×10^{10}
2100	2.5674×10^{-2}		2.1238×10^{-10}	2.1827×10^{7}	7.2028×10^{9}
2200	3.2516×10^{-2}		1.3671×10^{-9}	1.5389×10^{7}	2.5498×10^{9}
2300	4.0346×10^{-2}		7.5266×10^{-9}	1.1943×10^{7}	9.9426×10^{8}
2400	4.9125×10^{-2}		3.5818×10^{-8}	9.1348×10^{6}	4.1850×10^{8}
2500	5.8878×10^{-2}		1.5108×10^{-7}	7.1532×10^{6}	1.8915×10^{8}
2750	8.7466×10^{-2}		3.4380×10^{-6}	4.5426×10^{6}	3.3083×10^{7}
3000	1.2148×10^{-1}		4.6366×10^{-5}	2.6182×10^{6}	7.7108×10^{6}
3250	1.6040×10^{-1}		4.1812×10^{-4}	1.7527×10^{6}	2.2527×10^{6}
3500	2.0334×10^{-1}		2.7454×10^{-3}	1.1844×10^{6}	7.8109×10^{5}
3750	2.4939×10^{-1}		1.3948×10^{-2}	9.1496×10^{5}	3.1275×10^{5}
4000	2.9793×10^{-1}		5.7663×10^{-2}	6.9375×10^{5}	1.3880×10^{5}
4250	3.4839×10^{-1}				
4500	4.0085×10^{-1}				
4750	4.5188×10^{-1}				
5000	5.0405×10^{-1}				

[1] By permission, from NBS Circular 500, *Selected Values of Chemical Thermodynamic Properties*, 1 February 1952. The equilibrium constants are defined as follows: $K_{p,6} = p_{NO}/p_{N_2}p_{O_2}^{\frac{1}{2}}$, $\mathcal{K}_{p,7} = K_{p,7} = p_{C\,(c,\,diamond)}/p_{C\,(c,\,graphite)}$, $K_{p,8} = p_{C(g)}$ and $\mathcal{K}_{p,8} = p_{C(g)}/p_{C\,(c,\,graphite)}$, $\mathcal{K}_{f,9} = p_{CO}/p_{O_2}^{\frac{1}{2}}$ and $\mathcal{K}_{p,9} = p_{CO}/p_{C\,(c,\,graphite)}\,p_{O_2}^{\frac{1}{2}}$, $K_{p,10} = p_{CO_2}/p_{O_2}$, $\mathcal{K}_{p,10} = p_{CO_2}/p_{C\,(c,\,graphite)}\,p_{O_2}$.

Equilibrium constants with respect to the elements in their standard states[1]

T, °K	$K_{p,11}$	$K_{p,12}$	$K_{p,14}$	$K_{p,15}$
298.16	7.9159×10^{8}	2.2439×10^{-37}	3.4277×10^{-19}	6.9343×10^{-15}
300	6.5826×10^{8}	3.9264×10^{-37}	4.6238×10^{-19}	8.8105×10^{-15}
400	3.0896×10^{5}	2.8774×10^{-27}	9.0991×10^{-14}	1.3970×10^{-10}
500	2.6749×10^{3}	2.3496×10^{-21}	1.4060×10^{-10}	4.7163×10^{-8}
600	9.9937×10^{1}	2.0184×10^{-17}	1.9151×10^{-8}	2.3030×10^{-6}
700	8.9578	1.2794×10^{-14}	6.4908×10^{-7}	3.7282×10^{-5}
800	1.4135	1.5922×10^{-12}	9.2003×10^{-6}	3.0227×10^{-4}
900	3.2501×10^{-1}	6.7608×10^{-11}	7.2812×10^{-5}	1.5453×10^{-3}
1000	9.8288×10^{-2}	1.3372×10^{-9}	3.8300×10^{-4}	5.7161×10^{-3}
1100	3.6771×10^{-2}	1.5283×10^{-8}	1.4949×10^{-3}	1.6719×10^{-2}
1200	1.6073×10^{-2}	1.1564×10^{-7}	4.6666×10^{-3}	4.0992×10^{-2}
1300	7.9177×10^{-3}	6.3738×10^{-7}	1.2249×10^{-2}	8.7740×10^{-2}
1400	4.3311×10^{-3}	2.7473×10^{-6}	2.8074×10^{-2}	1.6877×10^{-1}
1500	2.5586×10^{-3}	9.6962×10^{-6}	5.7717×10^{-2}	2.9813×10^{-1}

T, °K	$K_{p,16}$	$K_{p,18}$	$K_{p,19}$	$K_{p,20}$
298.16	2.5468×10^{-11}	4.8978×10^{16}	5.3629×10^{9}	2.9648×10^{1}
300	3.0620×10^{-11}	3.8994×10^{16}	3.4206×10^{9}	2.9174×10^{1}
400	5.9965×10^{-8}	3.6813×10^{12}	1.8923×10^{7}	1.7100×10^{1}
500	5.7332×10^{-6}	1.3964×10^{10}	8.2433×10^{5}	1.2050×10^{1}
600	1.2086×10^{-4}	3.3450×10^{8}	1.0044×10^{5}	9.4406
700	1.0725×10^{-3}	2.3073×10^{7}	2.2126×10^{4}	7.8524
800	5.5373×10^{-3}	3.0825×10^{6}	7.0746×10^{3}	6.7920
900	1.9911×10^{-2}	6.4062×10^{5}	2.8987×10^{3}	6.0534
1000	5.5578×10^{-2}	1.8159×10^{5}	1.4158×10^{3}	5.5208
1100	1.2897×10^{-1}	6.4670×10^{4}	7.8705×10^{2}	5.1050
1200	2.6062×10^{-1}	2.7296×10^{4}	4.8128×10^{2}	4.7863
1300	4.7315×10^{-1}	1.3131×10^{4}	3.1747×10^{2}	4.5186
1400	7.8977×10^{-1}	7.0146×10^{3}	2.2233×10^{2}	4.3152
1500	8.1111×10^{-1}	4.0654×10^{3}	1.6297×10^{2}	4.1400

[1] By permission, from NBS Circular 500, *Selected Values of Chemical Thermodynamic Properties*, 1 February 1952. The equilibrium constants are defined as follows: $K_{p,11} = p_{CH_4}/p_{H_2}^2$ and $\mathcal{K}_{p,11} = p_{CH_4}/p_{C\ (c,\ graphite)}\,p_{H_2}^2$, $K_{p,12} = p_{C_2H_2}/p_{H_2}$ and $\mathcal{K}_{p,12} = p_{C_2H_2}/p_{C\ (c,\ graphite)}{}^2 p_{H_2}$, $K_{p,14} = p_{Cl}/p_{Cl_2}^{\frac{1}{2}}$, $K_{p,15} = p_{Br}/p_{Br_2}^{\frac{1}{2}}$, $K_{p,16} = p_I/p_{I_2}^{\frac{1}{2}}$, $K_{p,18} = p_{HCl}/p_{H_2}^{\frac{1}{2}}p_{Cl_2}^{\frac{1}{2}}$, $K_{p,19} = p_{HBr}/p_{H_2}^{\frac{1}{2}}p_{Br_2}^{\frac{1}{2}}$, $K_{p,20} = p_{HI}/p_{H_2}^{\frac{1}{2}}p_{I_2}^{\frac{1}{2}}$.

T, °K	$K_{p,13}$	$K_{p,17}$
298.16	1.998×10^{-21}	3.590×10^{-48}
300	2.908×10^{-21}	6.980×10^{-48}
400	1.319×10^{-14}	3.512×10^{-36}
500	1.399×10^{-10}	3.719×10^{-29}
600	7.019×10^{-7}	1.789×10^{-24}
700	6.095×10^{-6}	4.078×10^{-21}
800	1.767×10^{-4}	1.343×10^{-18}
900	2.439×10^{-3}	1.227×10^{-16}
1000	2.023×10^{-2}	4.558×10^{-15}
1200	4.874×10^{-1}	1.054×10^{-12}
1400	4.812	5.118×10^{-11}
1600	2.690×10^{1}	9.528×10^{-10}
1800	1.034×10^{2}	9.312×10^{-9}
2000	3.055×10^{2}	5.794×10^{-8}
2500	2.177×10^{3}	1.638×10^{-6}
3000	8.055×10^{3}	1.427×10^{-5}
3500	2.084×10^{4}	6.947×10^{-5}
4000	4.245×10^{4}	2.290×10^{-4}
4500	7.424×10^{4}	5.804×10^{-4}
5000	1.155×10^{5}	1.225×10^{-3}

[1] From L. G. Cole, M. Farber and G. W. Elverum, Jr., *J. Chem. Phys.* **20**: 586 (1952). The equilibrium constants are defined as follows: $K_{p,13} = p_F{}^2/p_{F_2}$, $K_{p,17} = p_{H_2}{}^{\frac{1}{2}}\,p_{F_2}{}^{\frac{1}{2}}/p_{HF}$. Equilibrium constants involving the interhalogens ClF, BrF, IF, BrCl, ICl, and IBr are given by L. G. Cole and G. W. Elverum, Jr., *J. Chem. Phys.* **20**: 1543 (1952).

By using the definition of the Gibbs free energy, we obtain from equation (3.38) the equivalent relation

$$\Delta H^\circ - T\Delta S^\circ = -RT\ln K_p \tag{3.39}$$

where ΔH^0 and ΔS^0 represent, respectively, the enthalpy and entropy changes for reaction (3.19) at a pressure of 1 atm and any arbitrary but fixed temperature T. The quantities ΔH^0 are readily computed from the standard heats of formation and heat capacities. Entropy changes ΔS^0 and standard free-energy changes ΔF^0 may be computed similarly by utilizing tables of standard entropies and free energies.

As one example of the application of these thermodynamic relations, consider the calculation of standard enthalpy changes from the temperature dependence of K_p. Dividing equation (3.38) by T we obtain

$$\frac{\Delta F^\circ}{T} = -R\ln K_p \tag{3.40}$$

and since

$$F^\circ = H^\circ - TS^\circ$$

it follows that

$$\frac{d}{dT}\left(\frac{F^\circ}{T}\right) = -\frac{H^\circ}{T^2} + \frac{1}{T}\left(\frac{dH^\circ}{dT} - T\frac{dS^\circ}{dT}\right) \tag{3.41}$$

But from the general thermodynamic relation

$$dH = TdS + Vdp$$

it follows that

$$\frac{dH^\circ}{dT} = T\frac{dS^\circ}{dT}$$

since F^0, H^0, and S^0 all refer to (constant) unit pressure. Hence,

$$\frac{d}{dT}\left(\frac{F^\circ}{T}\right) = -\frac{H^\circ}{R} \tag{3.42}$$

For a chemical reaction represented by equation (3.19)

$$\frac{d}{dT}\sum_{1}^{n}(\nu_j'' - \nu_j')\frac{F^\circ_{Mj}}{T} = \frac{d}{dT}\left(\frac{\Delta F^\circ}{T}\right) = -R\frac{d}{dT}\ln K_p$$

$$= -\sum_{1}^{n}(\nu_j'' - \nu_j')\frac{H^\circ_{Mj}}{T^2} = -\frac{\Delta H^\circ}{T^2} \qquad (3.43)$$

or

$$\frac{d}{d\left(\frac{1}{T}\right)}\ln K_p = -\frac{\Delta H_0}{R} \qquad (3.44)$$

Equation (3.44) shows the relation between the temperature variation of K_p and the enthalpy change for reaction occurring at a pressure of 1 atm. Thus, ΔH^0 may be obtained experimentally at any temperature by measuring the temperature variation of K_p at constant pressure.

Another example more directly related to evaluation of chemical propellants is the calculation of equilibrium composition and partial pressures using equilibrium constants. Consider the following reaction involving only ideal gases:

$$a_1 A_1 + a_2 A_2 \rightleftharpoons b_1 B_1 + b_2 B_2 \qquad (3.45)$$

Let $n^0(A_1)$, $n^0(A_2)$, $n^0(B_1)$, and $n^0(B_2)$ represent, respectively, the initial number of moles of A_1, A_2, B_1, and B_2 before equilibrium has been reached at a given temperature T. When equilibrium is reached according to (3.45), the following numbers of moles for each component will be present:

$$n_e(A_1) = n^\circ(A_1) - a_1\xi$$

$$n_e(A_2) = n^\circ(A_2) - a_2\xi$$

$$n_e(B_1) = n^\circ(B_1) + b_1\xi$$

$$n_e(B_2) = n^\circ(B_2) + b_2\xi$$

since for every $b_1\xi$ moles of B_1 formed, $b_2\xi$ moles of B_2 are formed, $a_1\xi$ moles of A_1 disappear, and $a_2\xi$ moles of A_2 disappear. From the definitions of K_n and K_p, it now follows that

$$K_n = \frac{(n^\circ(B_1)+b_1\xi)^{b_1}\,(n^\circ(B_2)+b_2\xi)^{b_2}}{(n^\circ(A_1)+a_1\xi)^{a_1}\,(n^\circ(A_2)+a_2\xi)^{a_2}} \qquad (3.46)$$

and

$$K_p = K_n\left(\frac{p_{Te}}{n_{T,e}}\right)^{b_1+b_2-a_1-a_2} \qquad (3.47)$$

where

$$n_{T,e} = n^\circ(A_1)+n^\circ(A_2)+n^\circ(B_1)+n^\circ(B_2)+\xi(b_1+b_2-a_1-a_2)$$

It is evident that for given values of K_n or K_p the value of ξ can be calculated readily for given initial concentrations of the various reactants.

Properties of Propellant Materials

Some representative chemicals which have been used or may be useful for the more important propulsion units are listed in the table on the following page.

Bipropellant mixtures consisting of a liquid oxidizer and a liquid reducing material are used extensively in rocket propulsion work. In general, satisfactory performance cannot be expected between any oxidizer listed in group (A) and any reducing compound listed in group (B). Practical utility depends on such factors as ease and speed of combustion, propellant density, toxicity, coolant charac-

A. Oxidizers in bipropellant systems: nitric acid (HNO_3), oxygen (O_2), ozone (O_3), fluorine (F_2), fluorine oxide (F_2O), nitrogen tetroxide (N_2O_4), chlorine trifluoride (ClF_3), hydrogen peroxide (H_2O_2), nitrogen trifluoride (NF_3), bromine pentafluoride (BrF_5).

B. Reducing materials in bipropellant systems: hydrogen (H_2), ammonia (NH_3), hydrazine (N_2H_4), hydrazine hydrate ($N_2H_4 \cdot H_2O$), diborane (B_2H_6), tetraborane (B_4H_{10}), pentaborane (B_5H_9), borazole ($B_3N_3H_6$), borimide [$B_2(NH_3)_3$], aluminium borohydride [$Al(BH_4)_3$], disiloxane [$(SiH_3)_2O$], disilane (Si_2H_6), trisilane (Si_3H_8), gasoline (C_5H_{12} to $C_{12}H_{26}$), kerosene (mixture of hydrocarbons with boiling points somewhat higher than gasoline), aniline ($C_6H_5NH_2$), methyl alcohol (CH_3OH), ethyl alcohol (C_2H_5OH), propyl alcohol (C_3H_7OH), acetylene (C_2H_2), ethylene (C_2H_4), methane (CH_4), other hydrocarbons, other alcohols [R—OH (R = an organic radical)], aldehydes ($R-\overset{H}{\overset{|}{C}}=O$), ketones ($R-\overset{\overset{O}{\|}}{C}-R'$).

C. Monopropellants: nitromethane (CH_3NO_2), dinitroethane [$C_2H_4(NO_2)_2$], hydrogen peroxide (H_2O_2), hydrazine (N_2H_4).

D. Gas-generating compounds: hydrazine (N_2H_4), hydrogen peroxide (H_2O_2).

E. Water-reactive chemicals: aluminum borohydride [$Al(BH_4)_3$], lithium (Li), sodium (Na), potassium (K), lithium hydride (LiH), sodium hydride (NaH), various alloys containing active metals.

F. Fuels for ramjets: any suitable liquid reducing compound, carbon (C), boron (B), carbon-metal mixtures.

G. Oxidizers in composite propellants: potassium perchlorate ($KClO_4$), ammonium nitrate (NH_4NO_3).

H. Fuels in composite propellants: polymers (i.e., high molecular weight compounds) containing mostly carbon and hydrogen.

J. Double-base propellants: homogeneous colloidal mixtures of roughly 50% nitrocellulose (containing in the neighborhood of 13% N) with roughly 50% nitroglycerin. In some double-base propellants the amount of nitroglycerin is reduced to about 20% and such substances as dinitrotoluene, potassium nitrate, etc., are added to act as stabilizers, plasticizers, flash suppressors, coloring or darkening agents, etc.

teristics, etc. It is noteworthy that the reducing and oxidizing compounds which have been chosen as liquid propellants generally yield combustion products of low molecular weight.

A propellant is useful as a monopropellant for rocket applications if it can be made to burn with the evolution of heat and the production of low molecular weight decomposition products. Gas-generating compounds must have similar properties, although it is generally desirable to have a maximum production of gases at relatively low temperatures.

Water-reactive chemicals are substances which react exothermically with water with the production of large volumes of gas. They are used in such devices as the hydroduct and hydropulse.

Ramjets, which do not carry their own supply of oxidizing agent, are best powered by the combustion products formed as the result of chemical reaction between a liquid reducing compound or a simple metal or nonmetal and atmospheric oxygen or nitrogen.

Composite propellants differ from double-base propellants by being more or less heterogeneous. Thus, they consist of a non-uniform mixture of oxidizing and reducing materials. Double-base propellants, on the other hand, consist of homogeneously compounded materials, the discontinuities in physical and chemical properties being of colloidal dimensions.

The more important characteristics of desirable propellant chemicals are summarized in the following table, page 93. The reasons for emphasizing the listed characteristics are, in some cases, closely related to the results obtained from a study of the thermodynamics of combustion. On the other hand, some of the desirable physical characteristics follow rather obviously from handling or cooling requirements in liquid-fuel rocket engines.

A detailed discussion of performance of selected bipropellant mixtures requires quantitative calculations on the thermodynamics of combustion. However, it is possible, even on the gasis of the qualitative remarks listed in the tables to draw some useful conclusions regarding performance. For example, the series of oxidizers

$$F_2,\ F_2O,\ NF_3,\ O_2,\ ClF_3,\ BrF_5$$

Desirable properties of propellants used in liquid-fuel rocket engines

(a) Small negative or preferably positive standard heats of formation of the propellants.

(b) The reaction products should have low molecular weights and large negative heats of formation. If conditions (a) and (b) are met, then the reaction products will consist of low molecular weight compounds at high temperatures.

(c) The propellants should have large densities in order to minimize the dead weight of storage tanks.

(d) The oxidizers and reducing agents are best handled as liquids. Hence it is desirable to obtain propellants which are normally liquid in the operating temperature range of service units (i.e., from about − 40 to + 60°C). For substances such as liquid oxygen and hydrogen special cooling units must be provided. This refrigeration equipment represents added dead weight, which the propulsion unit must carry, and is warranted only in the case of very high energy propellant mixtures.

(e) In normal propellant operation the combustion chamber temperatures may get excessively high. Hence it is necessary to provide special cooling equipment for the chamber walls. Cooling may be accomplished by forced convection involving passage of oxidizer and/or reducing agent through coils enveloping the chamber. In extreme cases, this cooling technique is inadequate and it is necessary to resort to sweat cooling, which is accomplished by passing a small amount of one or both of the propellants through small passages in the chamber wall, thus using the heat of vaporization, as well as the specific heat of the oxidizer and/or reducing agent, in order to cool the chamber wall. It is apparent that successful cooling can be accomplished the more readily the higher the specific heat and the heat of vaporization of the material involved. Hence it is customary to choose, if possible, at least one of the components of a bipropellant system with a high specific heat and/or large heat of vaporization.

(f) Since it may be necessary to store the propellants for long periods of time before use, good propellants should have high storage stability, i.e., they must not decompose or change chemically in any way during storage so that their use as a propellant is impaired.

(g) Since propellants are chemicals which have to be handled by service personnel, it may be desirable for some applications to use propellants of relatively low toxicity. Actually the art of propellant design has advanced at the present time to the point where practically every useful bipropellant component is toxic or represents a handling hazard for other reasons. As the result of this development, it has become important to educate service personnel on the proper handling of dangerous chemicals.

(h) For large-scale use it is, of course, imperative that propellants which are readily available and preferably also of low cost are employed. In practice this last requirement is inessential since experience has shown that rare and expensive chemicals, which are needed in large quantities, usually become cheap and readily available in the course of time.

(i) The bipropellant mixture in a liquid-fuel rocket should be spontaneously combustible with minimum time lag. Spontaneously combustible propellants are said to be hypergolic whereas non-spontaneously combustible propellants are said to be nonhypergolic. The time lag or ignition delay is the period of time preceding steady-state combustion. It is measured empirically and is a function of physical factors such as injection methods, motor configuration, etc., as well as of the chemical constitution of the propellant mixture. Long ignition delays may lead to the accumulation of large amounts of propellant in the combustion chamber before vigorous exothermic reaction occurs and initiates steady-state combustion. The accumulation of excessive amounts of propellant, before steady-state combustion, is usually accompanied by severe initial shock and very high initial pressures, which may lead to rupture of the combustion chamber.

(j) The reaction products should not be excessively corrosive or form solid deposits, thereby leading either to increased or decreased nozzle throat diameters. In the former case, steady-state combustion may cease altogether or else occur at such low pressures as to impair overall performance. Nozzle plugging, on the other hand, may lead to an excessive increase in chamber pressure followed by rupture of the combustion chamber.

(k) For application to guided missiles, the exhaust gases should not interfere with the guidance method which is used.

is listed in order of decreasing performance with a given reducing substance containing predominantly hydrogen. The performance differences are readily explained in terms of variation of the term $T_c / \bar{M}$ (T_c = combustion chamber temperature, $\bar{M}$ = average molecular weight of combustion products) which is of primary importance in determining the specific impulse.

For convenience in performance calculations, the physical properties as well as enthalpy, entropy, and heat capacity of transition, of selected chemical compounds are summarized in the following tables.

Substance	Process	Pressure, mm of Hg	Temperature, °K	ΔH, kcal/mole	ΔS, cal/mole-°K	ΔCp, cal/mole-°K
Br_2	$c \rightarrow l$	760	265.9	2.52	9.48	0.9
	$l \rightarrow g$	214	298.16	7.34	24.6	
C	$c \rightarrow g$	760	4620			
CH_4	$c \rightarrow l$	87.7	90.68	0.225	2.48	
	$l \rightarrow g$	760	111.67	1.955	17.51	
C_2H_2 (ethyne, acetylene)	$c \rightarrow l$	900	191.7	0.9	5	
	$l \rightarrow g$	900	191.7	4.2	22	
	$l \rightarrow g$	760	189.2	5.1	27	
C_2H_4 (ethene, ethylene)	$c \rightarrow l$	0.9	103.97	0.8008	7.702	
	$l \rightarrow g$	760	169.45	3.237	19.10	
C_2H_6 (ethane)	$c \rightarrow l$	0.006	89.89	0.6829	7.597	2.2
	$l \rightarrow g$	760	184.53	3.517	19.06	−11.5
CHF_3 (trifluoromethane)	$c \rightarrow l$		113			
	$l \rightarrow g$	760	189.0	4.4	2.3	
CH_5N (methylamine)	$c \rightarrow l$		179.70	1.466	8.16	
	$l \rightarrow g$	760	266.84	6.17	23.1	
C_2H_7N (dimethylamine)	$c \rightarrow l$		180.97	1.420	7.85	9.81
	$l \rightarrow g$	760	280.0	6.33	22.6	17.1
$C_2H_8N_2$ (2-dimethyl hydrazine)	$l \rightarrow g$	760	354			
CH_2O (formaldehyde)	$c \rightarrow l$		154.9			
	$l \rightarrow g$	760	253.9	5.85	23.0	
CH_4O (methanol)	$c, I \rightarrow l$		175.26	0.757	4.32	4.2
	$l \rightarrow g$	760	337.9	8.43	24.95	
CH_4O_2 (methyl hydrogen peroxide)	$l \rightarrow g$	34	298	7.9	26.5	

[1] By permission, from NBS Circular 500, *Selected Values of Chemical Thermodynamic Properties*, 1 February 1952.

Substance	Process	Pressure, mm of Hg	Temperature, °K	ΔH, kcal/mole	ΔS, cal/mole-°K	ΔCp, cal/mole-°K
C_2H_4O (ethylene oxide)	$c \rightarrow l$	760	160.71	1.236	7.69	3.45
	$l \rightarrow g$		283.72	6.101	21.50	−9.7
C_2H_6O (dimethylether)	$c \rightarrow l$		131.66	1.180	8.96	6.8
	$l \rightarrow g$		248.34	5.141	20.70	−10.6
C_2H_5OH (ethanol)	$c \rightarrow l$		158.6	1.200	7.57	5.70
	$l \rightarrow g$	760	351.7	9.22	26.22	
CH_4ON_2 (urea)	$c \rightarrow l$		405.8	3.60	8.9	
CH_3O_2N (nitromethane)	$c \rightarrow l$		244.78	2.319	9.47	
	$l \rightarrow g$	760	374.0			
CH_3O_2N (methyl nitrite)	$l \rightarrow g$	760	255	5.0	19.7	
CH_3O_3N (methyl nitrate)	$l \rightarrow g$	760	339.7	7.8	23.0	
$C_2H_5O_2N$ (nitroethane)	$c \rightarrow l$		183			
	$l \rightarrow g$	17	293	9.1	31	
$C_2H_5O_2N$ (ethyl nitrite)	$l \rightarrow g$	760	290.1	6.64	22.9	
$C_2H_5O_3N$ (ethyl nitrate)	$c \rightarrow l$		171			
	$l \rightarrow g$	760	361.9			
$C_2H_4O_6N_2$ (glycol dinitrate)	$c \rightarrow l$		250.9	4.5	18	
	$l \rightarrow g$	19	378			
$C(NO_2)_4$ (tetranitro-methane)	$c \rightarrow l$		286			
	$l \rightarrow g$	760	398.9	9.2	23	
CO	$l \rightarrow g$	760	81.67	1.444	17.68	
CO_2	$l \rightarrow g$	760	194.68	6.031	30.98	
Cl_2	$c \rightarrow l$		172.18	1.531	8.892	2.75
	$l \rightarrow g$	760	239.11	4.878	20.4	−8.76
ClF	$l \rightarrow g$	760	172.9	5.34	30.88	
Cl_2O_7	$l \rightarrow g$	760	354.7	7.88	22.2	
F_2	$c \rightarrow l$		55.20	0.372	6.74	1.86
	$l \rightarrow g$	760	85.24	1.51	17.7	−4.27
F_2O	$l \rightarrow g$	760	128.3	2.65	20.7	
H_2	$c \rightarrow l$	54.0	13.96	0.028	2.0	1.9
	$l \rightarrow g$	760	20.39	0.216	10.6	
HBr	$c \rightarrow l$		186.30	0.5751	3.087	1.64
	$l \rightarrow g$	760	206.44	4.210	20.39	−7.37
HCl	$c, I \rightarrow l$		158.97	0.4760	2.994	2.10
	$l \rightarrow g$	760	188.13	3.86	20.5	−7.14
HCN	$l \rightarrow g$	760	298.86	6.027	20.17	
HF	$c \rightarrow l$		190.09	1.094	15.756	2.55
	$l \rightarrow g$	760	293.1	1.8	6.1	−10.9
HI	$c \rightarrow l$					
	$c \rightarrow g$	0.31	298.16	14.88	49.91	
	$c \rightarrow l$		222.37	0.6863	3.086	1.10
HNO_3	$c \rightarrow l$		231.57	2.503	10.808	10.55
	$l \rightarrow g$	48	293	9.43	32.17	
H_2O	$c \rightarrow l$	760	273.16	1.4363	5.2581	8.911
	$l \rightarrow g$	4.58	273.16	10.767	39.416	−10.184
	$l \rightarrow g$	23.75	298.16	10.514	35.263	−9.971
	$l \rightarrow g$	760	373.16	9.717	26.040	−10.021

Substance	Process	Pressure, mm of Hg	Temperature, °K	$\triangle H$, kcal/mole	$\triangle S$, cal/mole-°K	$\triangle Cp$, cal/mole-°K
H_2O_2	$c \rightarrow l$		271.2	2.52	9.29	
	$l \rightarrow g$	2.1	298.16	13.01	43.64	
I_2	$c \rightarrow l$		386.8	3.74	9.67	
IF_7	$c \rightarrow l$	760	276.6	7.37	26.64	
N_2	$c, I \rightarrow l$	94	63.15	0.172	2.709	
	$l \rightarrow g$	760	77.36	1.333	17.231	
NH_3	$c \rightarrow l$	45.57	195.42	1.351	6.9133	
	$l \rightarrow g$	760	239.76	5.581	23.277	
N_2H_4	$c \rightarrow l$		274.7			
	$l \rightarrow g$	764	386.7	10	25.9	
NH_4N_3	$c \rightarrow g$	760	407	15.1	37.11	
NH_4NO_3	$c, V \rightarrow c, IV$	760	255	0.13	0.511	
	$c, IV \rightarrow c, III$	760	305.3	0.38	1.23	
	$c, III \rightarrow c, II$	6.32×10^5	336.5	0.20	0.594	
	$c, II \rightarrow c, I$	760	398.4	1.01	2.535	
	$c, I \rightarrow l$	760	442.8	1.3	12.94	
$N_2H_4 \cdot HNO_3$	$c \rightarrow l$		316			
$N_2H_4 NO_3$	$c, I \rightarrow l$		343.9			
$N_2H_4 \cdot H_2O$	$c \rightarrow l$		233			
	$l \rightarrow g$		118.5	391.7		
NH_2OH	$c \rightarrow l$		306.3			
	$l \rightarrow g$	22	331			
NO	$c \rightarrow l$	164.4	109.55	0.5495	5.016	6.0
	$l \rightarrow g$	760	121.42	3.292	27.113	11.8
N_2O	$c \rightarrow l$	658.9	182.34	1.563	8.5719	4.67
	$l \rightarrow g$	760	184.68	3.956	21.421	
N_2O_3	$c \rightarrow l$		162			
	$l \rightarrow g$	760	275	9.4	34.2	
N_2O_4	$c \rightarrow l$	139.78	261.96	3.502	13.368	6.12
	$l \rightarrow g$	760	294.31	9.110	30.954	
N_2O_5	$c \rightarrow g$	760	305.6	13.6	44.50	
NO_2F	$c \rightarrow l$		107.2			
	$l \rightarrow g$	760	200.8	4.31	21.46	
NO_3F	$c \rightarrow l$		92			
	$l \rightarrow g$	103	193			
O_2	$c, I \rightarrow l$	1.1	54.39	0.1063	1.95	1.74
	$l \rightarrow g$	760	90.19	1.6299	18.07	−6.00
O_3	$l \rightarrow g$	760	162.65	2.59	15.92	

Performance Evaluation of Chemical Propellants

For frozen chemical composition, the nozzle efflux velocity v_e may be calculated from the relation

$$\frac{1}{2} \bar{M} v_e^2 = \Delta H_c^e \tag{3.48}$$

where $\bar{M}$ represents the constant molecular weight of the gas mixture and ΔH_c^e is the molar enthalpy change between nozzle entrance and nozzle exit positions and is independent of pressure for ideal gases. If the relative concentrations of each component, as well as the numerical values of T_c and T_e, are known, then it is a simple matter to evaluate both $\bar{M}$ and ΔH_c^e. The composition of each constituent can be calculated by straightforward analysis.

The average molecular weight of a gas mixture of n components is given by the relation

$$\bar{M} = \sum_1^n X_j M_j \tag{3.49}$$

where X_j represents the mole fraction of the j^{th} component whose molecular weight is M_j. The value of ΔH_c^e for frozen chemical composition is evidently given by the relation

$$\Delta H_c^e = \sum_1^n X_j \left(H_j(T_c) - H_j(T_e) \right) \tag{3.50}$$

or

$$\Delta H_c^e = \sum_1^n X_j \int_{T_e}^{T_c} C_{p,j} \, dT \tag{3.51}$$

where $H_j(T)$ represents the molar enthalpy of component j at the temperature T, and $C_{p,j}$ represents the corresponding molar heat

capacity. Note that X_j remains constant during frozen chemical flow. Equation (3. 50) follows immediately from the expression for the enthalpy of an ideal gas mixture.

For adiabatic expansion of one mole of an ideal gas mixture doing only pressure - volume work, it follows from the First Law of Thermodynamics that

$$d\tilde{E} + p\,d\tilde{V} = 0 \tag{3.52}$$

But

$$\tilde{E} = \sum X_j \tilde{E}_j$$

whence

$$d\tilde{E} = \sum X_j\, d\tilde{E}_j = \sum X_j C_{v,j}\, dT \tag{3.53}$$

since X_j is constant for flow without composition change. The equation of state for one mole of ideal gas mixture is

$$p\tilde{V} = \sum X_j RT \; ; \quad \sum X_j = 1$$

whence

$$p\,d\tilde{V} = R\,dT \sum X_j - \tilde{V}\,dT = (R\,dT - RT\,d\ln p)\sum X_j \tag{3.54}$$

Introducing equations (3. 53) and (3. 54) into (3. 52), we obtain the relation

$$\sum X_j (C_{v,j} + R)\,dT = RT\,d\ln p \tag{3.55}$$

Integration between the limits T_e and T_c leads to the result

$$\frac{1}{R} \sum \chi_j \int_{T_o}^{T_c} C_{p,j} \, d\ln T = \ln\left(\frac{p_c}{p_e}\right) \qquad (3.56)$$

where the pressure ratio p_c/p_e is assumed specified. Molar heat capacities for selected chemical compounds at various temperatures are tabulated below.

Molar heat capacities C_p (cal/mole-°K)[1]

T, °K	$O_2(g)$	$H_2(g)$	$N_2(g)$	$O(g)$	$H(g)$	$N(g)$	$C(c$, graphite)	$C(c$, diamond)
298.16	7.017	6.892	6.960	5.2364	4.9680	4.9680	2.066	1.449
300	7.019	6.895	6.961	5.2338	4.9680	4.9680	2.083	1.466
400	7.194	6.974	6.991	5.1341	4.9680	4.9680	2.851	2.38
500	7.429	6.993	7.070	5.0802	4.9680	4.9680	3.496	3.14
600	7.670	7.008	7.197	5.0486	4.9680	4.9680	4.03	3.79
700	7.885	7.035	7.351	5.0284	4.9680	4.9680	4.43	4.29
800	8.064	7.078	7.512	5.0150	4.9680	4.9680	4.75	4.66
900	8.212	7.139	7.671	5.0055	4.9680	4.9680	4.98	4.90
1000	8.335	7.217	7.816	4.9988	4.9680	4.9680	5.14	5.03
1100	8.449	7.308	7.947	4.9936	4.9680	4.9680	5.27	5.10
1200	8.530	7.404	8.063	4.9894	4.9680	4.9680	5.42	5.16
1300	8.608	7.505	8.165	4.9864	4.9680	4.9680	5.57	
1400	8.676	7.610	8.253	4.9838	4.9680	4.9680	5.67	
1500	8.739	7.713	8.330	4.9819	4.9680	4.9680	5.76	
1600	8.801	7.814	8.399	4.9805	4.9680	4.9680	5.83	
1700	8.859	7.911	8.459	4.9792	4.9680	4.9681	5.90	
1800	8.917	8.004	8.512	4.9784	4.9680	4.9683	5.95	
1900	8.974	8.092	8.560	4.9778	4.9680	4.9685	6.00	
2000	9.030	8.175	8.602	4.9776	4.9680	4.9690	6.05	
2100	9.085	8.254	8.640	4.9778	4.9680	4.9697	6.10	
2200	9.140	8.328	8.674	4.9784	4.9680	4.9708	6.14	
2300	9.195	8.398	8.705	4.9796	4.9680	4.9724	6.18	
2400	9.249	8.464	8.733	4.9812	4.9680	4.9746	6.22	
2500	9.302	8.526	8.759	4.9834	4.9680	4.9777	6.26	
2750	9.431	8.667	8.815	4.9917	4.9680	4.9900	6.34	
3000	9.552	8.791	8.861	5.0041	4.9680	5.0108	6.42	
3250	9.663	8.899	8.900	5.0207	4.9680	5.0426	6.50	
3500	9.763	8.993	8.934	5.0411	4.9680	5.0866	6.57	
3750	9.853	9.076	8.963	5.0649	4.9680	5.1437	6.64	
4000	9.933	9.151	8.989	5.0914	4.9680	5.2143	6.72	
4250	10.003	9.220	9.013	5.1199	4.9680	5.2977		
4500	10.063	9.282	9.035	5.1495	4.9680	5.3927		
4750	10.115	9.338	9.056	5.1799	4.9680	5.4977		
5000	10.157	9.389	9.076	5.2102	4.9680	5.6109		

[1] By permission, from NBS, *Tables of Selected Values of Chemical Thermodynamic Properties*, Series III, Volume I, March 1947 to June 1949.

Molar heat capacities C_p (cal/mole-°K)[1]

T, °K	C(g)	CO(g)	NO(g)	OH(g)	$H_2O(g)$	$CO_2(g)$	$CH_4(g)$	$C_2H_2(g)$
298.16	4.9803	6.965	7.137	7.141	8.025	8.874	8.536	10.499
300	4.9801	6.965	7.134	7.139	8.026	8.894	8.552	10.532
400	4.9747	7.013	7.162	7.074	8.185	9.871	9.736	11.973
500	4.9723	7.120	7.289	7.048	8.415	10.662	11.133	12.967
600	4.9709	7.276	7.468	7.053	8.677	11.311	12.546	13.728
700	4.9701	7.451	7.657	7.087	8.959	11.849	13.88	14.366
800	4.9697	7.624	7.833	7.150	9.254	12.300	15.10	14.933
900	4.9693	7.787	7.990	7.234	9.559	12.678	16.21	15.449
1000	4.9691	7.932	8.126	7.333	9.861	12.995	17.21	15.922
1100	4.9691	8.058	8.243	7.440	10.145	13.26	18.09	16.353
1200	4.9697	8.167	8.342	7.551	10.413	13.49	18.88	16.744
1300	4.9705	8.265	8.426	7.663	10.668	13.68	19.57	17.099
1400	4.9725	8.349	8.498	7.772	10.909	13.85	20.18	17.418
1500	4.9747	8.419	8.560	7.875	11.134	13.99	20.71	17.704
1600	4.9783	8.481	8.614	7.973	11.34	14.1		
1700	7.9835	8.536	8.660	8.066	11.53	14.2		
1800	4.9899	8.585	8.702	8.152	11.71	14.3		
1900	4.9980	8.627	8.738	8.233	11.87	14.4		
2000	5.0075	8.665	8.771	8.308	12.01	14.5		
2100	5.0189	8.699	8.801	8.378	12.14	14.6		
2200	5.0316	8.730	8.828	8.828	12.26	14.6		
2300	5.0455	8.758	8.852	8.504	12.37	14.7		
2400	5.0607	8.784	8.874	8.561	12.47	14.8		
2500	5.0769	8.806	8.895	8.614	12.56	14.8		
2750	5.1208	(8.856)	8.941	8.733	12.8	14.9		
3000	5.1677	8.898	8.981	8.838	12.9	15.0		
3250	5.2150	8.933	9.017	8.931	13.1	15.1		
3500	5.2610	8.963	9.049	9.015	13.2	15.2		
3750	5.3043	8.990	9.079	9.092	13.2	15.3		
4000	5.3442	9.015	9.107	9.162	13.3	15.3		
4250	5.3800	9.038	9.133	9.228	13.4	15.4		
4500	5.4115	9.059	9.158	9.290	13.4	15.5		
4750	5.6375	9.078	9.183	9.350	13.5	15.5		
5000	5.9351	9.096	9.208	9.406	13.5	15.6		

T, °K	$Cl_2(g)$	$Br_2(g)$	$I_2(g)$	Cl(g)	Br(g)	I(g)	HCl(g)	HBr(g)	HI(g)
298.16	8.11	8.60	8.81	5.2203	4.9680	4.9680	6.96	6.96	6.97
300	8.12	8.60	8.82	5.2237	4.9680	4.9680	6.96	6.96	6.97
400	8.44	8.77	8.90	5.3705	4.9683	4.9680	6.97	6.98	7.01
500	8.62	8.86	8.95	5.4363	4.9708	4.9680	7.00	7.04	7.11
600	8.74	8.91	8.98	5.4448	4.9793	4.9680	7.07	7.14	7.25
700	8.82	8.94	9.00	5.4232	4.9973	4.9680	7.17	7.27	7.42
800	8.88	8.97	9.02	5.3887	5.0258	4.9682	7.29	7.42	7.60
900	8.92	8.99	9.04	5.3506	5.0632	4.9688	7.42	7.58	7.77
1000	8.96	9.01	9.06	5.3133	5.1066	4.9700	7.56	7.72	7.92
1100	8.99	9.03	9.07	5.2788	5.1529	4.9726	7.69	7.86	8.06
1200	9.02	9.04	9.09	5.2477	5.1192	4.9770	7.81	7.99	8.18
1300	9.04	9.05	9.10	5.2201	5.2434	4.9836	7.93	8.10	8.29
1400	9.06	9.07	9.12	5.1958	5.2839	4.9925	8.04	8.20	8.38
1500	9.08	9.08	9.13	5.1745	5.3199	5.0039	8.14	8.30	8.46
1600				5.1557	5.3510	5.0178			
1700				5.1392	5.3771	5.0340			
1800				5.1246	5.3984	5.0521			
1900				5.1117	5.4152	5.0718			
2000				5.1002	5.4279	5.0928			
2100				5.0900	5.4369	5.1147			
2200				5.0809	5.4427	5.1371			
2300				5.0727	5.4458	5.1597			
2400				5.0654	5.4464	5.1822			
2500				5.0588	5.4450	5.2045			
2750				5.0449	5.4347	5.2571			
3000				5.0339	5.4178	5.3039			
3250				5.0251	5.3972	5.3437			
3500				5.0179	5.3748	5.3762			
3750				5.0120	5.3518	5.4016			
4000				5.0070	5.3292	5.4205			
4250				5.0028	5.3074	5.4337			
4500				4.9993	5.2867	5.4419			
4750				4.9964	5.2672	5.4458			
5000				4.9941	5.2490	5.4462			

Molar heat capacities C_p (cal/mole-°K)[1]

T, °K	$F_2(g)$	$F(g)$	$HF(g)$
100	6.957	5.068	6.961
200	7.097	5.403	6.959
298.16	7.487	5.436	6.960
300	7.495	5.435	6.960
400	7.895	5.361	6.961
500	8.200	5.282	6.973
600	8.420	5.220	6.987
700	8.581	5.171	7.015
800	8.702	5.134	7.063
900	8.796	5.108	7.129
1000	8.872	5.084	7.210
1100	8.934	5.067	7.304
1200	8.987	5.053	7.401
1300	9.033	5.042	7.503
1400	9.074	5.033	7.604
1500	9.111	5.025	7.703
1600	9.145	5.019	7.798
1700	9.177	5.014	7.886
1800	9.206	5.009	7.974
1900	9.230	5.005	8.054
2000	9.262	5.002	8.129
2100	9.287	4.999	8.199
2200	9.313	4.996	8.264
2300	9.337	4.994	8.326
2400	9.361	4.992	8.383
2500	9.384	4.990	8.436
2600	9.407	4.989	8.486
2700	9.426	4.987	8.532
2800	9.453	4.986	8.576
2900	9.474	4.985	8.617
3000	9.496	4.984	8.656
3200	9.539	4.982	8.727
3400	9.580	4.980	8.790
3600	9.622	4.979	8.847
3800	9.664	4.978	8.899
4000	9.705	4.977	8.946
4200	9.745	4.976	8.990
4400	9.786	4.975	9.028
4600	9.826	4.975	9.066
4800	9.866	4.974	9.102
5000	9.906	4.974	9.135

[1] From L. G. Cole, M. Farber, and G. W. Elverum, Jr., *J. Chem. Phys.* **20**: 586 (1952).

The left hand side of equation (3. 56) can be wrwritten in the form

$$\frac{1}{R}\sum X_j \left(S_j^{\circ}(T_c) - S_j^{\circ}(T_e)\right)$$

which is more suitable for numerical calculation. The corresponding entropy data are tabulated below.

Molar entropies (cal/mole-°K)[1]

T, °K	$O_2(g)$	$H_2(g)$	$N_2(g)$	$O(g)$	$H(g)$	$N(g)$	$C(c$, graphite)	$C(c$, diamond)
298.16	49.00	31.21	45.77	38.47	27.39	36.61	1.361	0.5829
300	49.05	31.25	45.81	38.50	27.42	36.65	1.374	0.5918
400	51.09	33.25	47.82	39.99	28.85	38.07	2.081	1.14
500	52.72	34.81	49.39	41.13	29.96	39.18	2.788	1.76
600	54.10	36.08	50.69	42.05	30.87	40.09	3.474	2.39
700	55.30	37.17	51.81	42.83	31.63	40.85	4.127	3.01
800	56.36	38.11	52.80	43.50	32.30	41.52	4.740	3.61
900	57.32	38.95	53.69	44.09	32.88	42.10	5.314	4.18
1000	58.19	39.70	54.51	44.62	33.40	42.63	5.846	4.70
1100	58.99	40.40	55.26	45.09	33.88	43.10	6.342	5.18
1200	59.73	41.04	55.95	45.53	34.31	43.53	6.807	5.63
1300	60.42	41.63	56.61	45.93	34.71	43.93	7.247	
1400	61.06	42.19	57.22	46.30	35.08	44.30	7.663	
1500	61.66	42.72	57.79	46.64	35.42	44.64	8.057	
1600	62.23	43.22	58.33	46.96	35.74	44.96	8.43	
1700	62.76	43.70	58.84	47.27	36.04	45.26	8.79	
1800	63.27	44.15	59.32	47.55	36.32	45.55	9.13	
1900	63.75	44.59	59.79	47.82	36.59	45.82	9.45	
2000	64.21	45.01	60.23	48.07	36.84	46.07	9.76	
2100	64.66	45.41	60.65	48.32	37.09	46.31	10.05	
2200	65.08	45.79	61.05	48.55	37.32	46.54	10.34	
2300	65.49	46.16	61.44	48.77	37.54	46.76	10.61	
2400	65.88	46.52	61.81	48.98	37.75	46.98	10.88	
2500	66.26	46.87	62.16	49.19	37.96	47.18	11.13	
2750	67.15	47.69	63.00	49.66	38.43	47.65	11.73	
3000	67.98	48.45	63.77	50.10	38.86	48.09	12.29	
3250	68.74	49.16	64.48	50.50	39.26	48.49	12.80	
3500	69.46	49.82	65.14	50.87	39.63	48.87	13.29	
3750	70.14	50.44	65.76	51.22	39.97	49.22	13.74	
4000	70.78	51.03	66.34	51.55	40.29	49.55	14.18	
4250	71.38	51.59	66.88	51.86	40.59	49.87		
4500	71.96	52.12	67.40	52.15	40.88	50.18		
4750	72.50	52.62	67.89	52.43	41.15	50.47		
5000	73.02	53.10	68.35	52.69	41.40	50.76		

[1] By permission, from NBS, *Tables of Selected Values of Chemical Thermodynamic Properties*, Series III, Volume I, March 1947 to June 1949.

For equilibrium flow, the gas efflux velocity may be calculated from

$$\frac{1}{2}\tilde{M}_c v_e^2 = \tilde{H}_c - \frac{\tilde{M}_c}{\tilde{M}_e}\tilde{H}_e \qquad (3.57)$$

where

Molar entropies (cal/mole-°K)[1]

T, °K	OH(*g*)	NO(*g*)	C(*g*)	CO(*g*)	$CO_2(g)$	$H_2O(g)$	$CH_4(g)$	$C_2H_2(g)$
298.16	43.89	50.34	37.76	47.30	51.06	45.11	44.50	48.00
300	43.93	50.38	37.79	47.34	51.12	45.15	44.55	48.06
400	45.98	52.44	39.22	49.35	53.82	47.49	47.17	51.30
500	47.55	54.05	40.33	50.93	56.11	49.34	49.48	54.09
600	48.84	55.39	41.24	52.24	58.11	50.90	51.64	56.53
700	49.93	56.56	42.01	53.37	59.90	52.27	53.68	58.69
800	50.88	57.59	42.67	54.38	61.51	53.49	55.61	60.65
900	51.72	58.52	43.26	55.29	62.98	54.60	57.45	62.44
1000	52.49	59.37	43.78	56.12	64.33	55.62	59.21	64.10
1100	53.19	60.15	44.25	56.88	65.58	56.56	60.89	65.64
1200	53.85	60.87	44.68	57.59	66.75	57.45	62.50	67.08
1300	54.46	61.54	45.08	58.24	67.84	58.29	64.04	68.43
1400	55.03	62.17	45.45	58.86	68.86	59.08	65.51	69.71
1500	55.57	62.76	45.79	59.44	69.82	59.83	66.93	70.93
1600	56.08	63.32	46.12	59.98	70.72	60.55		
1700	56.56	63.84	46.42	60.50	71.58	61.24		
1800	57.03	64.33	46.70	60.99	72.40	61.90		
1900	57.07	64.80	46.97	61.45	73.17	62.53		
2000	57.89	65.25	47.23	61.90	73.92	63.14		
2100	58.30	65.68	47.47	62.32	74.63	63.72		
2200	58.66	66.09	47.71	62.77	75.31	64.29		
2300	59.07	66.49	47.93	63.11	75.96	64.83		
2400	59.43	66.86	48.15	63.49	76.59	65.36		
2500	59.78	67.23	48.35	63.85	77.20	65.86		
2750	60.61	68.08	48.84	63.69	78.62	67.07		
3000	61.37	68.86	49.29	65.46	79.92	68.19		
3250	62.09	69.58	49.70	66.17	81.14	69.23		
3500	62.75	70.25	50.09	66.84	82.27	70.22		
3750	63.38	70.87	50.45	67.46	83.33	71.15		
4000	63.97	71.46	50.80	68.04	84.32	72.04		
4250	64.53	72.01	51.12	68.59	85.26	72.86		
4500	65.06	72.54	51.43	69.10	86.15	73.63		
4750	65.57	73.03	51.73	69.59	86.99	74.37		
5000	66.05	73.50	52.00	70.06	87.80	75.08		

T, °K	$Cl_2(g)$	$Br_2(g)$	$I_2(g)$	Cl(*g*)	Br(*g*)	I(*g*)	HCl(*g*)	HBr(*g*)	HI(*g*)
298.16	53.29	58.64	62.28	39.46	41.81	43.18	44.62	47.44	49.31
300	53.34	58.69	62.33	39.49	41.84	43.21	44.66	47.48	49.36
400	55.72	61.20	64.88	41.01	43.27	44.64	46.66	49.49	51.37
500	57.63	63.16	66.87	42.22	44.37	45.75	48.22	51.05	52.94
600	59.21	64.78	68.51	43.21	45.28	46.66	49.51	52.34	54.25
700	60.56	65.16	69.89	44.05	46.05	47.42	50.60	53.45	55.38
800	61.74	67.36	71.10	44.77	46.72	48.09	51.57	54.43	56.38
900	62.79	68.41	72.16	45.41	47.31	48.67	52.43	55.31	57.29
1000	63.74	69.34	73.12	45.97	47.84	49.20	53.22	56.12	58.11
1100	64.59	70.22	73.98	46.47	48.34	49.67	53.95	56.86	58.88
1200	65.38	71.01	74.77	46.93	48.79	50.10	54.62	57.55	59.58
1300	66.10	71.73	75.50	47.35	49.21	50.50	55.26	58.20	60.24
1400	66.77	72.40	76.17	47.74	49.60	50.87	55.85	58.80	60.86
1500	67.39	73.03	76.80	48.09	49.96	51.22	56.41	59.37	61.44
1600	68.03	73.45		48.43	50.31	51.54	56.81	59.88	
1700	68.58	74.00		48.74	50.63	51.84	57.31	60.39	
1800	69.10	74.52		49.03	50.94	52.13	57.79	60.87	
1900	69.59	75.01		49.31	51.23	52.41	58.24	61.34	
2000	70.06	75.48		49.57	51.51	52.67	58.67	61.78	
2100	70.51	75.93		49.82	51.77	52.92	59.09	62.20	
2200	70.94	76.36		50.06	52.03	53.15	59.49	62.61	
2300	71.35	76.77		50.28	52.27	53.38	59.87	63.00	
2400	71.74	77.16		50.50	52.50	53.60	60.24	63.37	
2500	72.12	77.54		50.70	52.72	53.82	60.60	63.73	
2750				51.18	53.24	54.31			
3000	73.82	79.23		51.62	53.71	54.77	62.20	65.37	
3250				52.03	54.15	55.20			
3500	75.27	80.64		52.40	54.55	55.60	63.58	66.77	
3750				52.74	54.92	55.97			
4000	76.52	81.89		53.07	55.26	56.32	64.77	67.99	
4250				53.37	55.58	56.65			
4500	77.63	83.00		53.66	55.89	56.96	65.84	69.08	
4750					56.17	57.25			
5000	78.63	84.00		54.18	56.44	57.53	66.80	70.06	

Molar entropies (cal/mole-°K)[1]

T, °K	$F_2(g)$	F(g)	HF(g)
100	40.76	32.13	33.97
200	45.60	35.76	38.75
298.16	48.51	37.93	41.53
300	48.55	37.97	41.57
400	50.76	39.52	43.57
500	52.56	40.71	45.13
600	54.08	41.66	46.40
700	55.39	42.46	47.48
800	56.27	43.15	48.42
900	57.57	43.76	49.25
1000	58.50	44.29	50.01
1100	59.35	44.78	50.70
1200	60.13	45.22	51.34
1300	60.85	45.62	51.94
1400	61.52	45.99	52.50
1500	62.15	46.34	52.93
1600	62.74	46.66	53.52
1700	63.30	46.97	54.00
1800	63.82	47.26	54.45
1900	64.32	47.53	54.89
2000	64.79	47.78	55.30
2100	65.25	48.03	55.68
2200	65.68	48.26	56.08
2300	66.09	48.48	56.45
2400	66.50	48.69	56.81
2500	66.87	48.90	57.15
2600	67.24	49.09	57.48
2700	67.60	49.28	57.80
2800	67.94	49.46	58.12
2900	68.27	49.64	58.42
3000	68.60	49.81	58.71
3200	69.21	50.13	59.27
3400	69.79	50.43	59.80
3600	70.34	50.71	60.31
3800	70.86	50.98	60.79
4000	71.36	51.24	61.24
4200	71.83	51.48	61.68
4400	72.28	51.73	62.10
4600	72.72	51.93	62.50
4800	73.14	52.15	62.89
5000	73.54	52.35	63.26

$$\tilde{M}_c = \sum_j \chi_j(T_c, P_c)\, M_j \qquad (3.58)$$

and

$$\tilde{M}_e = \sum_j \chi_j(T_e, P_e)\, M_j \qquad (3.59)$$

In order to perform numerical calculations, it is convenient to consider that H_c and H_e represent the absolute molar enthalpies of the gas mixture referred to $T^* = 298.16^\circ K$ as reference point. Thus

$$\tilde{H}_c = \sum_j \chi_j(T_c, P_c)\left(\Delta H f_j^\circ + H_j(T_c) - H_j(T^*)\right) \qquad (3.60)$$

and

$$\tilde{H}_e = \sum_j \chi_j(T_e, p_e)\left(\Delta H f_j^\circ + H_j(T_e) - H_j(T^*)\right) \quad (3.61)$$

The factor $\bar{M}_c/\bar{M}_e$ in equation (3.57) corrects the molar enthalpy at the nozzle exit position to the enthalpy for the same weight of gas mixture for which $\bar{H}_c$ has been computed.

Choosing $\bar{M}_c$ as the fixed weight for which the analysis is to be carried out, the condition of isentropic flow may be expressed by the relation

$$S(T_c, p_c) = \frac{\tilde{M}_c}{\tilde{M}_e} S(T_e, p_e) \quad (3.62)$$

Here, $S(T, p)$ is the molar entropy of an ideal gas mixture at temperature T and pressure p, and substituting for these entropy values

$$\sum_j \chi_j(p_c, T_c)\left(S_j^\circ(T_c) - R\ln p_c - R\ln \chi_j(T_c, p_c)\right)$$

$$\frac{\tilde{M}_c}{\tilde{M}_e}\sum_j \chi_j(p_e, T_e)\left(S_j^\circ(T_e) - R\ln p_e - R\ln \chi_j(T_e, p_e)\right) \quad (3.63)$$

Equation (3.63) can be used to calculate T_e for any given propellant system. It should be noted that the use of this equation requires numerical calculation of $X_m(T_e, p_e)$ for each assumed value of T_e. For this reason, performance calculations for equilibrium flow are more laborious to carry out than performance calculations for frozen flow.

4. SOLID PROPELLANT ROCKET MOTORS

The propellant of a solid rocket motor is stored entirely within the combustion chamber in the form of one or more shaped blocks, called grains. The main characteristic of a solid-propellant rocket is its simplicity. The burning time may be from a few seconds or fractions of a second to as long as one or two minutes.

Once the rocket has been ignited the combustion generally proceeds until all the propellant is burnt; the thrust program is fixed.

It is possible, with suitable grain designs, to obtain a thrust which increases (progressive burning), remains constant (neutral), or decreases (regressive) with burning time. With constant-geometry nozzles, the thrust is approximately proportional to the chamber pressure. The following figure represents a typical record of a near-constant thrust motor. The time integral of the thrust gives the total impulse I .

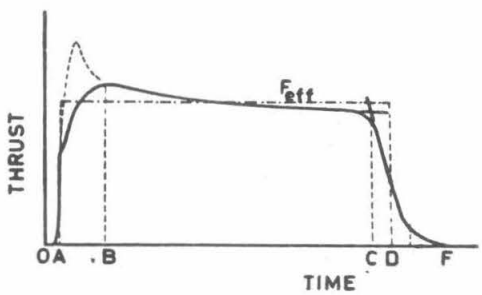

OA IGNITION DELAY
AB THRUST BUILD UP TIME
BC EQUILIBRIUM BURNING TIME
AD EFFECTIVE BURNING TIME ($F_D = 0.5 F_C$)

CF TAIL OFF TIME

$$\text{EFF. THRUST} = \frac{\int_o^{\prime} F\,dt}{AD}$$

Fig. 4. 1. Thrust law: typical recording of a near-constant thrust, together with some current definitions of durations and thrust values. The pressure-time diagram would be similar.

Combustion of Solid Propellants

The combustion of a solid propellant is a progressive phenomenon localized near the surface of the grain; the burning rate r is defined as the distance travelled per second by the flame front perpendicularly to the surface of the grain. The surfaces on which combustion must not take place are protected with an inhibiting material. Burning rates ranging from 0.01 to 10 in/sec, depending upon composition and pressure, are possible, but usual burning rates lie between 0.04 and 2 in/sec. An empirical relationship giving the burning rate r of a propellant as a function of the pressure p may be written

$$r = a + bp^n . \qquad (4.1)$$

For a given propellant, a and b are functions of the initial temperature of the grain and the exponent n is a constant. The constant a is usually of negligible importance. Then equation (4.1) is represented by a straight line in a logarithmic diagram. The burning rate of a composite propellant is shown in Fig. 4.2 as a function of pressure for several values of the initial temperature. The burning law written above is valid only within well specified ranges of pressure and temperature. For instance, below a certain pressure the combustion of a propellant becomes unstable and may stop completely. Even at normal operating pressures it is not always possible to represent the burning rate versus pressure relationship by a simple equation of the form given above. For instance, Fig. 4.3 represents the behavior of a plateau-burning composite propellant for which r is constant in a certain range of pressure. An even more complicated case is given in Fig. 4.4, which represents the burning rate versus pressure rela-

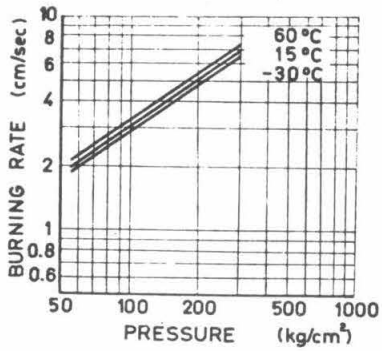

Fig. 4.2. Burning rate of a composite propellant as a function of pressure for several values of the initial temperature.

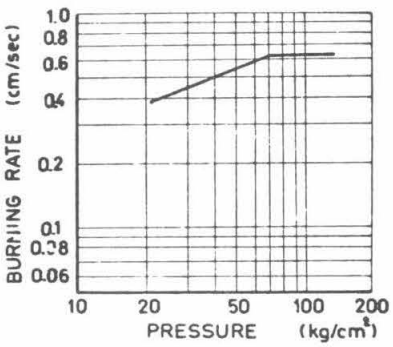

Fig. 4.3. Burning rate versus pressure relationship of a plateau-burning composite propellant at normal temperature.

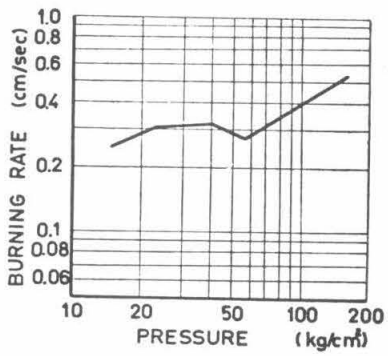

Fig. 4.4. Burning rate versus pressure relationship of a mesa-burning double-base propellant at normal temperature.

tionship of a mesa-burning double-base propellant.

As shown in Fig. 4. 2, if the initial temperature of the propellant decreases, the coefficient a diminishes together with the thrust and chamber pressure of the motor, but the burning time increases. The total impulse of the motor is only slightly smaller than at normal temperature.

If the initial temperature is too low, the chamber pressure may be too low to sustain smooth combustion, and intermittent burning, called chuffing, may occur. At high initial temperatures the total impulse rises somewhat, and the increase in chamber pressure may become important to the design of the chamber.

Figures 4. 5 and 4. 6 show the influence of the initial temperature upon the performance of solid-propellant motors. The thermal sensitivity of solid propellants limits the allowable range of exterior temperature.

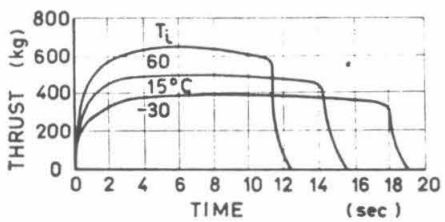

Fig. 4. 5. Influence of the initial temperature upon the thrust law of a solid-propellant motor.

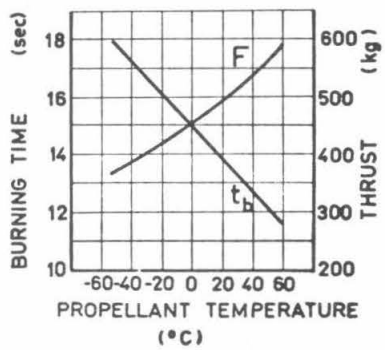

Fig. 4. 6. Influence of the initial temperature upon the performance of a solid-propellant motor.

Experimental data show that the burning rate r increases above its normal value with an increase in velocity of the combustion

gases parallel to the burning surface. Some data suggest that a threshold velocity exists below which the burning rate is unaffected by gas velocity. This phenomenon plays an important role in high performance designs, and is called erosive burning. It can be roughly represented by the empirical linear relation

$$r/r_o = 1 + k|V - V_{tv}|$$

where k is the erosion coefficient which is approximately constant and V the mean flow velocity parallel to the surface. The corrective term $k(V-V_{tv})$ is equal to zero for negative values of $(V-V_{tv})$. The values of k and V_{tv} depend upon pressure, propellant temperature, and the dimensions of the port area.

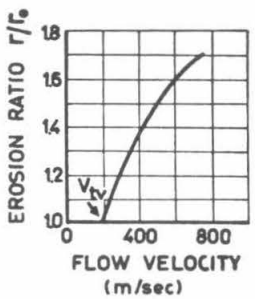

Fig. 4.7. Erosive burning: experimental relationship between the erosion ratio and the flow velocity.

Homogeneous Multi-Base Propellants

In a homogeneous propellant, both oxidant and fuel belong to the same molecule. Such propellants are often called double-base or colloidal propellants because they consist generally of colloidal mixtures of nitrocellulose and nitroglycerine.

Nitrocellulose (13.25% N_2) is a low-energy compound containing 21.25 gram-atoms of carbon, 25.96 g-at. of hydrogen, 36.63 g-at. of oxygen, and 9.46 g-at. of nitrogen per kg. It is underoxi-

dized by 301.8 g/kg. Nitroglycerine $C_3H_5(NO_3)_3$, which is a very high-energy explosive, is overoxidized by 35.2 g/kg.

The following table gives the composition and performance of the fairly energetic double-base Ballistite JPN. Its specific impulse and burning rate are high (I_s = 250 sec and r = 2.14 cm/sec at 100 kg/cm^2), but its combustion index n and thermal sensitivity τ are both poor, and its lower pressure limit for stable combustion is quite important (30 to 40 kg/cm^2). Owing to the elevated flame temperature, radiation plays an important role, bringing heat from the hot gases back to the grain. Carbon black is added in order to absorb radiant energy which otherwise would have heated the remaining translucent propellant. If the nitroglycerine content is lowered, the specific impulse decreases together with the burning rate and the flame temperature. For a propellant containing 32 percent of NG, 60 per cent of NC, and 8 per cent of additives, I_s = 228 sec, T_c = 2450°K, and r ranges from 0.5 to 1.2 cm/sec at 100 kg/cm^2 and 15°C.

Part B of the following table gives the composition and performance of the French S.D. whose nitroglycerine content is only 25 per cent.

The properties of double-base propellants are sometimes improved by adding to the nitrocellulose-nitroglycerine matrix a certain amount of finely-ground crystals of an inorganic oxidizer like potassium perchlorate or even an explosive compound. High explosives including trinitrotoluene and pentaerythritol tetranitrate can burn without detonation at rates comparable to those of propellants. Aluminum, magnesium, or other metallic powders can also be added.

A. Composition and Characteristics of JPN[3]

Composition	%
Nitrocellulose (13.25% N_2)	51.5
Nitroglycerine	43.0
Diethylphthalate	3.25
Potassium sulfate (flash-suppressing agent)	1.25
Ethyl centralite (*sym.*-diethyldiphenylurea)	1.0
Carbon black (added)	0.2
Wax (added)	0.08

Characteristics	
Burning rate	$r = 0.089p^{0.69} \exp [0.0038 (T_t - 15)]$ cm/sec
Density	$g_c \varrho_p = 1.62$ g/cm^3
Isobaric combustion temperature at 100 kg/cm^2	$T_c = 3125°K$
Molecular weight	$\mathfrak{M} = 26.4$
Specific heat ratio	$\gamma = 1.215$
Temperature of spontaneous ignition	300°K

B. Composition and Characteristics of the French S.D.[11]

Composition	%
Nitrocellulose	66
Nitroglycerine	25
Ethyl centralite	8
Miscellaneous	1

Characteristics	
Burning rate	$r = 0.0055p^{0.60} \exp [0.0032 (T_t - 20)]$ cm/sec
Density	$g_c \varrho_p = 1.59$ g/cm^3
Isobaric combustion temperature at 70 kg/cm^2	$T_c = 2170°K$
Molecular weight	$\mathfrak{M} = 22$
Specific heat ratio	$\gamma = 1.26$

Although the burning mechanism of double-base propellants has been studied in great detail, there does not exist a completely adequate quantitative theory.

During combustion, the solid is transformed into gas by pyrolysis and by chemical reactions. Even if the transformation occurs through the formation of an intermediate liquid phase, there exists a certain position, called the burning surface, where gas is being formed. The mechanism of the solid-phase decomposition is con-

sidered as the rate-controlling step of propellant burning, and the gas is being formed at a rate

$$\rho_p r = \rho_p B \exp\left(-\frac{E}{R_o T_s}\right) , \qquad (4.2)$$

where ρ_p is the density of the propellant, B the pre-exponential frequency factor, E the activation energy, R_o the universal gas constant and T_s the temperature of the gas at the burning surface.

With double-base propellants, the solid-phase processes, which take place in a very thin layer about 10^{-3} to 10^{-2} cm thick, are highly exothermic and are completed at a fairly low temperature in the neighborhood of 600°K if the burning rate is sufficiently slow. They include the thermal decomposition of nitroglycerine and nitrocellulose and the reactions between these substances and the stabilizers.

Figure 4.8 represents a model of the flame of a double-base propellant satisfactory from both the experimental and theoretical points of view. After the solid-phase decomposition has taken place, the gas-phase reactions can be divided into three layers: close to the burning surface, some exothermic reactions take place in the fizz zone; then, in the preparation or dark zone, activated products are

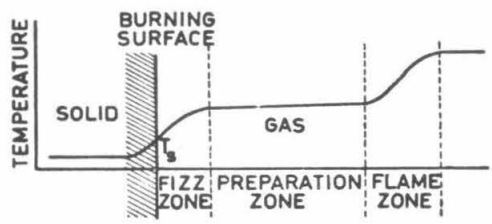

Fig. 4.8. Schematic model of the flame of a double-base propellant with the fizz, preparation, and flame zones.

formed without heat production; finally, when a sufficient concentration of activated products is achieved, the final reaction occurs in the flame zone at the end of which the isobaric combustion temperature is obtained.

The thickness of the zones diminishes when the pressure increases. At intermediate or low pressures, the thickness of the preparation zone is much greater than the thickness of the other zones and the heat transferred from the flame zone towards the surface can be neglected. Therefore, in that range of pressures, the burning rate and the surface temperature are determined mainly by the solid phase decomposition and by the heat evolved within the fizz zone. The pressure dependence of r is very complex and depends strongly upon composition and additives which may act as catalysts of the solid-phase and fizz-zone reactions.

At fairly high pressures, the dark zone almost disappears, and a significant amount of heat from the flame zone is conducted back to the burning surface. Therefore, the burning rate increases smoothly with pressure and, for a given pressure, the compositions having the highest combustion temperatures exhibit the highest burning rates.

At very low pressures, the thickness of the dark zone increases very rapidly. The flame-zone reactions become sluggish and may cease completely while the propellant still continues to react. When this happens, the chamber pressure drops to atmospheric but the temperature of the surface layers remains relatively high.

Composite Propellants

In a composite propellant, oxidizer and fuel are separate compounds intimately mixed together. The stoichiometric mixture ratio, which corresponds roughly to maximum combustion temperature and specific impulse, is always fairly small; it ranges between 0.5 and 0.05. Figure 4.9 represents the calculated combustion temperature, the molecular weight, the specific heat ratio, and the specific impulse as functions of oxidizer percentage of a typical ammonium perchlorate-polyester composition at the pressure of 70 kg/cm^2. When the oxidizer content increases towards stoichiometric, the combustion temperature

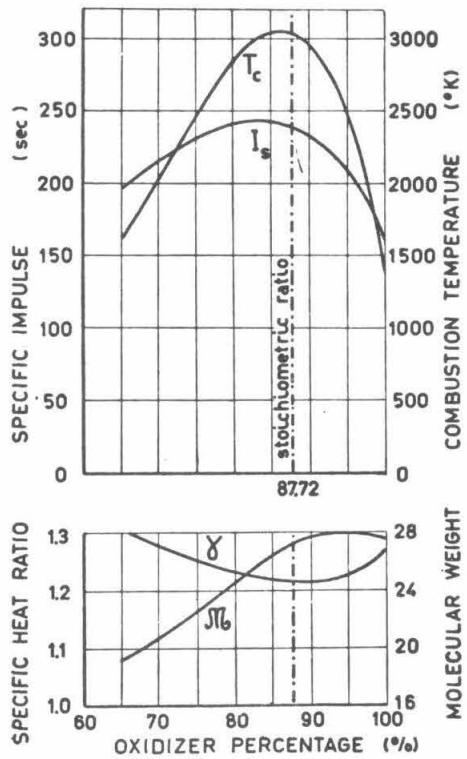

Fig. 4.9. Calculated isobaric combustion temperature, molecular weight, specific heat ratio, and specific impulse of a typical ammonium perchlorate-polyester composite propellant, as functions of the oxidizer percentage (p_c = 70 kg/cm^2).

rises sharply, but the increase in specific impulse is more gradual. The optimum values of T_c and I_s are on the fuel-rich side because of dissociation, the variation of molecular weight, and the specific heat ratio.

Actual compositions seldom contain more than 80 per cent or 85 per cent of oxidizer because physical properties of the propellant are provided entirely by the fuel. Moreover, the susceptibility to detonation of some propellants increases with the oxidizer content.

The number of available solid oxidizers is fairly limited. They are generally crystalline inorganic salts like potassium, sodium, lithium, or ammonium nitrates or perchlorates, but organic compounds like ammonium picrate $C_6H_2(NO_2)_3ONH_4$ are also used. In addition to high heat release and low molecular weight of the gaseous combustion products, the oxidizers must have a high available oxygen content corresponding to a fairly low stoichiometric ratio. The table below gives the molecular weight, the percentage of available oxygen, the heat of formation, the combustion products, and the density of various inorganic oxidizers.

Oxidizer	*Molecular weight*	*Available oxygen % of weight*	*Heat of formation kcal/mole*	*Products of complete combustion*	*Density g/cm³*
$LiClO_4$	106.397	60.152	—106.00*	LiCl	2.429
$NaClO_4$	122.454	52.265	— 92.18	NaCl	—
$KClO_4$	138.553	46.192	—103.6	KCl	2.52
NH_4ClO_4	117.497	34.043	— 69.42	N_2, HCl, H_2O	1.95
$LiNO_3$	68.948	58.015	—115.28	Li_2O	2.38
$NaNO_3$	89.005	47.056	—101.54	Na_2O	2.261
KNO_3	101.104	39.563	—117.76	K_2O	2.109
NH_4NO_3	80.048	19.988	— 87.27	N_2, H_2O	1.725

* Other values sometimes quoted are: —110.5 and, more recently, —91.8 kcal/mole.

Ammonium perchlorate forms the mainstay of today's high-energy composite propellants; with commonly used fuels, it gives specific impulses between 220 and 250 sec with low combustion indexes and low temperature sensitivities. The burning rate of that family of propellants ranges from 0.4 to 2 cm/sec and even more. In general, it increases with the oxidizer content, together with specific impulse and density, but for the same composition it can be adapted within fairly wide limits by the choice of oxidizer particle size and by adding suitable catalysts.

For instance, for the same composition (oxidizer 75%, fuel 25%), it is possible to increase the burning rate from 0.575 to 1.05 cm/sec by varying the particle mean diameter from coarse (150 μ) to fine (25 μ). However, very large particles may not burn completely in the chamber. Catalysts like manganese dioxide, ferric oxide, copper chromite, or many others (Cr_2O_3, SnO_2, TiO_2, ZnO) are also used for increasing r .

The following table gives the performance of two typical ammonium perchlorate and one ammonium nitrate composite propellants.

A wide variety of fuel-binders may be used ranging from asphalt to polymers like polysulfide, polyester, epoxy, synthetic rubbers, polyurethane, polyvinyl, polyacrylate, polyamide, polyethylene, polystyrene, polysiloxane, polybutadiene, polyisobutylene, and phenolic or cellulosic resins. Depending upon the fuel-binder, the physical properties of composite propellants can range from hard, tough, and brittle to soft and resilient. The nature of the fuel-binder has a strong influence upon the value of the stoichiometric mixture ratio.

CALCULATED CHARACTERISTICS OF METALLIZED COMPOSITE PROPELLANTS

Composition	*67.5% NH_4ClO_4 22.5% binder* 10% Al*	*63.75% NH_4ClO_4 21.25% binder 15% Al*	*72% NH_4ClO_4 18% binder 10% Al*	*68% NH_4ClO_4 17% binder 15% Al*	*67.5% NH_4ClO_4 22.5% binder 10% Mg*	*71.25% NH_4ClO_4 23.75% binder 5% B***
Isobaric combustion temperature T_c (°K)	3002	3221	3290	3519	2915	2481†
Molecular weight	20.21	18.954	21.813	20.905	20.823	22.508
Specific heat ratio	1.2665	1.2775	1.2500	1.2635	1.2615	1.2475
% of solid matter in the combustion products	18.9	27.85	18.85	27.9	16.6	0†
Specific impulse†† (sec)	248.3	253	252.6	254	243.4	241

* The fuel-binder is a polyester whose gross formula is $C_{23}H_{28}O_4$.

** This last formulation merely provides an indication of the energetic possibilities of boron; indeed powdered elemental boron cannot be expected to burn completely[37].

† At chamber temperature, B_2O_3 is gaseous: it condenses only within the nozzle.

†† The specific impulse takes into account the loss due to condensed matter in the flow . Indeed, available data suggest that Al_2O_3 is already condensed at chamber temperature[23]. With boron, condensation of B_2O_3 within the nozzle has been taken into account and equilibrium flow has been assumed in order to compute I_s.

Composition	*75% NH_4ClO_4 25% fuel and additives*	*80% NH_4ClO_4 20% fuel and additives*	*80% NH_4NO_3 20% fuel and additives*
Molecular weight	24	25.5	22
Specific heat ratio	1.24	1.22	1.26
Isobaric flame temperature T_c (°K)	2420	2790	1755
Characteristic velocity c^* (m/sec)	1396	1460	1219
Specific impulse I_s at 70 kg/cm^2 (sec)	224	236	195
Combustion index at 70 kg/cm^2	0.4	0.4	0.4
Burning rate at 70 kg/cm^2 (cm/sec)	0.5–1.5	0.8–2.0	0.2–0.3
Density (g/cm^3)	1.66	1.72	1.55
Current temperature sensitivity coefficient τ (°K^{-1})	0.0012–0.0024	0.0012–0.0024	0.0025

The fuel-binder does not have a strong influence upon the specific impulse of the propellant if the heat of formation is not too low. However, fuels containing a high hydrogen to carbon ratio, perhaps some nitrogen but little sulphur, must be favored in this respect, but they often have relatively low stoichiometric ratios.

The performance of composite propellants can be improved by adding high-energy metallic elements or compounds which give highly stable but condensed combustion products. In the simplest approach, powdered metals are added to the main composition. Taking into account the correction introduced by the presence of condensed matter in the exhaust, the gain in specific impulse may be as much as 10 or 15 seconds. The following table gives the calculated performance of an ammonium perchlorate - polyester formulation boosted with various percentages of aluminum, magnesium, and boron.

Our understanding of the burning mechanism of composite propellants is at best of conceptual significance. All proposed descriptions of the process make use of the same fundamental assumption as

is used for homogeneous propellants, i.e., that the regression rates of both fuel and oxidizer are governed by equation (4.2), which expresses the solid-phase decomposition rate as a function of the surface temperature T_s.

For the steady-state burning of a composite solid propellant, it is reasonable to assume that the mean linear rates of regression of the oxidizer and fuel surfaces are very roughly equal:

$$r_f \simeq r_o$$

or

$$B_f \exp\left(-\frac{E_f}{R_o T_{sf}}\right) \simeq B_o \exp\left(-\frac{E_o}{R_o T_{so}}\right) \quad . \tag{4.3}$$

In general, the pre-exponential factor and the activation energy of the fuel and of the oxidizer are not equal. It follows that T_{so} must be different from T_{sf}. That assumption constitutes the base of the "two-temperatures postulate" of the theory of composite propellant burning.

Because of the difference in pyrolysis rates (r versus T_s), one constituent gasifies relatively faster, and the slower-burning component is left protruding from the surface. The faster-pyrolizing constituent is then in contact with a cooler region of the flame than the slower-burning constituent.

In order to take advantage of this model, some assumptions must be made upon the process which controls the heat exchange between the flame and the surface. It appears that two different processes can be considered: the thermal decomposition of the oxidizer, and the diffusion flame.

The oxidizer thermal decomposition model has been satisfacto-

rily developed in the case of an ammonium nitrate propellant in which the pyrolysis rate of the oxidizer is the faster. Figure 4. 10 represents the pyrolysis rates of NH_4NO_3 and of a typical fuel as a function of surface temperature. It is assumed that the regression is completely governed by the heat exchange between the surface and the products of the decomposition of NH_4NO_3, acting as a monopropellant.

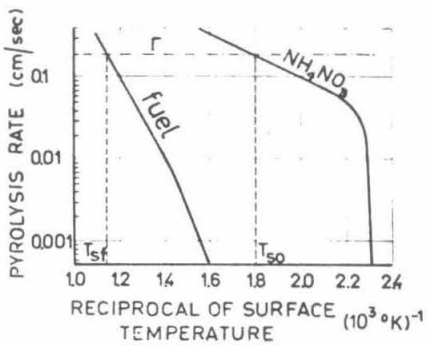

Fig. 4. 10. Pyrolysis rate of NH_4NO_3 and of a typical fuel, as a function of the reciprocal of the surface temperature.

At the outer boundary of the decomposition zone the temperature is 1250°K, corresponding to the combustion of NH_4NO_3 alone. If the surfaces of both fuel and oxidizer were in the same plane, their temperatures would be roughly equal. The regression rate of the oxidizer would be greater and the fuel would protrude into the higher temperature layers of the decomposition zone until both rates eventually became equal. This is a self-regulating process, and the mean burning rate of the propellant is equal to the regression rate of the oxidizer alone, since there are always enough oxidizer surfaces to carry on the flame propagation.

With potassium perchlorate propellants, flame pictures suggest that the oxidizer particles are protruding over the fuel matrix,

and a model has developed in which heat reaching the surface comes from the diffusion flamelets at the boundaries of the oxidizer and fuel vapor. A substantial elaboration of such a model is required to describe the propellant behavior. Summerfield has proposed such a model, in which, as the propellant is heated, fuel vapor pockets are expelled through the solid surface. This model further involves a finite chemical time and the effect of high turbulence level.

The situation is different with ammonium perchlorate propellants in which the decomposition of NH_4ClO_4 into N_2, O_2, HCl, and H_2O gives a temperature of about 1430°K, and the oxidizer thermal decomposition model may be considered.

If the oxidizer-decomposition model is taken for granted, the burning rate dependence on pressure can probably be explained, and the increase in burning rate due to a finer granulation or to the fuel nature can be viewed as the result of the interaction between the oxidizer and fuel pyrolysis.

Combustion Chamber Equilibrium

Inasmuch as the rate of propellant consumption depends upon the pressure in the chamber, it is apparent that some relation exists between the pressure, chamber volume, and rate of propellant consumption which is fundamental in determining the rocket thrust. Likewise, it is clear that the propellant consumption process may or may not be stable, depending upon the manner of dependence of burning rate upon chamber pressure. For example, if the rate of propellant consumption increases very rapidly with pressure, the increase in burn-

ing rate may cause the pressure in the chamber to rise so rapidly that the result is catastrophic. Therefore, not only must the equilibrium operating conditions be investigated for a solid propellant rocket of given characteristics, but also the stability of the operation.

The operation of a solid propellant rocket depends upon the gross conservation of mass in a manner which may be expressed as:

Mass of Propellant Consumed = Gas Stored in Chamber + Gas Ejected from the Nozzle .

Assuming the flow through the rocket nozzle to be given by the isentropic relations previously developed, each term of this relation may be expressed in analytic form. The gas ejected from the nozzle is given by

$$\text{Rate of Gas Discharge} = \Gamma' \frac{A_t p_c}{a_c} \tag{4.4}$$

where p_c is the pressure in the chamber and a_c depends only upon the propellant combustion temperature (i.e., the chamber temperature) and the gas properties. The rate of gas storage in the combustion chamber volume may be written

$$\text{Rate of Storage} = \frac{d}{dt} (\rho_c V_c) \tag{4.5}$$

where ρ_c and V_c are the instantaneous gas density and volume of the combustion chamber. It is important to note that the flow process is not steady because of the fact that the combustion chamber volume is changing throughout the rocket burning period. Finally, the rate of gas generation is

$$\text{Rate of Generation} = r A_c \rho_p \tag{4.6}$$

where r is the rate of propellant burning at the existing combustion chamber pressure, ρ_p is the density of the propellant, and A_c is the surface of the propellant which is accessible to combustion. The above equation may then be written simply in the form

$$rA_c\rho_p = \frac{d}{dt}(\rho_c V_c) + \frac{\Gamma' A_t p_c}{a_c} \quad . \tag{4.7}$$

Now it is known that under considerable variation of the combustion chamber pressure, the chamber temperature T_c is very nearly constant. In particular, this value does not vary according to the simple thermodynamic relations for constant volume. Hence, it will be assumed that RT_c = constant, so that the above relation may be written

$$rA_c(RT_c\rho_c) = \frac{d}{dt}(V_c RT_c \rho_c) + \frac{\Gamma' A_t p_c RT_c}{\sqrt{\gamma RT_c}} \quad . \tag{4.8}$$

For convenience, an effective "pressure" of the propellant may be defined according to the perfect gas law; that is

$$p_p = \rho_p RT_c \, . \tag{4.9}$$

This is a fictitious pressure which has no particular physical significance, but will serve as a notation. Then, using this pressure,

$$rA_c p_p = \frac{d}{dt}(V_c p_c) + \Gamma\sqrt{RT_c}\, A_t p_c \, , \tag{4.10}$$

where $\Gamma = 1/\sqrt{\gamma}\,\Gamma'$. Now because of variation of the volume V_c with time, it is necessary to relate the rate of change of combustion chamber volume to the rate of propellant consumption. If the volume of the combustion chamber at the start of burning is denoted by $V_c^{\,o}$, the volume at any later time may be expressed as the sum of the initial volume and the volume of propellant consumed during that time. If

the burning rate is r and the combustion surface is A_c, the rate of volume increase is simply rA_c so that the volume of the combustion chamber at any time t is

$$V_c = V_c^{\,o} + \int_0^t rA_c\,dt \tag{4.11}$$

where the time $t = 0$ has been chosen as that corresponding to the initiation of combustion. Using this relation, the derivative in equation (4.10) may be simplified to give

$$\frac{d}{dt}(V_c p_c) = V_c \frac{dp_c}{dt} + p_v \frac{dV_c}{dt} = V_c \frac{dp_c}{dt} + rA_c p_c . \tag{4.12}$$

Upon substitution into equation (4.9), and collecting terms

$$V_c \frac{dp_c}{dt} = rA_c(p_p - p_c) - \Gamma\sqrt{RT_c}\,A_t p_c . \tag{4.13}$$

This is clearly a differential equation for p_c, provided that the other principal variables, V_c, r, and T_c, can be expressed as functions of the chamber pressure and the time alone. The linear burning rate has been written previously as a function of the chamber pressure (equation 4.1), and consequently, the differential equation for the chamber pressure of the solid propellant rocket is

$$V_c \frac{dp_c}{dt} = ap_c^{\,n}(p_p - p_c)A_c - \Gamma\sqrt{RT_c}\,A_t p_c . \tag{4.14}$$

The combustion equilibrium will be achieved when the value of $dp_c/dt \approx 0$, that is, when the chamber pressure is nearly invariant with time. The term "nearly invariant" is used because there will always be some long period effects which prevent the pressure from being exactly constant. Among these are slow variation of the propellant grain temperature with time, heating of the combustion chamber itself

and consequent change in the radiation conditions, etc. However, for theoretical considerations, it will be quite sufficient to assume that combustion equilibrium is defined by $dp_c/dt = 0$. This implies that all transient phenomena and pressure perturbations have died out.

Inspection of the differential equation (4. 14) leads one to wonder whether any stable equilibrium exists. Because of the dependence of the burning rate upon the pressure, it appears possible that the burning rate will increase so rapidly with combustion chamber pressure that no equilibrium will be reached. Reasoning from equation (4. 14), this observation means that as p_c increases, the right hand side of the equation will be positive, indicating a positive value of dp_c/dt. Therefore, the chamber pressure will increase even further with time, indicating an unstable process. The stability of the calculated equilibrium operating condition will be investigated subsequently.

Denote by a superscript * the conditions for which equilibrium is reached, that is $dp_c/dt = 0$. Then, from equation (4. 14),

$$a p_c^{*n} A_c (p_p^* - p_c^*) = \Gamma \sqrt{R T_c^*}\, A_t p_c^* . \qquad (4.15)$$

The stability of this solution may be checked by studying the transient behavior of the chamber pressure in the neighborhood of this point. If the process is stable to small disturbances of the combustion chamber pressure, the assumption of an equilibrium operating point was correct. If the process is unstable, the assumption leads to a contradiction, and no equilibrium operating point exists.

Consider a disturbance in chamber pressure p_c' where $p_c'/p_c^* \ll 1$, so that the instantaneous chamber pressure is

$$p_c = p_c^* + p_c' \tag{4.16}$$

Inasmuch as the equilibrium pressure p_c^* does not depend upon the time, $dp_c/dt \equiv d/dt(p_c^* + p_c') = dp_c'/dt$. The value of T_c^*, and consequently the value of p_p^*, is unchanged by the pressure perturbation p_c' which has been imposed. Now because $p_c'/p_c^* \ll 1$, an approximation may be made in calculating the value of p_c^n which occurs in the linear burning rate. That is

$$p_c^n \equiv (p_c^* + p_c')^n = p_c^{*n}\left(1 + \frac{p_c'}{p_c^*}\right)^n \approx p_c^{*n}\left(1 + n\frac{p_c'}{p_c^*}\right). \tag{4.17}$$

Substituting these results into equation (4.14), it appears that

$$V_c \frac{dp_c'}{dt} \approx a p_c^{*n}\left(1 + n\frac{p_c'}{p_c^*}\right)(p_p^* - p_c^* - p_c')A_c - \Gamma\sqrt{RT_c^*}\,A_t(p_c^* + p_c'). \tag{4.18}$$

This equation may be simplified by noting that equation (4.15) gives a general relation among the variables in the equilibrium state. By subtracting equation (4.15) from (4.18) and neglecting second and higher order terms in p_c', it follows that

$$V_c \frac{dp_c'}{dt} \approx a p_c^{*n}\left[-1 + n\left(\frac{p_p^*}{p_c^*} - 1\right)\right]A_c p_c' - \Gamma\sqrt{RT_c^*}\,A_t p_c'. \tag{4.19}$$

Employing equation (4.15) again, it is seen that $\Gamma\sqrt{RT_c^*}\,A_t = a p_c^{*n-1}A_c(p_p^* - p_c^*)$, so that the differential equation for the pressure perturbation is just

$$V_c \frac{dp_c'}{dt} \approx a p_c^{*n} A_c\left[-1 + (n-1)\left(\frac{p_p^*}{p_c^*} - 1\right)\right]p_c'. \tag{4.20}$$

Now, inasmuch as $V_c > 0$ and certainly $a p_c^{*n} A_c > 0$, the sign of the

derivative depends entirely upon the signs of p_c' and $-1 + (n-1)\left\{p_p^*/p_c^* - 1\right\}$. In general, the value of the fictitious propellant pressure, p_p, is greatly in excess of the combustion chamber, its value being numerically of the order of 10^5 pounds per square inch because of its high density.

To investigate the stability of the combustion chamber flow process, consider a small pressure disturbance p_c' and, for convenience, consider $p_c' > 0$. Then, for stability

$$dp_c'/dt < 0 ,$$

for neutral stability

$$dp_c'/dt = 0 ,$$

and for instability

$$dp_c'/dt > 0 .$$

If the pressure disturbance is considered to be general so that it may be either positive or negative, the corresponding stability criteria are

$$\begin{aligned} &\text{Stable:} && 1/p_c'(dp_c'/dt) < 0 , \\ &\text{Neutral:} && 1/p_c'(dp_c'/dt) = 0 , \\ &\text{Unstable:} && 1/p_c'(dp_c'/dt) > 0 . \end{aligned} \qquad (4.21)$$

The sign of the pressure derivative, and hence the stability of the system, is completely determined by the quantity $-1 + (n-1)\left(\frac{p_p^*}{p_c^*} - 1\right) \equiv k$. Then we have

$$\begin{aligned} &\text{Stable:} && k < 0 , \\ &\text{Neutral:} && k = 0 , \\ &\text{Unstable:} && k > 0 . \end{aligned} \qquad (4.22)$$

This stability criterion is completely adequate, but is somewhat inconvenient to apply because it involves the combustion chamber equi-

librium conditions as well as the characteristic exponent of the propellant burning rate. Within the accuracy of approximation and, more important than that, within the accuracy that the theoretical criterion may be applied to the actual rocket, it may be said that $(p_p^*/p_c^* - 1) \approx p_p^*/p_c^*$. Furthermore, for any value of n significantly different from unity

$$|n-1| >> p_c^*/p_p^* .$$

Therefore, the stability parameter is approximately n-1, and the classification of stable chamber operation may be classified in terms of the characteristic exponent n alone:

Stable:	$n < 1$,	
Neutral:	$n = 1$,	(4.23)
Unstable:	$n > 1$.	

The equilibrium equation (4.15) holds only when $n<1$, since only under this condition does a stable equilibrium exist. Fortunately, the values of n for various solid propellants lie in the range $0.4<n<0.8$.

Before returning to the calculation of performance under the equilibrium conditions, it is of interest to estimate the time required for the decay of a pressure disturbance in the combustion chamber. To be practically useable, a chamber - nozzle configuration should be such that the pressure disturbances decay in a period of time which is short compared with the duration of rocket burning. To estimate the rate of decay of a pressure disturbance in the chamber, the differential equation (4.20) for the perturbation chamber pressure must be solved as a function of time. The approximation, discussed in the last paragraph, will be made that $(n-1)(p_p^*/p_c^*-1) >> 1$, so that the

right side of equation (4.20) becomes $-\Gamma\sqrt{RT_c^*}\,A_t(1-n)p_c'$. If, further, V_c^* denotes the combustion chamber volume at the onset of the disturbance, then the instantaneous chamber volume is

$$V_c = V_c^* + \int_0^t r A_c^* \, dt \tag{4.24}$$

where the zero of the time scale has now been moved to the time disturbance instigation. It will be assumed that the disturbance is sufficiently small that the burning rate r is unchanged over the period of interest. Therefore,

$$V_c \approx V_c^* + rA_c^* t . \tag{4.25}$$

With these approximations, the differential equation (4.20) becomes

$$(V_c^* + rA_c^* t)\frac{dp_c'}{dt} \approx -\Gamma\sqrt{RT_c^*}\,A_t(1-n)p_c' , \tag{4.26}$$

which may be easily solved by separation of variables. In fact,

$$\frac{dp_c'}{p_c'} = -\frac{(1-n)\Gamma\sqrt{RT_c^*}\,A_t}{rA_c^*}\,\frac{d(rA_c^* t)}{V_c^* + rA_c^* t} .$$

If at time $t = 0$ a pressure disturbance p_{c0}' is introduced into the combustion chamber, then the history of this pressure disturbance is given by the solution of the differential equation

$$p_c'/p_{c_o}' = \left(1 + \frac{rA_c^* t}{V_c^*}\right)^{-(1-n)\Gamma\left[\sqrt{RT_c^*}/r\right](A_t/A_c^*)} . \tag{4.27}$$

Consequently, as has already been shown from the stability analysis, the disturbances die out in time so long as $n<1$. However, it is further seen that they die out more quickly the smaller the value of n. Likewise, it appears that the ratio of throat area to combustion surface

area is important in this regard. The larger the ratio A_t/A_c^*, the more rapidly will combustion chamber equilibrium be restored. The condition that the chamber disturbance vanishes in a time which is short compared with the rocket burning time may be applied to equation (4.27) to estimate the permissible values of the variables which may be used. If the bracketed term of (4.27) is written as

$$1 + \frac{rA_c^* t_b}{V_c^*} \frac{t}{t_b} \equiv 1 + \frac{V_p}{V_c^*} \frac{t}{t_b}$$

where V_p is the total volume of propellant in the rocket motor, it is noted that V_p/V_c^* is of the order of 1 over most of the burning time. Consequently, if the life of the disturbance is very small compared with the burning time, the right side of (4.27) may be expanded in a binomial series and sufficient accuracy obtained with only the linear term in time. Therefore,

$$\frac{p_c'}{p_{c_0}} \approx 1 - (1-n)\Gamma \frac{\sqrt{RT_c^*}\, A_t t_b}{V_c^*} \frac{t}{t_b} \quad . \tag{4.28}$$

Hence, for this to vanish for values of t such that $t/t_b \ll 1$, the following inequality must be satisfied:

$$(1-n)\Gamma \frac{\sqrt{RT_c^*}\, A_t t_b}{V_c^*} \gg 1 \, . \tag{4.29}$$

The quantity $\sqrt{RT_c^*}\, A_t t_b$ is proportional to the volume of gas ejected from the nozzle, and since this is much greater than the combustion chamber volume V_c^*, it is usually possible to satisfy this inequality if n is not too nearly equal to unity.

Returning now to the question of the actual equilibrium oper-

ating condition, now that the conditions under which it exists are understood, equation (4.15) may be rewritten

$$p_c = \left(\frac{a(p_p - p_c)}{\Gamma \sqrt{RT_c}} \frac{A_c}{A_t} \right)^{1/(1-n)} . \qquad (4.30)$$

This has not actually been solved for p_c since it still occurs in the right hand term. However, the quantity $p_p - p_c$ is dominated by the effective propellant pressure p_p, and only a small error is made in approximating this by

$$p_c \approx \left(\frac{a p_p}{\Gamma \sqrt{RT_c}} \right)^{1/(1-n)} \left(\frac{A_c}{A_t} \right)^{1/(1-n)} = (a \rho_p c^*)^{1/(1-n)} K_N^{1/(1-n)} . \qquad (4.31)$$

Here the area ratio A_c/A_t has been denoted K_N and the definition of the characteristic velocity $c^* = (\sqrt{\gamma RT_c})/\Gamma'$ has been used. The term $a\rho_p c^*$ is entirely determined by the chemical nature of the solid propellant employed, while the ratio K_N is a matter of physical dimension and may therefore be varied even for the same propellant. Furthermore, the exponent $1/(1-n)$ is rather large for usual values of n, ranging between 2 and 5. Therefore, the chamber pressure is quite critically affected by the combustion area - throat area ratio.

It is also of interest to investigate, using the present results, the effect of varying the nozzle throat area for a given combustion chamber and propellant. Near the ideal expansion point, the thrust coefficient C_F is nearly independent of the chamber pressure p_c so long as the expansion ratio across the nozzle is large. Then the thrust may be written in the form

$$F = C_F p_c A_t . \qquad (4.32)$$

Now from equation (4.31), the chamber pressure is proportional to $A_t^{-(1/(1-n))}$ when the area of the combustion surface and the propellant composition are fixed. Then the thrust is proportional to

$$F \sim A_t A_t^{-(1/(1-n))} = A_t^{-(n/(1-n))} . \qquad (4.33)$$

Therefore, the rocket thrust decreases as the throat area increases, with a rate depending upon the exponent n. For usual propellants, the rate of decrease is between A_t^{-1} and A_t^{-4}. For propellants having a value of n close to unity, the thrust is extremely sensitive to the throat area.

For most large rocket motors, the required proportions of the chamber necessitate large cylindrical combustion surfaces, with the consequence that the gaseous products of combustion flow in the chamber passage toward the nozzle, and in doing so may attain velocities of considerable magnitude. A pressure gradient along the grain results from this flow process, the pressure decreasing from the front end of the grain (F) to the nozzle end of the grain (N). This pressure variation along the burning surface causes the grain to burn more rapidly at the front end.

On the other hand, the erosive effect of gas velocity past the propellant surface causes an increase in the propellant burning rate. In the unrestricted burning rocket, the mass of propellant gas flowing by any cross section increases toward the nozzle end of the grain, and consequently, the local velocity past the grain is larger toward the nozzle end than it is toward the front. This variation of gas velocity causes varying decrees of erosion over the propellant surface; in particular, it causes the propellant to burn more rapidly at the nozzle

end. In the simple analysis which follows, it will be assumed that the burning rate is uniform over the grain surface.

From the nature of the internal ballistic problem for the usual solid rocket, it is clear that some rather far-reaching assumptions must be made before any theoretical analysis may be considered. In general, it will be assumed that:

1) The process may be described as the one-dimensional, non-viscous flow of a perfect gas;

2) The effects of pressure and gas velocity on burning rate cancel each other over the grain so that the burning rate is constant;

3) The calculations may be based upon steady-state flow processes.

According to the first assumption, the effects of viscosity in producing a frictional pressure loss in the combustion chamber passages and losses in the flow separation at the nozzle end of the grain will be neglected. This is not a serious restriction so far as exhibiting the physical phenomenon is concerned. The second assumption is, however, a limitation, inasmuch as experimental results show considerable effect of erosion for long tubular charges. However, the results will be completely satisfactory for grains of short and medium length, and not in serious error for long grains. The assumption of a quasi-stationary analysis is quite adequate so long as the periods of pressure and velocity variation are long with respect to the stabilization time of the chamber - nozzle system. Other specific assumptions made in the course of analysis will be noted as they are made.

The idea of the following analysis is simply one of relating the

conditions within the tubular chamber of the rocket to those of an equivalent rocket with uniform pressure along the grain, and then utilizing the results of the previous analysis. This process will be divided into two main parts, that of relating the nozzle end pressure and mass flow to those of the previous analysis, and finally relating the effective combustion-chamber pressure to the front end pressure from which the burning rate of the propellant is determined.

Let p_c and T_c be effective chamber-pressure and stagnation-gas temperature, respectively. Then from the nozzle analysis, the mass of gas passing through the nozzle is

$$m = (\Gamma / \sqrt{RT_c})\, p_c A_t . \tag{4.34}$$

The value of T_c is a known constant of the propellant combustion process. However, the effective value of p_c is not known. If it is assumed that the gas flow from the grain port outlet to the nozzle is a reversible adiabatic process, then the effective value of p_c is simply the stagnation pressure corresponding to the velocity v_N and pressure p_N. The velocity v_N satisfies the relation

$$v_N^2 = 2C_p T_c (1 - T_N/T_c) , \tag{4.35}$$

and because the process is adiabatic and reversible, the pressure ratio p_N/p_c may be used.

$$v_N^2 = 2C_p T_c \left(1 - (p_N/p_c)^{(\gamma-1)/\gamma}\right) . \tag{4.36}$$

Clearly, the mass flow through the grain port is

$$m = \rho_N v_N A_p , \tag{4.37}$$

where A_p, the port area, is the entire area accessible to the flow at the nozzle end of the grain. Utilizing the isentropic feature again, the

density ρ_N may be expressed as

$$\rho_N/\rho_c = (p_N/p_c)^{1/\gamma}, \tag{4.38}$$

so that the mass flow may be written as

$$m = \rho_c v_N A_p (p_N/p_c)^{1/\gamma} = (p_c/RT_c) v_N A_p (p_N/p_c)^{1/\gamma}. \tag{4.39}$$

Now employing the value of the velocity at the nozzle end from equations (4.36), the mass flow is just

$$m = \frac{p_c A_p}{\sqrt{RT_c}} \left(\frac{p_N}{p_c}\right)^{1/\gamma} \sqrt{\frac{2\gamma}{\gamma-1}\left(1 - \left(\frac{p_N}{p_c}\right)^{(\gamma-1)/\gamma}\right)}. \tag{4.40}$$

By continuity, this mass is equal to that flowing through the nozzle, described by equation (4.34) in terms of the effective chamber pressure. Equating these two relations, it follows that

$$\frac{A_t}{A_p} = \frac{1}{\Gamma}\left(\frac{p_N}{p_c}\right)^{1/\gamma} \sqrt{\frac{2\gamma}{\gamma-1}\left(1 - \left(\frac{p_N}{p_c}\right)^{(\gamma-1)/\gamma}\right)} \tag{4.41}$$

where A_t/A_p is a known geometric factor. Hence, equation (4.41) gives the ratio of the grain nozzle end pressure to the effective chamber pressure, although the relation is implicit.

In any actual design, the pressure ratio p_N/p_c is not far from unity, so that within the accuracy of the analysis, certain approximations may be made. Considering the right side of equation (4.41), it is obvious that the value of this expression is determined by the term $1 - (p_N/p_c)^{(\gamma-1)/\gamma}$ which is very sensitive to the value of the pressure ratio. The term $(p_N/p_c)^{(1/\gamma)}$ outside the radical will not be influential in the calculations. By writing

$$\Gamma^2(A_t/A_p)^2 = (p_N/p_c)^{2/\gamma} \frac{2\gamma}{\gamma-1}\left(1 - (p_N/p_c)^{(\gamma-1)/\gamma}\right)$$

$$= \frac{2\gamma}{\gamma-1}\left(1 + (p_N/p_c - 1)\right)^{2/\gamma}\left[1 - \left(1 - (1 - p_N/p_c)\right)^{(\gamma-1)/\gamma}\right]$$

Each of the terms including the small term $(p_N/p_c - 1)$ may be expanded in a binomial series which, retaining only the first power of the small quantity , becomes

$$\Gamma^2\left(\frac{A_t}{A_p}\right)^2 \approx \frac{2\gamma}{\gamma-1}\left[1 + \frac{2}{\gamma}\left(\frac{p_N}{p_c} - 1\right)\right]\frac{\gamma-1}{\gamma}\left(1 - \frac{p_N}{p_c}\right) \approx 2\left(1 - \frac{p_N}{p_c}\right) . \qquad (4.42)$$

The pressure ratio p_N/p_c is then approximately

$$p_N/p_c \approx 1 - \frac{\Gamma^2}{2}(A_t/A_p)^2 . \qquad (4.43)$$

In terms of this nozzle end pressure, the mass rate of flow from the nozzle, and hence that from the grain port, may be approximated as

$$m \approx \frac{\Gamma}{\sqrt{RT_c}} \frac{p_N A_t}{1 - \frac{\Gamma^2}{2}\left(\frac{A_t}{A_p}\right)^2} , \qquad (4.44)$$

where use has been made of equations (4.34) and (4.43). If the mass flow may be expressed in terms of the linear burning rate, r , as

$$m = r\rho_p A_c , \qquad (4.45)$$

then, by substitution into equation (4.44), the pressure at the nozzle end of the grain is expressed as

$$p_N = \frac{r\rho_p A_c \sqrt{RT_c}\left(1 - \frac{1}{2}\Gamma^2(A_t/A_p)^2\right)}{\Gamma A_t} . \qquad (4.46)$$

Here, ρ_p denotes the propellant density and A_c the total combustion surface of the propellant grain. Equation (4.45) is an approximation

in that the gas being stored in the combustion chamber due to the reduction of propellant volume is neglected. The correct expression for the mass ejected from the nozzle is clearly

$$m = rA_c(\rho_p - \rho) \tag{4.47}$$

where ρ is the density of the propellant gas generated by combustion.

The actual value of the nozzle end chamber pressure, p_N, may not be determined from equation (4.48) because of the unknown linear burning rate r. This burning rate is not simply related to the pressure p_N because the burning rate is increased above the expected value due to the erosive effect of gas velocity past the propellant surface. The only point at which the burning rate can be calculated is at the front end of the grain where the gas velocity vanishes. Since the burning rate is assumed constant over the entire grain, the value found at this point will hold everywhere. Therefore, the pressure p_F at the front end of the chamber must be computed.

The difference of pressure between the two ends of the propellant grain is caused by the continuous production of gas along the flow passage and the consequent acceleration of the gas along the constant area passage. In order to investigate this phenomenon, equations of continuity and momentum must be developed which apply to a flow of varying mass. If ρ and v are the local gas density and velocity, respectively, then $\rho v A_p$ would be a constant value were it not for the gas generated at the combustion surface. However, considering a section of length dx along the direction of flow between the planes at x and $x+dx$, the change of mass flow between these two planes is

$$d(\rho v A_p) \tag{4.48}$$

This may be expressed in another manner by considering the mass of gas generated by the burning surface. The mass added to the flow per unit length is then

$$\frac{\rho_p r A_c}{L} \tag{4.49}$$

Consequently, the gas added to the flow may be set equal to that generated by burning over the length dx to give

$$d(\rho v A_p) = \frac{\rho_p r A_c}{L} dx \tag{4.50}$$

which is the extension of the one-dimensional continuity equation for systems with mass addition. The momentum relation may be developed in a similar manner. The momentum change across the two planes is easily expressed as

$$d(\rho v^2 A_p) \tag{4.51}$$

which accounts for both the effects of velocity change and mass addition. This change of momentum is accounted for by the pressure force between the two faces

$$-A_p dp \tag{4.52}$$

and any component of momentum in the direction of flow possessed by the combustion gas from the propellant. It will be assumed that the escape from the propellant surface is such that no mean momentum is contributed to the gas stream. Then the momentum relation is

$$d(\rho v^2 A_p) = -A_p dp \tag{4.53}$$

It will be assumed further, in good agreement with known results, that the stagnation temperature of the propellant gas is a fixed quantity

$c_p T_c$ and is relatively independent of the pressure or propellant temperature. Then the energy equation which is appropriate to the gas flow is

$$\frac{1}{2} v^2 + \frac{\gamma}{\gamma - 1} \frac{p}{\rho} = c_p T_c \tag{4.54}$$

Of the three equations defining the flow (equations 4.50, 4.53, and 4.54), the first two may be integrated directly starting from the front end of the propellant grain. At this point, the pressure is p_F, the velocity of the gas vanishes ($v_F = 0$), and the value of x will be chosen $x = 0$. Then the continuity equation integrates to

$$\rho v A_p = \rho_p r A_c \frac{x}{L} \tag{4.55}$$

expressing the evident fact that the mass of gas flowing by a cross section taken at the ordinate x is equal to the mass of gas generated by propellant burning from the point x to the chamber front. The momentum equation may likewise be integrated to give

$$\rho v^2 A_p = A_p (p_F - p) \tag{4.56}$$

where advantage has been taken of the fact that the momentum vanishes at the grain front. Then equation (4.56) says simply that the entire gas momentum is generated by the difference between the local pressure and the pressure at the grain front. To summarize, the relations which will be employed in investigating the distribution of pressure along the grain face, and in particular, to find the front end pressure, p_F, are

$$\rho v A_p = \rho_p r A_c \frac{x}{L} \tag{4.55}$$

$$\rho v^2 A_p = A_p (p_F - p) \tag{4.56}$$

$$\frac{1}{2} v^2 + \frac{\gamma}{\gamma - 1} \frac{p}{\rho} = c_p T_c \tag{4.54}$$

Now from equation (4.56), the term ρv^2 is just

$$\rho v^2 = (p_F - p) \tag{4.57}$$

while the local gas density itself may be found by squaring the continuity equation (4.55) and dividing by the momentum relation (4.56). This gives

$$\rho = \frac{(\rho_p r A_c)^2}{A_p^2} \left(\frac{x}{L}\right)^2 \frac{1}{p_F - p} \tag{4.58}$$

The momentum per unit area and the local gas density may now be employed to eliminate the velocity and density terms from equation (4.54), the energy relation. Making this substitution, it is found that

$$\frac{1}{2}(p_F - p) + \frac{\gamma}{\gamma - 1} p = c_p T_c \left(\rho_p r \frac{A_c}{A_p}\right)^2 \left(\frac{x}{L}\right)^2 \frac{1}{p_F - p} \tag{4.59}$$

This expression gives the local pressure p in terms of the pressure at the front of the grain and known parameters inasmuch as the burning rate r is determined by the pressure p_F. Reasoning in the opposite manner, this equation may be employed to give the pressure p_F in terms of a known local pressure. The local pressure which may be employed to this purpose is that at the nozzle end of the grain p_N which occurs when x = L. Making this substitution and collecting terms in the form of p_F/p_N, it follows that

$$\left(\frac{p_F}{p_N}\right)^2 + \frac{2}{\gamma - 1}\left(\frac{p_F}{p_N}\right) - \left[\frac{\gamma + 1}{\gamma - 1} + 2 c_p T_c \left(\frac{\rho_p r}{p_N} \frac{A_c}{A_p}\right)^2\right] = 0 \tag{4.60}$$

This quadratic is easily solved for the pressure ratio p_F/p_N to give

$$\frac{p_F}{p_N} = -\frac{1}{\gamma-1} + \frac{\gamma}{\gamma-1}\sqrt{1+2\left(\frac{\gamma-1}{\gamma}\right)^2 c_p T_c \left(\frac{\rho_p r}{p_N}\frac{A_c}{A_p}\right)^2} \qquad (4.61)$$

where the choice of sign for the radical is obvious.

This solution is merely formal, however, inasmuch as the propellant burning rate still depends upon the chamber front pressure. However, this form has the advantage of allowing an approximation by means of which the solution to the complete problem may be obtained. Consider the physical significance of the second term in the radical. This may be written

$$2\left(\frac{\gamma-1}{\gamma}\right) R T_c \left(\frac{\rho_p r A_c}{p_N A_p}\right)^2$$

Now since p_N is approximately the chamber pressure, it follows closely that

$$p_N \approx R \rho_c T_c$$

so that the above expression may be written approximately

$$2(\gamma-1)\frac{(\rho_p r A_c)^2}{\rho_c^2 \gamma R T_c A_p^2} = 2(\gamma-1)\left(\frac{\rho_p r A_c}{\rho_c a_c A_p}\right)^2$$

The quadratic $(\rho_p r A_c)/(\rho_c a_c A_p)$ has a simple physical significance by means of which its value may be estimated. The numerator is the mass of propellant consumed by the combustion process per unit time; the denominator is the mass which would flow through the propellant port area A_p if the gas moved with the sonic velocity of the combustion chamber. Usually the mass flow through the port passage (equal to that generated by the propellant combustion) is such that a binomial expansion of this radical, retaining only the first order term, is appropriate. To good accuracy

$$\frac{p_F}{p_N} \approx -\frac{1}{r-1} + \frac{r}{r-1}\left[1 + \left(\frac{r-1}{r}\right)^2 c_p T_c \left(\frac{\rho_p r A_c}{p_N A_p}\right)^2\right] = 1 + RT_c\left(\frac{\rho_p r A_c}{p_N A_p}\right)^2 \qquad (4.62)$$

It should be mentioned again that this relation does not give p_F explicitly in terms of p_N and known constants because the burning rate r still depends upon p_F.

Now the result can actually be put into a convenient form most easily by referring to the approximate value of the nozzle end pressure p_N which is given by equation (4.46). By substituting this value of p_N for its equivalent in the denominator of the second right hand term of the above equation, it follows immediately that

$$\frac{p_F}{p_N} \approx 1 + \frac{r^2 A_t^2}{A_p^2}\left(\frac{1}{1 - \frac{1}{2} r^2 (A_t/A_p)^2}\right) \approx 1 + r^2\left(\frac{A_t}{A_p}\right)^2 \qquad (4.63)$$

Here, terms of order $(A_t/A_p)^4$ and higher have been dropped because A_t/A_p is not greater than 0.5 as a rule. It is conventional to use as parameters the area ratios

$$\begin{aligned} K_I &\equiv A_c/A_p \\ K_N &\equiv A_c/A_t \end{aligned} \qquad (4.64)$$

both of which are greatly in excess of unity. The ratio of the front to nozzle end pressures may be expressed in terms of these ratios as

$$\frac{p_F}{p_N} \approx 1 + r^2\left(\frac{K_I}{K_N}\right)^2 \qquad (4.65)$$

Clearly, this reduces to the result that $p_F = p_N = p_c$ for the restricted burning rocket since the ratio K_I/K_N is quite small, and its square may be neglected.

Through application of this relatively simple relation between the front pressure and nozzle end pressure, the absolute value of the grain front pressure may be calculated directly. Solving equation (4.65) for the nozzle end pressure p_N, entering the result in (4.46), for p_N, and writing the propellant burning rate as $r = ap_F^n$, it follows that

$$\frac{p_F}{1+\Gamma^2\left(\frac{K_I}{K_N}\right)^2} = \frac{a p_F^n \rho_p A_c \sqrt{RT_c}}{\Gamma A_t}\left[1-\frac{1}{2}\Gamma^2\left(\frac{K_I}{K_N}\right)^2\right] \qquad (4.66)$$

This may be solved for the grain front pressure, again neglecting quantities of order $(K_I/K_N)^4$ and higher;

$$p_F \approx \left\{a\rho_p \frac{\sqrt{RT_c}}{\Gamma} K_N\left[1+\frac{1}{2}\Gamma^2\left(\frac{K_I}{K_N}\right)^2\right]\right\}^{\frac{1}{1-n}} \qquad (4.67)$$

Consequently the value of p_F is now known directly in terms of rocket and grain geometry and the propellant properties.

The reliability of the performance calculation may be improved by employing the experimental value of c^* for the propellant used. Usually, the experimental value of c^* is about 90 per cent of the theoretical value, that is, the effective combustion temperature is in the neighborhood of 80 per cent of the calculated value. Then it is appropriate to employ, where experimental values are available,

$$p_F = \left[a\rho_p c^*_{exp} K_N\right]^{\frac{1}{1-n}}\left[1+\frac{1}{2}\Gamma^2\left(\frac{K_I}{K_N}\right)^2\right]^{\frac{1}{1-n}}$$

If the effective combustion chamber pressure is defined as

$$p_c' = \left[a \rho_p C^*_{exp} K_N \right]^{\frac{1}{1-n}} \tag{4.68}$$

then the pressure at the front end of the propellant grain may be expressed as a correction to this pressure by writing

$$p_F \approx p_c' \left[1 + \frac{\Gamma^2}{2(1-n)} \left(\frac{K_I}{K_N} \right)^2 \right] \tag{4.69}$$

Aside from the chemical properties of the propellant, the value of p_c' depends upon the nozzle area ratio, while the pressure at the front end of the chamber depends upon both the nozzle area ratio K_N and this internal area ratio K_I.

The pressure distribution along the propellant grain may be calculated from equation (4.59) using the now known value of p_F. Regrouping the terms in equation (4.59) in the form

$$\frac{1}{2}\left(\frac{\gamma+1}{\gamma-1}\right)\left(\frac{p}{p_F}\right)^2 - \frac{1}{\gamma-1}\frac{p}{p_F} + \left[C_p T_c \left(\frac{\rho_p r A_c}{p_F A_p} \right)^2 \left(\frac{x}{L} \right)^2 - \frac{1}{2} \right] \tag{4.70}$$

the resulting quadratic expression may be solved to give

$$\frac{p}{p_F} = \frac{1}{\gamma+1} + \frac{\gamma}{\gamma+1} \sqrt{1 - \frac{\gamma^2-1}{\gamma^2} 2 C_p T_c \left(\frac{\rho_p r A_c}{p_F A_p} \right)^2 \left(\frac{x}{L} \right)^2} \tag{4.71}$$

By the same argument used in connection with the simplification of equation (4.61), it follows that to a good approximation

$$\frac{p}{p_F} \approx 1 - R T_c \left(\frac{\rho_p r A_c}{p_F A_p} \right)^2 \left(\frac{x}{L} \right)^2 = 1 - \Gamma^2 \left(\frac{K_I}{K_N} \right)^2 \left(\frac{x}{L} \right)^2 \tag{4.72}$$

Then, in terms of the effective chamber pressure p_c, the local pressure on the grain surface is

$$p/p_c' \approx \left[1 + \frac{r^2}{2(1-n)}\left(\frac{K_I}{K_N}\right)^2\right]\left[1 - r^2\left(\frac{K_I}{K_N}\right)^2\left(\frac{x}{L}\right)^2\right] \qquad (4.73)$$

This result indicates that the local pressure and, in particular, the pressure at the nozzle end of the grain may or may not fall below the effective chamber pressure depending upon the value of n , the exponent in the propellant burning law.

5. LIQUID PROPELLANT ROCKET MOTORS

Propellants and Propellant Evaluation

A chemical propellant system consists of an oxidizer and a fuel; the oxidizer consists mainly of atoms such as oxygen, chlorine, and fluorine; the fuel consists mainly of such atoms as hydrogen, lithium, beryllium, boron, carbon, sodium, magnesium, aluminum, and silicon. If the oxidizer and the fuel have no chemical affinity at normal temperature and can be mixed to form a single liquid, we have a composite monopropellant. If the fuel and oxidant atoms are both joined in the same molecule, we have a simple monopropellant such as propyl nitrate. In this case, the exothermic reaction consists in a decomposition, such as occurs with hydrogen peroxide or hydrazine.

Usually, however, the liquids (oxidizer and fuel) are injected separately, and such a system constitutes a bipropellant. When the two components of a bipropellant react immediately upon contact with one another, the propellant is denoted hypergolic. The most usual oxidizers available for bipropellants are:

hydrogen peroxide, H_2O_2

nitric acid, HNO_3

liquid oxygen, O_2

ozone, O_3

tetranitromethane, $C(NO_2)_4$

nitrogen peroxide, N_2O_4

fluorine, F_2

oxygen fluoride, F_2O

chlorine, Cl_2

chlorine trifluoride, ClF_3

nitrogen trifluoride, F_3N

perchloryl fluoride, ClO_3F

fluorazine, N_2F_4

The fuels that can be used along with these oxidizers are very numerous; they include compounds of:

carbon:	saturated and unsaturated hydrocarbons amines alcohol
boron:	boranes B_nH_{n+4}
nitrogen:	ammonia hydrazine
hydrides:	HLi
organometallics:	$(C_2H_5)_3Al$

Consider first those fuel elements which react with a simple oxidizer such as oxygen itself, as shown in Fig. 5.1. The elements of greatest interest are those which occur at the center of the period, the maximum of energy being obtained from beryllium and aluminum. Combustion temperatures (Fig. 5.2) follow virtually the same law, these same elements yielding the optimum. High temperatures can also be obtained from certain heavy metals, such as thorium burning in oxygen (4700°K) and zirconium (4800°K), but the resulting molecules are heavy and the choice is limited to the first, second, and

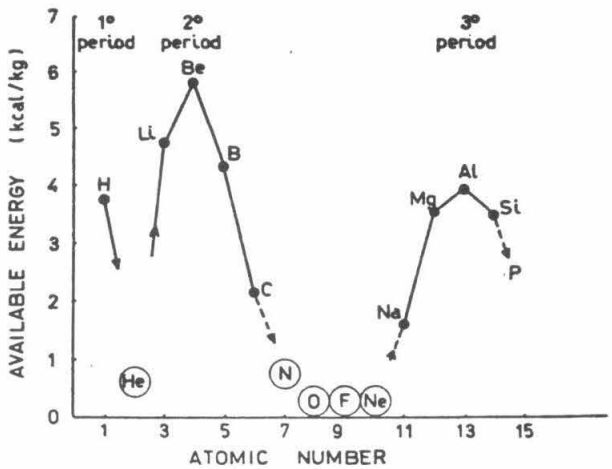

Fig. 5.1. Available energy E of the light elements associated with oxygen (stoichiometric mixture and element taken at the standard temperature of 298.16°K).

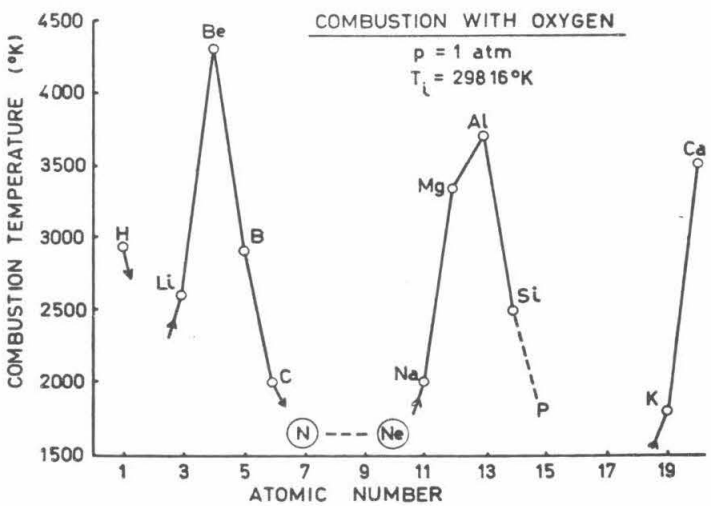

Fig. 5.2. Adiabatic combustion temperature (oxidizer: oxygen. p = 1 atm, T_i = 298.16°K).

third periods. Comparing the elements with one another by reference to the available energy gives only a first approximation, and it is better to base the comparison on the specific impulse. This is illustrated by the following table, which compares fluorine-hydrogen and oxygen-hydrogen at maximum of performance.

Propellant (liquid) :	F_2+H_2	O_2+H_2
Available energy of stoichiometric mixture (kcal/kg)	3110	3600
Optimum equivalence ratio	3.33	2.27
Temperature (^oK)	3323	2760
Molecular weight	10.01	9.0
Specific impulse (sec) for $p_c/p_e = 20/1$ (equilibrium flow)	364	350

Although the hydrogen-oxygen system has higher available energy than the hydrogen-fluorine system, its performance is lower. Such differences are due to dissociation phenomena which depend on the nature of the molecules formed at the end of combustion as in the present case where water (H_2O) is more easily dissociated than hydrofluoric acid (HF).

The available energy of the (fluorine-lithium) propellant is higher than that of (fluorine-hydrogen), but calculation indicates the specific impulse of (F_2+Li) to be lower than that of (F_2+H_2). This difference is illustrated in Fig. 5.3. Even though the combustion temperature is higher for lithium than for hydrogen, which is in accordance with the classification based on available energy, the fact of the molecular weights being markedly lower in the (F_2+H_2) system than in

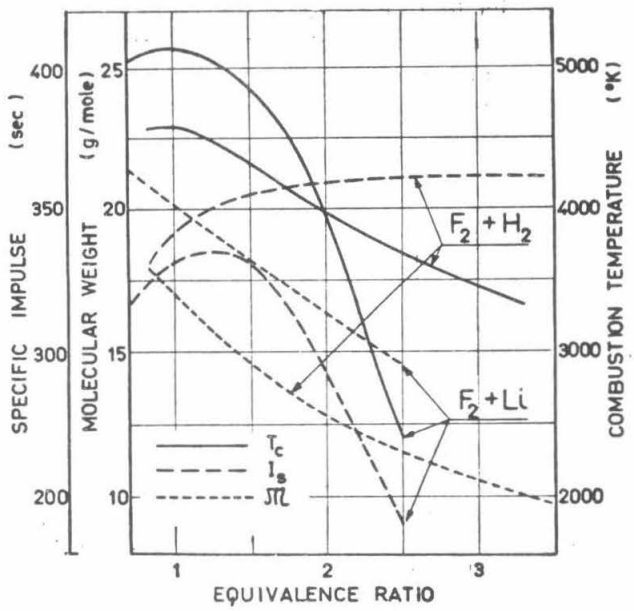

Fig. 5.3. Comparison between the performance of the propellants (fluorine-hydrogen) and (fluorine-lithium): p_c = 20 atm, expansion ratio = 20/1.

the (F_2+Li) system explains the result.

This observation serves to stress once again the necessity for calculating specific impulses when comparing propellants with one another.

The mixture ratio Φ or the equivalence ratio Φ^* may modify the specific impulse. For specific impulse, the optimum lies in the direction of rich mixtures ($\Phi^* > 1$) and its position depends on the elements present. The maximum depends strongly on the proportion of hydrogen in the mixture. On the other hand, the highest temperature is obtained close to the stoichiometric mixture, but with $\Phi^* > 1$. This fact is shown in Fig. 5.3, which shows that for the propellant (F_2+H_2) the maximum of specific impulse occurs around $\Phi^* = 3$.

In general, the specific impulse increases with the combustion

pressure, but in order to isolate its significance, it is necessary to assume a constant expansion ratio, that is, that the nozzle has a certain geometric form. In Fig. 5.4, the characteristic velocity is seen to be insensitive to changes in chamber pressure, for when this pressure is multiplied by two, the characteristic velocity increases by only one per cent, this due to a slight increase in combustion temperature with pressure.

It has been shown that the specific impulse corresponds to the product of two terms: the characteristic velocity and the thrust coefficient:

$$I_s = \frac{c^* C_F}{g} \tag{5.1}$$

Although the characteristic velocity is not greatly affected by the chamber pressure, the thrust coefficient depends more sensitively on

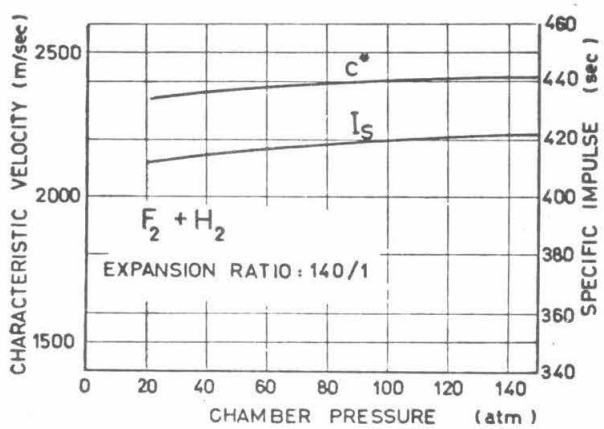

Fig. 5.4. Variations of the characteristic velocity and specific impulse as functions of chamber pressure. Propellant F_2+H_2; expansion ratio 140/1 ($\Phi^* = 1$).

the expansion ratio.

The specific impulse can be appreciably imporved by appropriate choice of the expansion ratio or the nozzle geometry. Figure

5. 5 shows that the specific impulse is increased by over 30 per cent when the expansion ratio changes from 10 to 100. The gain is due mainly to recombination during the expansion. To show this effect,

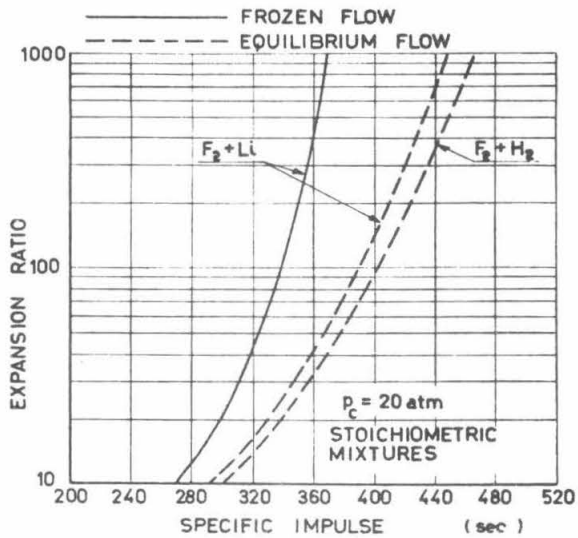

Fig. 5. 5 Variations of specific impulse as a function of the expansion ratio (stoichiometric mixture; p_c = 20 atm).

two extreme assumptions have been considered, namely frozen and equilibrium flows. The difference between these becomes marked when the expansion ratio increases. Therefore, it is necessary to specify the equivalence ratio and the expansion ratio when evaluating the specific impulse of high energy propellants.

Although propellants may be compared on the basis of specific impulse, such classification fails to account for the volume required by the propellant-powerplant combination. To account for volumetric requirements, the parameter which should be used for comparison is the volumetric specific impulse $I_s \delta$, where δ is the density of the propellant.

PERFORMANCE OF THE PROPELLANT (F_2+H_2)

p_c = 20.4 atm.

Parameters	$\Phi^* = 1$				$\Phi^* = 3.3$			
	p_e = 1 atm		p_e = 0.1149 atm		p_e = 1 atm		p_e = 0.1149 atm	
	Frozen	Equilibrium	Frozen	Equilibrium	Frozen	Equilibrium	Frozen	Equilibrium
I_s(sec)	312.8	341.5	363.4	420.7	351.7	364.6	411.0	430.7
c^*(m/sec)	2221	2343	2221	2343	2489	2558	2489	2558
C_F	1.381	1.429	1.604	1.761	1.386	1.398	1.619	1.651
$\frac{A_e}{A_t}$	3.049	3.987	12.25	21.30	3.154	3.384	13.00	14.24
T_e (°K)	2074	3456	1112	2749	1597	1882	884	1075

The performance of different oxidizers will depend on the fuels associated with them. Figure 5.6 shows how I_s and $I_s\delta$ compare when different oxidizers are used with a fuel containing carbon and hydrogen, such as kerosene of the general formula C_nH_{2n}, or with a fuel containing nitrogen and hydrogen, such as ammonia. The oxidizers with a fluorine base give the highest performance, but it should be remarked that the fluorine-ammonia propellant is better than the

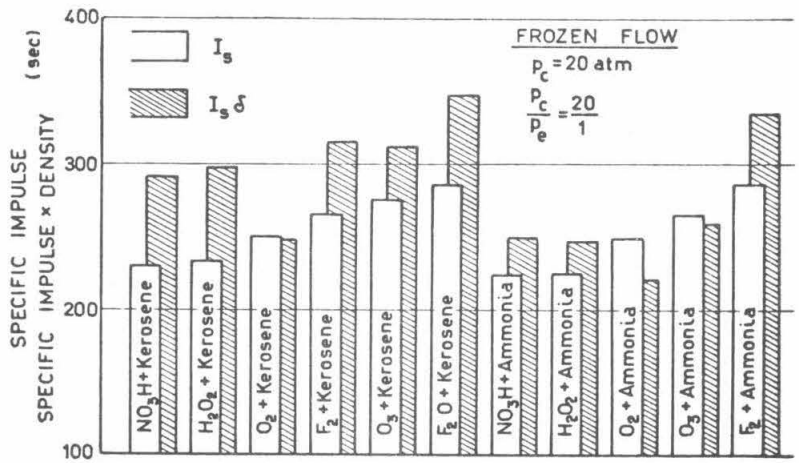

Fig. 5.6. Comparison between several oxidizers used with two fuels (frozen flow, p_c = 20 atm, p_c/p_e = 20/1).

fluorine - kerosene system even though, when the fluorine is replaced by oxygen, both propellants have about the same specific impulse. This is due partly to the strong dissociation of molecules based on fluorine and carbon such as CF_4, C_2F_2, CF_3, ... so that energy is derived solely from the combination of hydrogen with fluorine.

It is advantageous if the curve of specific impulse as a function of the equivalence ratio is flat near its maximum, for then any variations that may occur in the thrust and in the duration of combustion as the result of possible changes in the mixture ratio will be minimized. As the oxidizer and fuel have different specific gravities, the maximum values of I_s or of $I_s\delta$ do not coincide with the same values of the mixture ratio. In most cases, the maximum of $I_s\delta$, by comparison with the maximum of I_s, occurs closer to the poorer mixtures. It is well to have available, for each propellant, under standard conditions of expansion, three curves showing the theoretical varuations of I_s, of $I_s\delta$, and of the temperature at the end of combustion expressed as functions of Φ or Φ^*. Such graphs (similar to that shown in Fig. 5.7) constitute a characteristic diagram for the propellant.

The comparisons have so far been based on the theoretical performances of the propellant. Therefore, it is important to know how closely the results obtained experimentally approach these theoretical performances. Three quality factors may be introduced to aid in this comparison:

$$\zeta_s = \frac{(I_s)_{exp}}{(I_s)_{th}}, \qquad \zeta_b = \frac{(C^*)_{exp}}{(C^*)_{th}}, \qquad \zeta_F \frac{(C_F)_{exp}}{(C_F)_{th}}$$

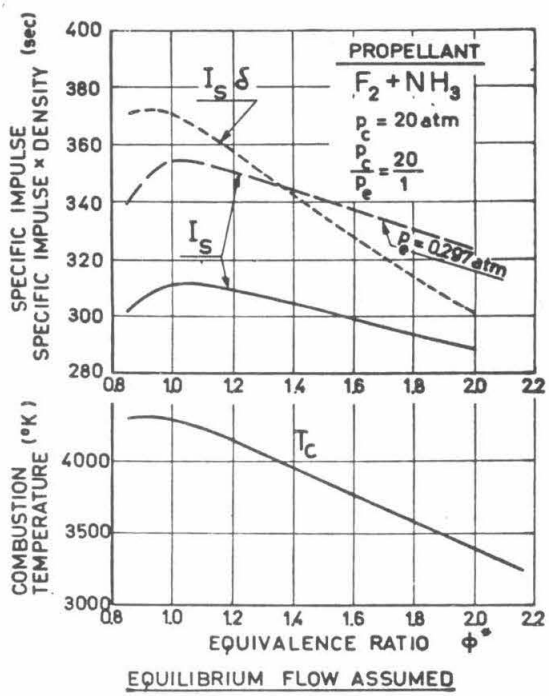

Fig. 5.7. Performance of a propellant.

these being related by the relation

$$\xi_s = \xi_F \cdot \xi_b$$

The divergence between the theoretical and experimental specific impulse is measured by the parameter ξ_s; for the usual propellants, the parameter ξ_F depends mainly on the geometry of the nozzle and only slightly on the nature of the propellant. This being so, comparison between propellants is based in fact upon ξ_b. Figures 5.8 and 5.9, obtained with the propellants HNO_3-U. D. M. H. and O_2-H_2, show that the values of ξ_b lie between 0.9 and 1.0.

For more energetic propellants or for longer nozzles in which recombination reactions are possible, it is necessary to base comparisons on ξ_s. In this case, the recombination modifies the values both

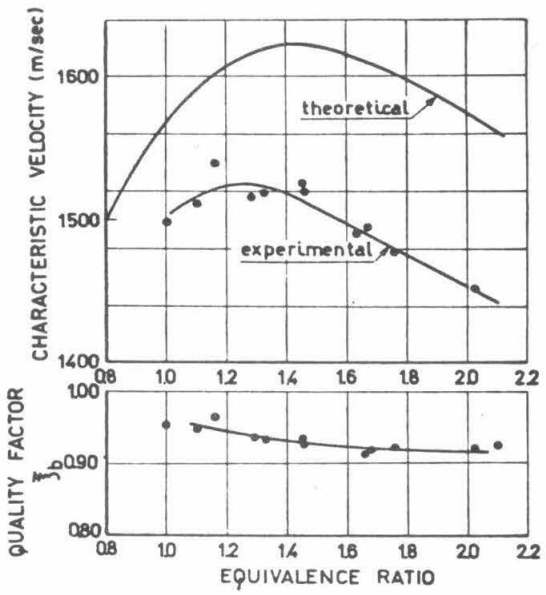

Fig. 5.8. Variations of the theoretical and experimental values of the characteristic velocity as functions of the equivalence ratio Φ^*. Propellant HNO_3-U. D. M. H. ; p_c = 20 atm; injector with premixing.

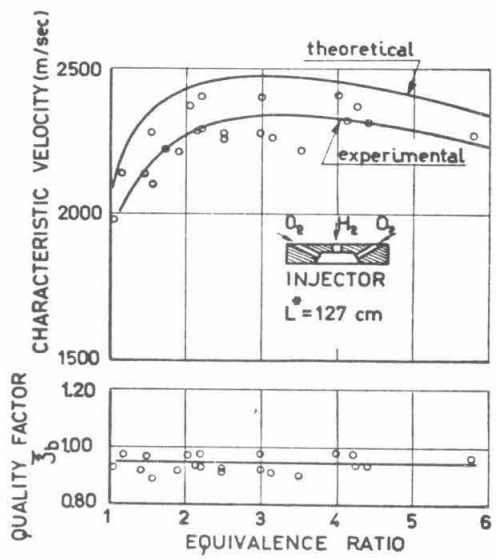

Fig. 5.9. Variations of the theoretical and experimental values of the characteristic velocity of the propellant[H_2-O_2], L^* , 127 cm.

of ξ_b and of ξ_F.

The Combustion Chamber

The processes of vaporization, diffusion, heat transfer, combustion, etc. take place successively in the chamber once the propellant has been injected until complete combustion has taken place. These processes are so complex that it is difficult to follow them in any detail. On entering the combjstion chamber, the oxidizer and fuel are suitably atomized and mixed. If the oxidizer and the fuel have no chemical affinity for each other in the liquid state, atomization and mixing will be carried out to as high a degree as possible in order to obtain very rapid vaporization of the liquids and formation of a homogeneous gaseous phase ready for combustion. If the oxidizer and fuel, however, react in the liquid state (hypergolic propellant), this exothermal reaction will be used to vaporize the mixture and to bring about as quickly as possible the gaseous phase preceding ignition. Schematic diagrams showing possible processes taking place are shown in Figs. 5.10 and 5.11. From the quantitative point of view, it is difficult to determine the time required for each process. It is possible, however, to determine the characteristic time intervals required for certain partial or complete processes, and the characteristic volume necessary for obtaining complete combustion.

Consider the change of specific volume v from the time the propellant enters the combustion chamber until the burnt gases are obtained. Consider first the case of concentrated combustion, Curve I, Figure 5.12.

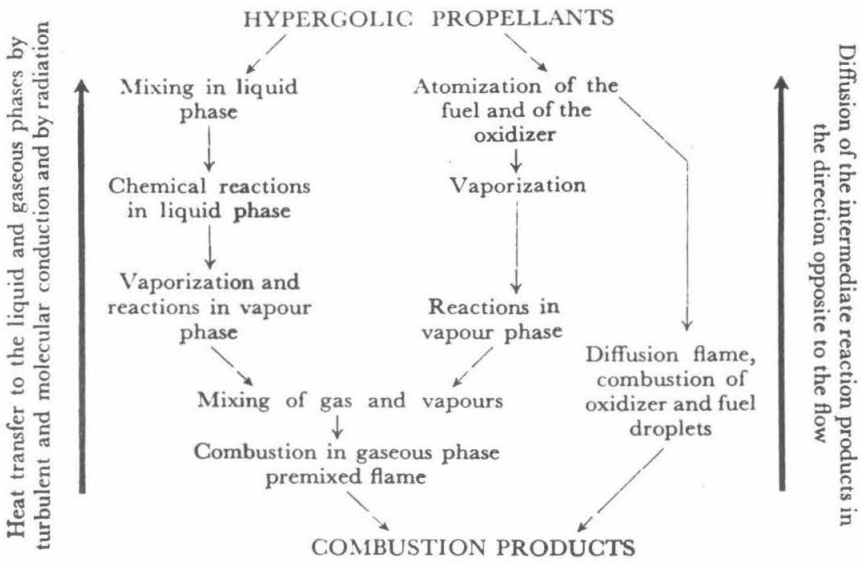

Fig. 5.10

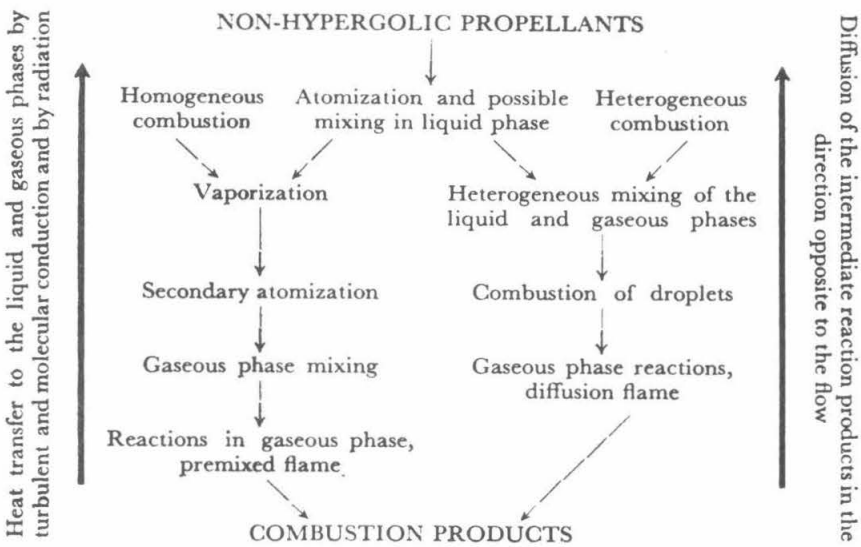

Fig. 5.11

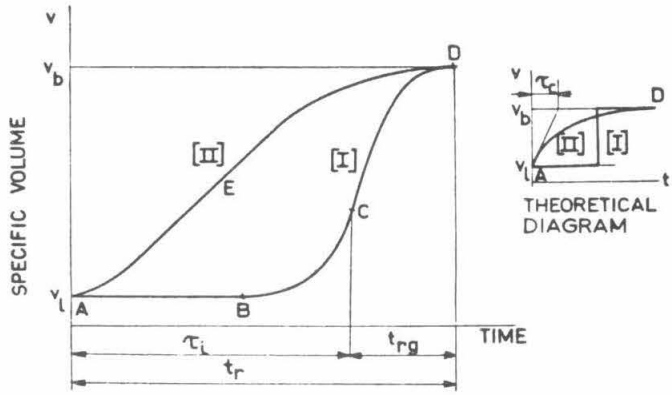

Fig. 5.12. Variation of the specific volume in the combustion chamber as a function of time.

At the origin time (point A), the propellant enters the combustion chamber in liquid phase. It is atomized; oxidizer and fuel are then mixed, and if we assume a certain delay before the chemical phenomena and vaporization take place, the change in volume starts at B. The increase is at first slow but then becomes more rapid. After point C, the combustion reactions start and continue until point D, the nozzle entrance. In this case we can assume:

(1) That the propellant does not burn immediately on entering the combustion chamber, but only after a certain time interval known as the ignition delay τ_i during which the particles of oxidizer and fuel are suitably mixed and absorb the amount of energy necessary to initiate combustion.

(2) That the gases resulting from combustion stay during a certain time t_{rg} in the combustion chamber until combustion is complete.

The processes undergone by the propellant are thus defined by

two characteristic times:

- the time τ_i during which the liquid phase predominates;
- the time t_{rg} during which the gaseous phase predominates.

The total residence time is, therefore, equal to:

$$t_r = \tau_i + t_{rg}$$

Consider now the case of distributed combustion, Curve II, Fig. 5.12. We assume that the chemical reaction first starts in the liquid phase and continues in the gaseous phase when the propellant enters the chamber. It is no longer possible to distinguish τ_i and t_{rg}; nevertheless, it is possible to define a time constant due to the combustion τ_c and a time constant θ for the chamber. If, for example, we assume a first-order chemical reaction to take place in the propellant, τ_c is equal to the reciprocal of the specific reaction velocity, and this time is defined by the tangent to the exponential curve at time $t = 0$. The time constant for the chamber is equal to the residence time of the gaseous mass. It is thus possible in both cases to introduce two characteristic times, τ_i or τ_c for the combustion, and t_{rg} or θ for the chamber.

The minimum volume required for satisfactory combustion must take into account τ_i or τ_c, which we shall refer to by the letter τ, and the residence time t_{rg}. To define the minimum volume we can write

$$\frac{L^*}{c^*} = f_1(\tau) + f_2(t_{rg}) \qquad (5.2)$$

where L^* is the characteristic length:

$$L^* = \frac{V_c}{A_t} = \frac{\text{volume of the chamber}}{\text{nozzle throat area}} \quad . \qquad (5.3)$$

It is, therefore, necessary to know $f_1(\tau)$ and $f_2(t_{rg})$ in order to determine L^*, the characteristic velocity c^* being known. To a first approximation, the characteristic time τ can be neglected, so that the residence time t_{rg} can be defined as the ratio of the mass of gas m_c residing in the chamber to the amount of propellant injected $\dot{m}$ per unit time:

$$t_{rg} = \frac{m_c}{\dot{m}} \tag{5.4}$$

According to the elementary theory, the assumption is made that under steady-state conditions, an average specific mass $\overline{\rho}_c$ holds for the entire volume V_c of the thrust chamber, including the volume of the combustion chamber and the volume of the convergent section, and is equal to the specific mass of the burnt gases. Then

$$t_{rg} = \frac{\overline{\rho}_c V_c}{\dot{m}} = \frac{\overline{\rho}_c}{p_c} \cdot c^* L^* \tag{5.5}$$

and we obtain

$$f_2(t_{rg}) = \frac{p_c}{\overline{\rho}_c} \frac{1}{c^{*2}} \cdot t_{rg} \tag{5.6}$$

Assuming that γ is constant throughout expansion, we obtain

$$\frac{p_c}{\overline{\rho}_c} \cdot \frac{1}{c^{*2}} = \gamma \left(\frac{2}{\gamma+1} \right)^{\frac{\gamma+1}{\gamma-1}} \frac{\rho_c}{\overline{\rho}_c} = \Gamma^2 \frac{\rho_c}{\overline{\rho}_c} \tag{5.7}$$

relating the characteristic velocity c^*, the characteristic length L^*, and the residence time of the gaseous mass t_{rg}. Taking the value of γ to be 1.2, $\Gamma = 0.6485$, and assuming $\overline{\rho}_c = \rho_c$, it follows

$$t_{rg} = \frac{1}{\Gamma^2} \frac{L^*}{c^*} = 2.38 \frac{L^*}{c^*} \tag{5.8}$$

Thus, for a motor having $L^* = 2$ m and $c^* = 1500$ m/sec, $t_{rg} = 3.17 \times 10^{-3}$ sec, and usually $2 \times 10^{-3} < t_{rg} < 7 \times 10^{-3}$ sec. The residence time t_{rg} depends on the nature of the propellant and the injection system. With the aid of chambers having transparent walls, it can be shown that this residence time varies from 2 to 7 milliseconds, depending on the type of injector.

To a first approximation, therefore, it is possible, for a given type of injector and a given propellant, to calculate the volume of the chamber using the relationship:

$$V_c = t_{rg} \Gamma^2 c^{*2} \frac{\dot{m}}{p_c} = K \frac{\dot{w} T_c}{p_c M_c} \approx K' \frac{F}{p_c} \frac{T_c}{M_c} \qquad (5.9)$$

where F is the motor thrust and K, K' are constants. In determining the minimum volume, however, the characteristic times τ and t_{rg} must both be taken into account according to the relation:

$$V_c = A_t c^* \left[f_1(\tau) + f_2(t_{rg}) \right] \qquad (5.10)$$

where f_1 is a function of the injection-pressure drops Δp_O and Δp_H of the oxidizer and the fuel, the chamber pressure p_c, the nature of the combustion gases and their temperature, the turbulence, and the position and arrangement of the oxidizer and fuel jets. Examination of high-speed films taken in combustion chambers with transparent walls shows heterogeneous conditions of temperature, composition, and velocity. There is no flame front in a plane perpendicular to the axis of the chamber. On the contrary, what is actually seen is a series of luminous trails in the longitudinal direction, which indicates a stratified flow. It is even possible to detect products of combustion

proceeding upstream and recirculation behind the injection zone, and and generally the intensity of the transverse flow is not sufficient to mix this longitudinal stratification. The intensity of this recirculation modifies the effective volume of the combustion chamber and thus the characteristic length necessary for complete combustion.

Instead of a characteristic time, one may consider a characteristic length where the combustion process is observed in each point x along the axis of the chamber with origin in the plane of injection. The parameters representing the combustion process are then:

$$\xi_{\dot{m}} = \frac{\dot{m}_b(x)}{\dot{m}_i} = \frac{\text{propellant burnt at the abscissa x}}{\text{propellant injected}} \qquad (5.11)$$

or another parameter which is equivalent to the above:

$$\xi_{c^*} = \frac{c^*(x)}{c^*(L)} = \qquad (5.12)$$

$$\frac{\text{characteristic velocity at the abscissa x}}{\text{characteristic velocity at the end of the combustion chamber}} \; .$$

The classical method is to carry out a series of tests using motors of different length and to measure in each case the characteristic velocity c^*. In this way curves similar to those of Fig. 5.13 are obtained and they determine the optimum length for the combustion chamber. These curves are valid for a given propellant and a given injection system, while the ratio

$$\varepsilon_c = \frac{A_c}{A_t} = \frac{\text{chamber cross-section}}{\text{throat area}} \qquad (5.13)$$

and the mixture ratio are constant. This optimum length, however, depends on the mixture ratio. This is indicated in Fig. 5.14 for the propellant nitric acid-UDMH. It is possible to define a surface using

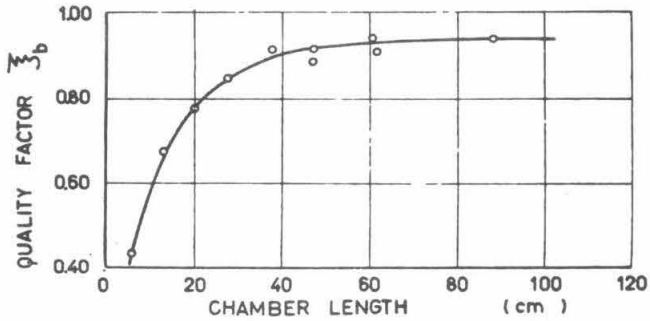

Fig. 5.13. Variation in the characteristic velocity as a function of the length of the combustion chamber.

the coordinates (L^*, c^*, Φ^*), the top of which determines the geometry and the optimum operating conditions of the combustion chamber. We note in particular that the optimum performance shifts towards richer mixtures when shorter combustion chambers or shorter characteristic lengths are used. From the practical point of view, therefore, it is necessary to carry out numerous tests in order to decide on the shape

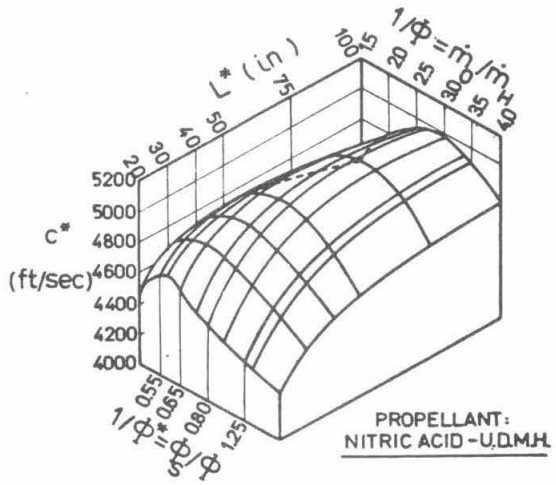

Fig. 5.14. Characteristic velocity as a function of characteristic length L^* and equivalence ratio (propellant: nitric acid-UDMH).

of the combustion chamber giving optimum performance.

This length also depends on the nature of the propellant as indicated below for various propellants:

nitric acid-hydrocarbons	$2 < L^* < 3$ m
nitric acid-UDMH	$1.5 < L^* < 2$ m
liquid oxygen-ethyl alcohol	$2.5 < L^* < 3$ m
liquid oxygen-kerosene	$1.5 < L^* < 2.5$ m
fluorine-ammonia	$1 < L^* < 1.5$ m

The ratio ε_c defining the optimum cross-section to be given to the combustion chamber depends above all on the size of the motor and decreases as the thrust of the motor increases. In early practice, motors had values of ε_c between 4 and 15, while current practice tends toward longer chambers with $1.2 < \varepsilon_c < 4$; for instance, $\varepsilon_c = 3$ to 4 (F = 1 ton), $\varepsilon_c = 2$ to 3 (F = 10 tons), $\varepsilon_c = 1.2$ to 2 (F = 100 tons). The choice of ε_c is equivalent to giving a certain value to the flow rate per unit area:

$$\frac{\dot{w}}{A_c} = \frac{g\, p_c}{c^*} \cdot \frac{1}{\varepsilon_c} \qquad (5.14)$$

Rocket Nozzle Cooling

The heat transfer between the combustion gases and the walls of the chamber and nozzle takes place by convection and by radiation.

Consider a fluid at a high temperature moving along the wall of a conducting body. At a point of the wall where the velocity and the temperature of main flow are V_g and T_g, the wall temperature is T_w and the heat flow per unit area is Φ_c :

If we assume an average specific heat at constant pressure c_p, the stagnation temperature T_{tot} corresponding to the total enthalpy is

$$T_{tot} = T_g + \frac{V_g^2}{2c_p} \tag{5.15}$$

At the wall, the fluid generally has a temperature T_f slightly different from the stagnation temperature T_{tot}. The difference between T_{tot} and T_f is taken into account by a coefficient known as the local recovery factor

$$r = \frac{T_f - T_g}{T_{tot} - T_g} = \frac{T_f - T_g}{V_g^2/2c_p} \tag{5.16}$$

The local heat-flow rate per unit area is proportional to the temperature difference $(T_f - T_w)$ so that we can define a local film or convection coefficient

$$h = \frac{\Phi_c}{T_f - T_w} \tag{5.17}$$

Since the fluid is motionless at the wall, the transfer of heat through the fluid film next to the wall takes place by thermal conduction. Fourier's law gives an expression for the thermal flux and the film coefficient:

$$\frac{\Phi_c}{T_f - T_w} = \frac{-k \left(\frac{\partial T}{\partial y}\right)_{y=0}}{T_f - T_w} = h \tag{5.18}$$

k is the thermal conductivity of the fluid at the wall temperature and y is an ordinate perpendicular to the surface. The study of heat transfer in rocket nozzles involves the following dimensionless groups:

Nusselt number $$Nu = \frac{h D}{k}$$

Prandtl number $$P_r = \frac{c_p \mu}{k}$$

Reynolds number $$R_e = \frac{\rho V_g D}{\mu}$$

Mach number $$M = \frac{V_g}{a}$$

where D is a characteristic length, μ and ρ are the absolute viscosity and the mass density of the fluid, and a is the local velocity of sound.

Analysis and experiments on heat transfer by forced convection lead to relations of the type

$$Nu = g_1 (R_e, M, P_r)$$

$$r = g_2 (R_e, M, P_r)$$

Experimental results show that the recovery factor r depends upon the Prandtl number, and in the case of a turbulent boundary layer,

$$r = P_r^{0.33} \qquad (5.19)$$

The convective heat transfer coefficient h is given by the Nusselt number; in the case of a flat plate,

$$Nu = 0.0296 R_e^{0.8} \frac{P_r}{1 + 2.1 R_e^{-0.1} (P_r - 1)} \qquad (5.20)$$

The length involved in the Reynolds number is the distance measured from the leading edge of the plate.

Experimental studies on rocket motors lead to relations of the type

$$Nu = 0.0162\, Pr^{0.82} Re^{0.82} \left(\frac{T_f}{T_w}\right)^{0.55} \qquad (5.21)$$

in which the Reynolds number is calculated using the diameter of the combustion chamber. The Nusselt number is sometimes replaced by the Stanton number

$$St = \frac{h}{\rho c_p V_g} = Nu\, Pr^{-1} Re^{-1} \qquad (5.22)$$

In general, the determination of the heat transfer coefficient in a rocket motor is an extremely complex problem because the values of μ, ρ, c_p, k vary considerably through the boundary layer. For this reason, average values are often taken between these two extreme temperatures, for example $T = \frac{1}{2}(T_g + T_w)$, or use is made of T_g or T_w. Chemical reactions may also take place in the boundary layer, and these can modify the temperatures; it may occur that dissociated species recombine. Generally, the speed of reaction plays a secondary part in determining the mass concentrations of the different chemical species and modifies the local film coefficient only slightly. The heat liberated by recombination reactions appears as an additional "enthalpy potential". There may, in some instances, be a catalytic effect due to the wall which causes local changes in the chemical composition. In many cases, the wall material sublimates or ablates under the effect of the heat transfer; the mass addition leads to a reduced heat transfer rate.

If, as indicated in Fig. 5.15, $T_{w\ell}$ is the temperature on the wall in contact with the liquid and T_ℓ is the temperature of the liquid, the heat flow rate per unit area is

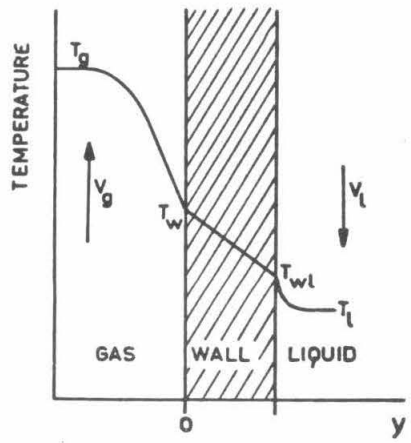

Fig. 5.15. Temperature variation in the boundary layer.

$$\Phi_c = \frac{q}{A} = h_l (T_{wl} - T_l) \tag{5.23}$$

where h_l is the coolant-liquid film coefficient. The laws determining h_l are similar to those for exchange between the gas and the wall, and we get

$$Nu = 0.023 R_e^{0.8} P_r^{0.33} \tag{5.24}$$

In this expression the values of μ, c_p, and k are generally calculated at an average temperature in the liquid boundary layer

$$\tilde{T} = \frac{1}{2}(T_{wl} + T_l)$$

The characteristic length D_l involved in the Reynolds number and the Nusselt number is defined by

$$D_l = \frac{4 A_l}{P_l} \tag{5.25}$$

where A_l is the passage area of the liquid and P_l is the wetted perimeter. Some details of cooling passages are shown in Fig. 5.16.

Under some conditions, the thermal flux may be such that the temperature of the wall T_{wl} on the liquid side is greater than the

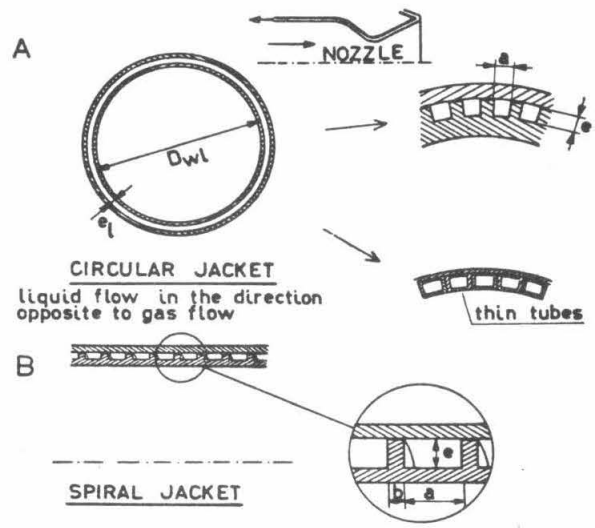

Fig. 5.16. Cooling-jacket shapes.

critical temperature of the liquid at the pressure considered. This results in local boiling which increases the amount of heat that the liquid is capable of absorbing. At higher temperatures, a vapor film is formed in contact with the wall. Near the boiling point, one obtains results similar to those of Fig. 5.17, which shows the change in q/A as a function of $(T_{w\ell} - T_{\ell})$. In general, there exist the four conditions represented in Fig. 5.18 which correspond to:

(1) convection (liquid-wall),

(2) the presence of nuclei in contact with the surface and brought to the boiling point; the formation of vapor bubbles,

(3) the presence of a partial gaseous film,

(4) the presence of a gaseous film over the entire surface.

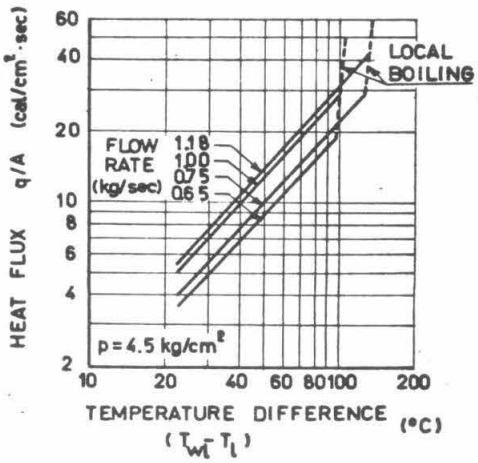

Fig. 5.17. Forced convection with and without local boiling (nitric acid).

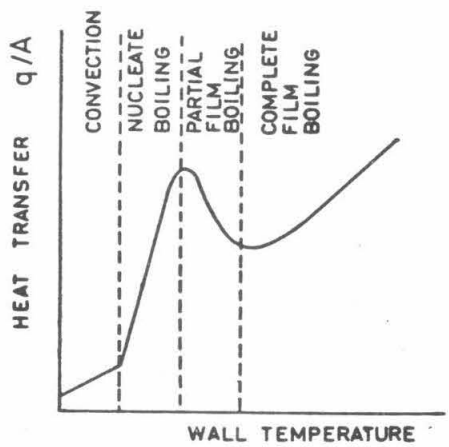

Fig. 5.18. Typical heat-transfer curve.

For liquid-propellant rockets, either the oxidizer or the fuel, or both, may be employed as cooling agents. The liquid is circulated, either through a jacket or in a helicoidal channel covering the surface of the chamber.

The conventional design for a combustion chamber having a double wall is shown in Fig. 5.19. The liquid enters at the end of the divergent section and is guided along the wall of the nozzle by means

of a jacket leaving a passage for the fluid. The passage area is smaller at the throat in order to increase the heat transfer in this region. The liquid then passes through the cylindrical combustion chamber and and leaves on the side near the injection system.

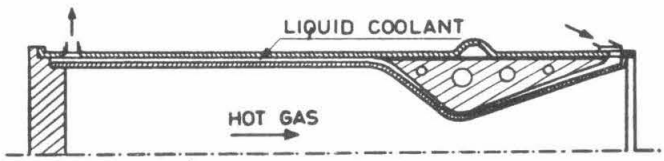

Fig. 5.19. Circulation of the coolant liquid parallel to the hot gases.

More recent designs of regenerative cooling systems use a bundle of tubes in which the coolant circulates under pressure. Such a solution is represented schematically in Fig. 5.20. The cross section of each tube has two flat parts and two circular parts. Such a

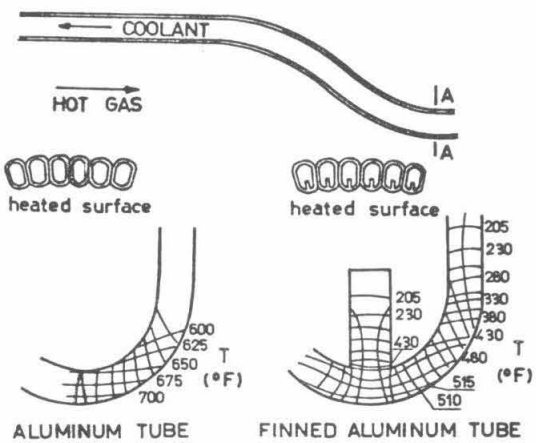

Fig. 5.20. Circulation of the coolant liquid parallel to the hot gases (tube bundles).

cooling system is very efficient since the metal between the gas and the liquid is very thin. It is difficult to manufacture a combustion chamber of this type, because it is necessary to weld the tubes in

such a way that they withstand the pressures and thermal stresses encountered. In addition, the cross section of the throat determines the number of tubes so that it may be necessary to use tubes of varying cross sections. For the divergent nozzle, a V-shaped arrangement must be adopted such that it covers the entire surface, this being particularly important when the area ratio is large. Whatever the case, it is possible with this method to accommodate any chamber and nozzle shape, and the weight saving over conventional methods is considerable.

Use may also be made of a helicoidal thread or rib to construct coolant passages. The wire is welded onto the wall, and the diameter of the wire fixes the distance between the two walls within which the coolant circulates. If a thread is machined in the wall of the chamber, the temperature in the metal is not uniform. The thickness of the thread must be such that it does not disturb the transmission of heat to the wall and there is no hot spot on the wall at the thread.

The liquid employed in the cooling circuit should not exceed its boiling point, or at least the temperature of the wall $T_{w\ell}$ should remain below a certain value, above which nucleate boiling takes place. We can thus define the limiting temperature $(T_{w\ell})_{\ell}$, and for $T_{w\ell} > (T_{w\ell})_{\ell}$, the thermal flux Φ_t increases abruptly; this transition point is associated with a value of Φ_t equal to $\Phi_{u\ell}$, which is the heat flux at the upper limit of nucleate boiling. This value of $\Phi_{u\ell}$ can be used as a criterion to calculate a cooling efficiency of the propellant. In general, $\Phi_{u\ell}$ passes through a maximum for a certain pressure and hardly varies when the pressure lies between 0.3 and 0.7 times the critical

pressure. It decreases when T_ℓ increases, increases with the velocity of the liquid V. A true comparison of the different propellants cannot be made simply by considering the properties of the liquids. Bartz has compared them from the theoretical point of view by using them in a standard motor having the following characteristics: a thrust of the order of 25 tons (metric), a chamber pressure of 20 kg/cm^2, a characteristic length of 100 cm, a throat diameter of 31 cm, a convergent area ratio $A_c/A_t = 2/1$, a divergent area ratio $A_e/A_t = 7/1$, a convergent half-angle of 30°, a divergent half-angle of 15°, and a pressure drop in the cooling system of 5.25 kg/cm^2. The table on page 176 results from the analysis.

In the process of film cooling and sweat cooling, a liquid or gaseous film is introduced between the combustion products and the wall to form a thermal barrier. In the case of the liquid, the film vaporizes and may play a part in the combustion. In the case of a fuel, the richness of the mixture in this region reduces the combustion temperature and hence the thermal flux penetrating the wall. This film is obtained either by injecting the fuel through carefully situated orifices in the wall (film cooling) or by using the transpiration of one of the liquids through the porous material constituting the chamber wall (sweat cooling). Film cooling has been the most favored, and in liquid-propellant rockets, the fuel injection orifices are distributed in a cross section of the chamber, either near the injection head or in the convergent section of the nozzle.

In solid-propellant rockets, the nozzle might be protected by a gaseous film produced from the combustion of a special propellant

Sections	*1*	*2*	*3*	*4*	*5*	*6*	*7*	*8*	*9*	*10*	*11*	*12*	*13*	*14*
$(T_{wg})_2$ °K	728	752	883	1065	1155	1079	1005	941	884	830	783	738	698	662
$(T_{wg})_3$ °K	732	727	881	1112	1189	1101	1014	941	880	833	783	740	709	684
Φ_c cal/cm² · sec	42.05	46.0	82.12	136.4	157.9	139.1	121.1	106.6	94.9	85.5	76.5	68.9	62.7	57.8
Φ_t cal/cm² · sec	58.2	60.7	93.9	145.2	163.9	144.7	126.1	111.1	98.76	88.9	79.3	71.1	64.3	58.9

TABLE 15

Coolant liquid	*Other liquid*	*1* *Mixture ratio*	*2* T_c °K	*3* Φ_t *cal/cm² · sec*	*4* $\dot{w}$ *kg/sec*	*5* e_t *cm*	*6* V_t *m/sec*	*7* T_t °K	*8* Φ_{nt} *cal/cm² · sec*	*9* T °K *(26.2atm)*	*10* $(T_t)_{ex}$ °K
a RFNA	UDMH	0.40	2664	228	71.67	0.277	18.53	355	344	453	390
b Corporal	SFNA	0.33	2743	198	26.90	0.182	15.03	390	320	578	454
c DETA	SFNA	0.33	2671	196	26.0	0.184	17.86	374	281	666	425
d 50An50FA	SFNA	0.33	2753	192	27.03	0.183	15.24	386	211	633	447
e JP_3	N_2O_4	0.33	2892	192	25.31	0.181	19.32	387	205	627	449
f NH_3	RFNA	0.45	2347	218	32.07	0.156	22.10	306	207	333	333
g Isopropanol	SFNA	0.30	2636	205	25.08	0.189	19.2	370	176	561	418
h NH_3	O_2	0.71	2712	255	38.69	0.175	23.77	306	227	333	330
i JP_3	O_2	0.44	3098	235	28.21	0.194	20.45	409	201	627	464
j ClF_3	N_2H_4	0.4	3267	228	65.77	0.232	17.62	374	166	399	424

1 = mixture ratio
2 = 90% of the theoretical value
3 = thermal flux at the throat
4 = total coolant flow rate
5 = thickness of the cooling jacket
6 = velocity of the liquid at the throat
7 = temperature of the liquid at the throat (inlet temperature 311°K for all substances except for NH_3, for which we have 273°K)
8 = upper limit of heat flux with nucleate boiling
9 = saturation temperature.

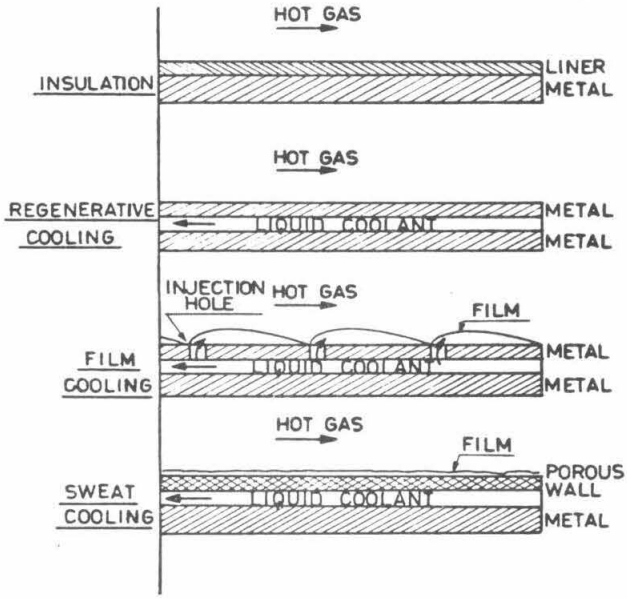

Fig. 5.21. Cooling systems.

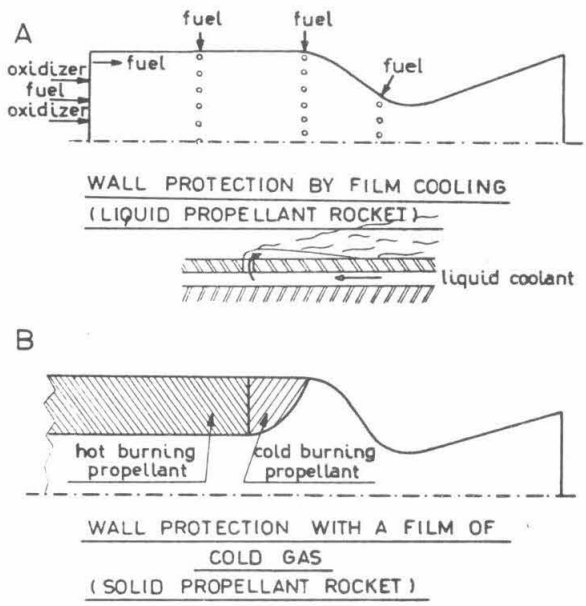

Fig. 5.22. Wall protection by film cooling.

having a relatively low combustion temperature. The thermal flux Φ_t to the wall is modified by this mass addition. Fig. 5.23 shows that Φ_t changes slowly when the flow rate $\dot{m}_c$ is low (main flow rate $\dot{m}_m$),

since Φ_t decreases linearly with $f = \dot{m}_c/\dot{m}_m$ up to a certain value of f of the order of 0.10; after this, Φ_t remains practically constant. The effect is greatest in the section near the throat.

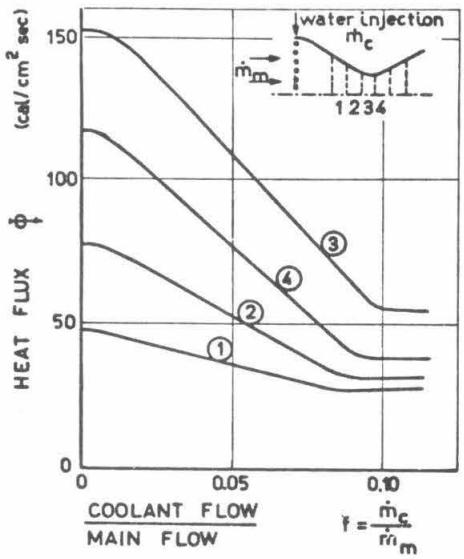

Fig. 5.23. Transmission of heat to the wall as a function of the ratio of the coolant flow to main flow.

These results show that for the film cooling to be efficient, it is necessary to inject up to 10 per cent of the main fuel flow with a corresponding decrease in overall specific impulse.

One of the problems which arises when using film cooling is the stability of the film. Slight disturbances are observed, their wavelength being of the order of 10 times the thickness of the film, and these disturbances are independent of the liquid flow. These disturbances decrease when the Reynolds number for the gaseous flow increases. If the velocity of the liquid at the injector exit exceeds a certain critical value, the wavelength of the disturbances increases and droplets start to be carried off by the gas flow.

Consider the sweat-cooled plate represented in Fig. 5.24: the flow velocity is $V_{x,b}$ at temperature T_b; the gas is injected at velocity $V_{y,w}$ and is assumed to have the same properties as the main fluid; the temperature of the wall is T_w. The parameter characterizing these two flows is $\lambda = (V_{y,w}/V_{x,b})(R_e)^{0.5}$, the Reynolds number being equal to $V_{x,b} \cdot x/\nu$. For different values of λ, the values for the film coefficients h and h_c with and without sweat cooling are

λ = 0	0.25	0.375	0.5
h/h_c = 1	0.496	0.282	0.107

For low values of λ, h/h_c varies linearly with λ, i.e., with the injection velocity of the fluid in the porous surface.

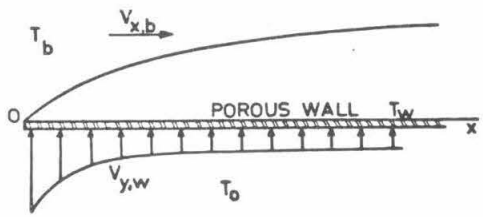

Fig. 5.24. Sweat cooling.

Propellant Feed System

It is the task of the feed system to supply the liquid-propellant motor with the amounts of propellant that it requires at each time. We shall consider below the two types of feed system; (a) the gas-pressure system, and (b) the turbopump system.

Gas-pressure systems differ according to the nature of the gases introduced into the tanks:

(a) The cold gas-pressure system: a neutral gas stored at high pressure is expanded into the tanks.

b) The feed system employing the combustion gases of a small solid-propellant grain;

c) The hot gas-pressure feed system: a small quantity of solid propellant is burnt in a neutral gas under pressure.

The cold gas system is represented schematically in Fig. 5.25. It consists of a high-pressure tank of volume V, a pressure regulator, and a check valve at the outlet of which there is a low-pressure distributor connected to the oxidizer and fuel tanks. This low pressure forces the liquid into the combustion chamber and, for a particular pressure in the tanks, a state of equilibrium is established between the flow through the nozzle throat and the injector discharge rate. In rockets with a gas-pressure feed system, the high-pressure tank represents an important item in the weight balance of the missile. It is, therefore, advisable to reduce its volume to the minimum compatible with satisfactory operation.

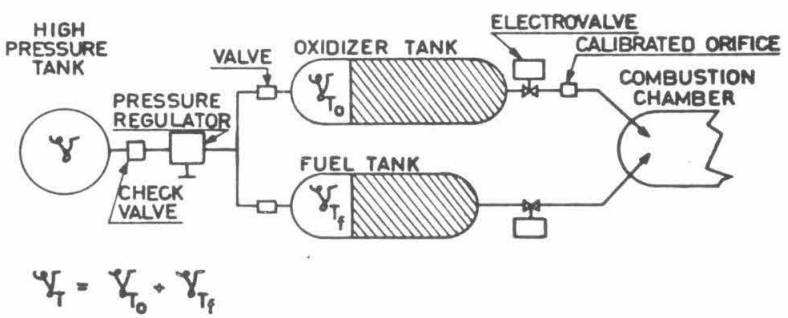

Fig. 5.25. Feed system using pressurized gas.

Although the high-pressure tank may not be too large, it must have a volume sufficiently great to ensure that the combustion chamber is properly supplied throughout the entire period of operation. The

tank pressure must always be high enough, compared with the feed pressure, not to give rise to oscillations which would result in pressure instability in the combustion chamber.

In practice, it is difficult to determine the optimum gaseous volume necessary to ensure proper emptying of the propellant tanks, and certain assumptions must be made. We shall make use of the following symbols:

known data

V_T = volume of the oxidizer and fuel tanks $V_{T_O} + V_{T_H}$

p_i = initial pressure in the high-pressure tank

T_i = initial temperature in the high-pressure tank

p_T = pressure in the propellant tanks: feed pressure

unknown

The practical volume V of the high-pressure tank. Let us introduce here the dimensionless variable $k = V/V_T$.

intermediate parameters

p_f, T_f = final pressure and temperature in the high-pressure tank,

W_i, W_f = weight of gas contained in the high-pressure tank at the beginning and end of operation,

T_T = final gas temperature in the propellant tanks,

W_T = weight of compressed gas contained in the oxidizer and fuel tanks at the end of delivery.

Let us now write the gas equations for the following conditions:

-- initial state of the gas in the high-pressure tank:

$$p_i V = W_i R T_i$$

-- final state of the gas in the high-pressure tank:

$$p_f V = W_f R T_f$$

-- final state of the gas in the oxidizer and fuel tanks:

$$p_T V_T = W_T R T_T$$

At the end of the feed period, all the gas is distributed between the feed tank and the oxidizer and fuel tanks:

$$W_i = W_f + W_T$$

so that we can write

$$k = \frac{V}{V_T} = \frac{p_T}{T_T} \Big/ \left(\frac{p_i}{T_i} - \frac{p_f}{T_f} \right) \tag{5.26}$$

The expansion of the gas in the tank between p_i and p_f cannot be regarded as adiabatic since it exchanges heat with the wall. By introducing a coefficient for polytropic expansion,

$$\frac{T_f}{T_i} = \left(\frac{p_f}{p_i} \right)^{n\left(\frac{\kappa-1}{\kappa}\right)} = \left(\frac{p_f}{p_i} \right)^{n} = \tag{5.27}$$

and, if a_2 denotes the ratio T_T/T_i, the parameter k equals

$$k = \frac{a_1}{a_2} \left(\frac{p_T}{a_1 p_i - p_T} \right) \tag{5.28}$$

where a_1 and a_2 are empirical coefficients. Regarding the value of n, there is some difference of opinion between the various authors. The values for n range between 0.1 and 0.3. Values for a_2 for different values of the ratio p_i/p_f are:

p_i/p_f	10	7	4	2
a_2	0.75	0.80	0.87	0.90

Since the operation of the pressure valve must be accurate and free from instability at the end of the feed period, there is every justifica-

tion for a safety margin in choosing p_f. For all values of p_i below 200 kg/cm^2, we shall take:

$$p_f = p_T + 10 \text{ kg/cm}^2$$

A higher value of Δp would require an undesirably large high-pressure tank.

The parameters a_1 and a_2 can be found analytically if certain assumptions are made and new experimental parameters are introduced. For an adiabatic process, neglecting the Joule-Thomson effect, the First Law of Thermodynamics gives

$$W_i c_v T_i = W_f c_v T_f + W_T c_v T_T + p_T V_T \tag{5.29}$$

where c_v is the specific heat at constant volume. Using the equation of state,

$$\frac{p_i V c_v}{R} = \frac{p_f V c_v}{R} + \frac{p_T V_T c_v}{R} + p_T V_T$$

and

$$k = \frac{V}{V_T} = \frac{c_v + R}{c_v} \left(\frac{p_T}{p_i - p_f} \right) = \frac{\gamma p_T}{p_i - p_f} \tag{5.30}$$

The curves represented in Fig. 5.26 have been calculated numerically; the value of k is given as a function of the feed pressure, the initial storage temperature T_i being regarded as an auxiliary parameter. The use of storage pressures lower than 150 kg/cm^2 leads to very large tank volumes, while for values higher than 350 kg/cm^2 the advantage of the reduced gas volume hardly compensates for the increased tank weight.

The turbopump feed system is employed for rockets with a high thrust and a long burning time, and is therefore of interest when the volume of the propellant tanks is large. The main advantages of such

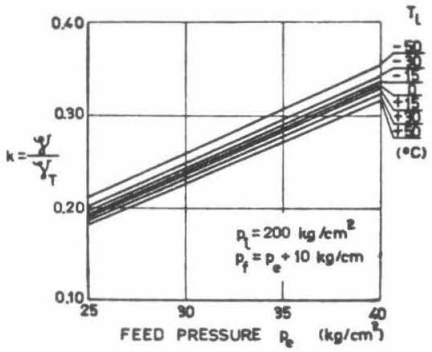

Fig. 5.26. Value of k as a function of p_e, for p_i = 200 kg/cm^2 ($p_f = p_e$ + 10 kg/cm^2 and n = 0.11).

an arrangement are:

(1) good flexibility in operation can be obtained through controlling the pump speed;

(2) high, stable pressures can be obtained, the pressure remaining practically constant for a given set of operating conditions;

(3) high power-to-weight ratio and small volume requirements.

Pumps can be classified according to the geometry of the impeller and the path of the fluid. There are three categories of pumps (Fig. 5.27); centrifugal or radial, mixed flow, and axial. Pumps for rocket motors are usually of the first or second types.

We introduce the following notation, see Fig. 5.28:

V_a = absolute velocity of the fluid

V_e = peripheral velocity of the blade

V_r = relative velocity

α = angle between V_a and V_e at a given point

β = angle between velocity V_r and direction V_e

ω = angular velocity = $2\pi N$ (N = number of revolutions per sec)

A = the cross section at the point considered

r = radius of the cross section

and denote conditions at the impeller inlet and discharge by the subscripts 1 and 2. The torque T applied to the impeller is

$$T = \int_{A_2} r_2 V_{a2} \cos\alpha_2 \, d\dot{m} - \int_{A_1} r_1 V_{a1} \cos\alpha_1 \, d\dot{m} \qquad (5.31)$$

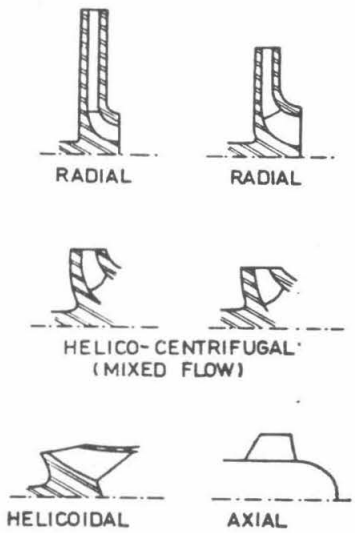

Fig. 5.27. Turbopump types.

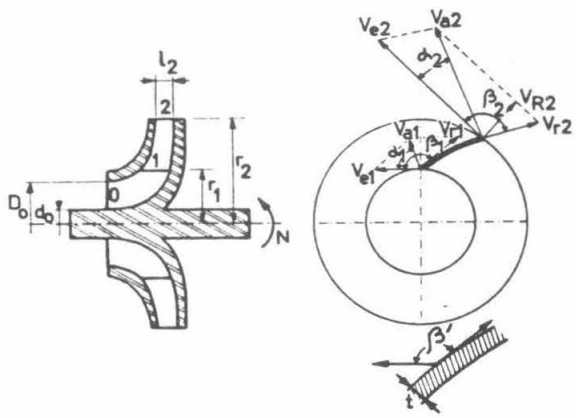

Fig. 5.28. Diagram showing the operation of a pump.

and the theoretical power P delivered to the impeller is:

$$P = T\omega = \int_{A_2} V_{\theta 2}\, V_{a2} \cos\alpha_2\, d\dot{m} - \int_{A_1} V_{\theta 1}\, V_{a1} \cos\alpha_1\, d\dot{m} \qquad (5.32)$$

The power divided by the weight flow rate through the impeller, denoted by the letter H_{th}, is the theoretical head given by Euler's formula:

$$H_{th} = \frac{P}{\dot{m} g} = \frac{1}{\dot{m} g}\left[\int_{A_2} V_{\theta 2}\, V_{a2} \cos\alpha_2\, d\dot{m} - \int_{A_1} V_{\theta 1}\, V_{a1} \cos\alpha_1\, d\dot{m}\right] \qquad (5.33)$$

Without losses, the increase in stagnation pressure between the inlet and the outlet of the pump is

$$\Delta p_{th} = \rho_p g\, H_{th} \qquad (5.34)$$

where ρ_p is the mass density of the fluid passing through the pump. If the velocities are uniform at all points, and if the mass flow in the impeller is denoted $\dot{m}$, we obtain

$$T = \dot{m}\left[r_2 V_{a2} \cos\alpha_2 - r_1 V_{a1} \cos\alpha_1\right] \qquad (5.35)$$

and

$$\Delta p_{th} = \rho_p\left[V_{\theta 2}\, V_{a2} \cos\alpha_2 - V_{\theta 1}\, V_{a1} \cos\alpha_1\right] \qquad (5.36)$$

The ratio of experimental and theoretical pressure rises is written

$$\eta_p = \frac{\Delta p_{real}}{\Delta p_{theoretical}} \qquad (5.37)$$

where η_p takes into account all losses.

To represent the performance of a pump, the independent variables normally chosen are the volumetric discharge Q and the angular velocity of the shaft $\omega = 2\pi N$ so that the pressure rise Δp, the torque T, the power P delivered by the motor, and the efficiency η are ex-

pressed in the following manner:

$$\begin{aligned} \Delta p &= f(Q,\omega) \\ T &= f'(Q,\omega) \\ P &= f''(Q,\omega) \\ \eta &= f'''(Q,\omega) \end{aligned} \tag{5.38}$$

These characteristics are not independent; if two of them are known, the others can be found with the aid of the relations

$$\begin{aligned} P &= T\omega \\ \eta &= \frac{\Delta p \cdot Q}{P} \end{aligned} \tag{5.39}$$

The characteristic curves usually are represented at a constant angular velocity; Fig. 5.29 shows the curves $\Delta p = f(Q)$, $P = f''(Q)$, and $\eta = f'''(Q)$.

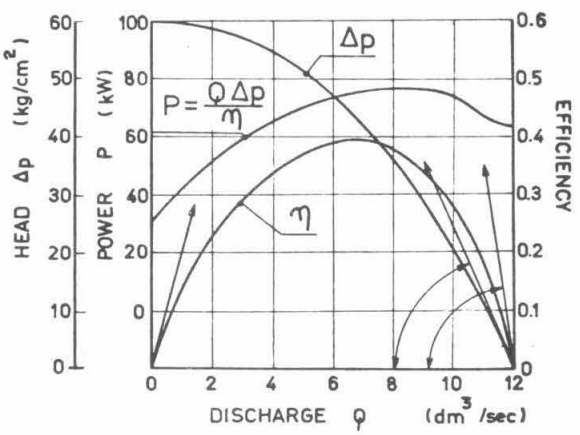

Fig. 5.29. Pump characteristics: variations in the power P, pressure rise Δp, and efficiency η as functions of the flow Q (N = 333 revolutions per sec).

For various angular velocities, the pressure-discharge characteristics of a given pump are shown in Fig. 5.30. They may be deduced from each other with the aid of rules of similitude. The flow Q is proportional to N, the head or the pressure rise Δp being propor-

tional to N^2. The homologous points lie on parabolas corresponding to constant values of Q/N or to constant efficiencies.

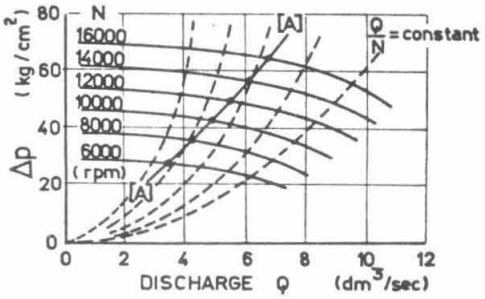

Fig. 5.30. Pressure-flow characteristics at different speeds.

In the case of a rocket motor with a variable thrust, obtained by variation of the pump speed, the operating point does not generally follow a curve of constant efficiency; the locus of the points is a distinct curve (A) and the ratio Q/N decreases with the speed.

The fundamental quantities involved in selecting a pump are the discharge Q, the pressure rise ΔP, or the head $H = \Delta p/\rho_p g$, the mass density ρ_p, and the shaft speed N or ω. The head H is proportional to $\omega^2 r_2^2$ and the volumetric flow to ωr_2^3, so that:

$$H = \frac{\Psi}{g} \omega^2 r_2^2 \tag{5.40}$$

and

$$Q = \Phi \omega r_2^3 \tag{5.41}$$

Eliminating r_2, we get:

$$\Phi \left(\frac{g}{\Psi}\right)^{3/2} = \frac{\omega^2 Q}{H^{3/2}} \tag{5.42}$$

If, now, we consider the pump which is geometrically similar to the one of interest, working at the same operating point, with a discharge

of 1 m^3/sec and a head of 1 m , the angular velocity of such a pump is the <u>specific speed</u> ω_s :

$$\omega_s^2 = \Phi \left(\frac{g}{\psi}\right)^{3/2} \tag{5.43}$$

For the real pump, therefore, we have

$$\omega_s = \omega \sqrt{Q}\, H^{-3/4} \tag{5.44}$$

or, introducing the shaft speed in revolutions per second,

$$N_s = N \sqrt{Q}\, H^{-3/4} \tag{5.45}$$

If, instead of expressing Q in m^3/sec and H in m, we employ gallons per minute and feet, we obtain

$$N_s \text{ (British Units)} = 51.6\, N_s \text{ (metric Units)} \tag{5.46}$$

The performance of a pump is limited by cavitation, which appears as soon as the static pressure p at some point falls below the vapor pressure p_v of the liquid. If this phenomenon is to be avoided, $p > p_v$; if this condition is not fulfilled, bubbles will form locally and these collapse abruptly when they reach a region of pressure higher than p_v . In regions of condensation, violent shocks are produced leading to rapid erosion of the surfaces. It can be noted that for a given suction pressure the experimental characteristic line suddenly breaks away from the normal characteristic line and falls rapidly; this break is associated with cavitation.

If cavitation is to be avoided, the minimum pressure in the pump p_{min} must be greater than or at least equal to the saturated vapor pressure of the liquid p_v, that is, $p_{min} > p_v$. The minimum pressure is produced in the neighborhood of the leading edges of the

blades, on their rear face. It is given by the expression:

$$p_1 - p_{min} = \lambda \rho_p \frac{V_{r1}^2}{2} \tag{5.47}$$

where p_1 is the pressure immediately before entering the impeller blades, V_{r1} is the relative velocity of the fluid at this same point, and ρ_p is the mass density of the fluid. The coefficient λ is in practice between 0.2 and 0.4.

For a rocket pump whose geometric suction head and suction pressure loss are negligible, pressure p_1 is related to the suction pressure p_{suc} :

$$p_1 = p_{suc} - \rho_p \frac{V_{a1}^2}{2} \tag{5.48}$$

where V_{a1} is the absolute velocity of the fluid just before entry to the impeller blades. Combining the last two relations, we get:

$$p_{suc} - p_{min} = \frac{\rho_p}{2} \left(V_{a1}^2 + \lambda V_{r1}^2 \right) \tag{5.49}$$

Let us try to find the lower limit of suction pressure which can be permitted without the risk of cavitation, and let us call this pressure $(p_{suc})_\ell$. Taking into account the necessity of a certain safety margin, we can write:

$$(p_{suc})_\ell - p_v = \frac{\rho_p \phi}{2} \left(V_{a1}^2 + \lambda V_{r1}^2 \right) \tag{5.50}$$

where ϕ is a factor of safety lying between 1.2 and 1.4. Let us assume that the triangle of inlet velocities has a right angle; then

$$V_{r1}^2 = V_{a1}^2 + V_{e1}^2$$

and

$$(p_{suc})_\ell - p_v = \frac{\rho_p \varphi}{2}\left[(1+\lambda) V_{a1}^2 + \lambda V_{e1}^2\right] \qquad (5.51)$$

Dividing by the pressure rise of the pump Δp, the preceding relation gives:

$$\frac{(p_{suc})_\ell - p_v}{\Delta p} = \frac{\rho_p V_{e2}^2}{\Delta p}\,\frac{\varphi}{2}\left[(1+\lambda)\left(\frac{V_{a1}}{V_{e1}}\right)^2 + \lambda\left(\frac{V_{a1}}{V_{e2}}\right)^2\right] \qquad (5.52)$$

The head coefficient is:

$$\psi = \frac{\Delta p}{\rho_p V_{e2}^2}$$

For a given pump and similar operating conditions:

V_{a1}/V_{e1} = constant, V_{a1}/V_{e2} = constant, ψ = constant

and hence:

$$\frac{(p_{suc})_\ell - p_v}{\Delta p} = \text{constant} = a$$

Introducing the specific speed, which is also a constant for the operating conditions in similitude;

$$N_s = N Q^{1/2} H^{-3/4} \qquad (5.53)$$

$$H = \frac{\Delta p}{\rho_p g} = \left(\frac{N\sqrt{Q}}{N_s}\right)^{4/3} \qquad (5.54)$$

and finally

$$(p_{suc})_\ell - p_v = a \rho_p g \left(\frac{N\sqrt{Q}}{N_s}\right)^{4/3} \qquad (5.55)$$

or, in terms of the heads,

$$(H_{suc})_\ell - H_v = a\left(\frac{N\sqrt{Q}}{N_s}\right)^{4/3} \qquad (5.56)$$

where $(H_{suc})_\ell - H_v$ is often called the required suction head above vapor pressure. Replacing the specific speed N_s by the values corresponding to the radial pumps employed in rocket motors, we arrive at the following formula:

$$(p_{suc})_\ell = p_v + \rho_p g \cdot 10^{-3} \left(\frac{N\sqrt{Q}}{\beta} \right)^{4/3} \qquad (5.57)$$

in which the pressures are expressed in atmospheres and where β is between 13 and 17, N is the number of shaft revolutions per second, Q is the volumetric flow rate in m^3/sec, and $g\ \rho_p$ is the specific weight in kg/m^3. From this relation, we can deduce the maximum shaft speed when the suction pressure is fixed:

$$N_{max} = \frac{\beta}{\sqrt{Q}} \left(\frac{H_{suc} - H_v}{10} \right)^{3/4} \qquad (5.58)$$

The power necessary for driving the feed pumps is obtained from a gas turbine. As represented in Fig. 5.31, an auxiliary combustion chamber is used as a high-pressure gas generator to feed the turbine. The latter drives the two pumps for the oxidizer and the fuel either by direct drive between the turbine and the pumps using the same shaft, or by a gear box if the turbine speed is higher than that of the pumps. The turbines used in rocket motors are generally of the impulse type with one or at most two velocity stages. The expansion of the gases takes place entirely in the nozzle of the gas generator. The symbols employed are indicated in Fig. 5.32. As for the turbopump, the torque T_t of a turbine is

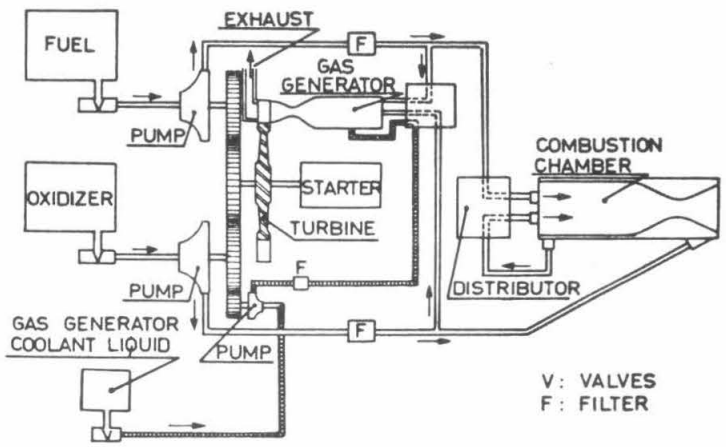

Fig. 5.31. Diagram of a turbopump feed system.

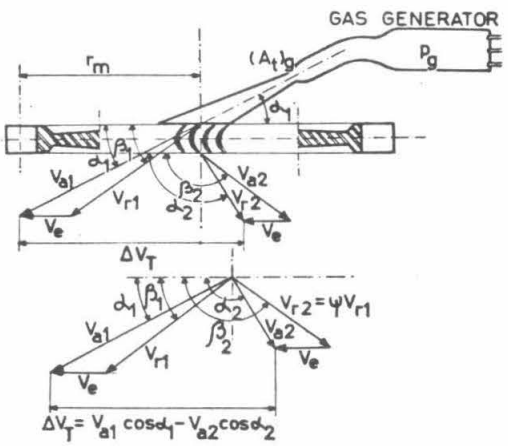

Fig. 5.32. Velocity triangles for a turbine.

$$T_t = \int_{A_1} r_1 V_{a1} \cos\alpha_1 \, d\dot{m}_T - \int_{A_2} r_2 V_{a2} \cos\alpha_2 \, d\dot{m}_T \qquad (5.59)$$

and the useful power P supplied by the fluid to the turbine is equal to:

$$P = T_t \omega = \int_{A_1} V_{e1} V_{a1} \cos\alpha_1 \, d\dot{m}_T - \int_{A_2} V_{e2} V_{a2} \cos\alpha_2 \, d\dot{m}_T \qquad (5.60)$$

For an impulse turbine $V_{e2} = V_{e1} = V_e$, so that

$$P = V_e \dot{m}_T (V_{a1} \cos\alpha_1 - V_{a2} \cos\alpha_2) \tag{5.61}$$

$$T_t = r_m \dot{m}_T (V_{a1} \cos\alpha_1 - V_{a2} \cos\alpha_2) \tag{5.62}$$

where r_m is the mean radius of the wheel at the level of the blades. The efficiency η_T of the wheel is the ratio of the useful power to the kinetic energy contained in the fluid at the nozzle exit:

$$\eta_T = \frac{2 V_e (V_{a1} \cos\alpha_1 - V_{a2} \cos\alpha_2)}{V_{a1}^2} \tag{5.63}$$

The turbine efficiency η_u is equal to the product of the nozzle efficiency and the efficiency of the wheel. The efficiency of the nozzle is ϕ^2; ϕ is the ratio of the actual exhaust velocity to the isentropic exhaust velocity. Therefore,

$$\eta_u = \frac{2 V_e (V_{a1} \cos\alpha_1 - V_{a2} \cos\alpha_2) \psi^2}{V_{a1}^2} \tag{5.64}$$

Defining

$$\psi = \frac{V_{r2}}{V_{r1}} = \text{velocity coefficient of the moving blades}$$

and

$$\xi = \frac{V_e}{V_{a1}}$$

the useful power can be written:

$$P = \dot{m}_T V_{a1}^2 \xi \left(1 - \frac{\cos\beta_2}{\cos\beta_1} \psi\right)(\cos\alpha_1 - \xi) \tag{5.65}$$

If the moving blades are symmetrical, $\beta_2 = 180° - \beta_1$

$$P = \dot{m}_T V_{a1}^2 \xi (1+\psi)(\cos\alpha_1 - \xi) \tag{5.66}$$

and the turbine efficiency becomes:

$$\eta_u = 2\varphi^2 \zeta (1+\psi)(\cos\alpha_1 - \zeta) \tag{5.67}$$

a function of the second degree in ζ, which at $\zeta = \frac{1}{2}\cos\alpha$, has a maximum value

$$\eta_{u\,max} = \varphi^2(1+\psi)\frac{\cos^2\alpha_1}{2} \tag{5.68}$$

In rocket motors, the value of ζ usually lies between 0.2 and 0.25. The torque T_t depends on the nozzle mass flow of the gas generator

$$\dot{m}_T = \frac{p_g \cdot (A_t)_g}{c^*_g}$$

where p_g is the pressure in the generator, $(A_t)_g$ is the area of the throat, and c^*_g is the characteristic velocity of the propellant employed in the generator. The torque T_t is thus given by the expression:

$$T_t = \frac{p_g (A_t)_g r_m}{c^*_g}(V_{a_1}\cos\alpha_1 - V_{a2}\cos\alpha_2) \tag{5.69}$$

The term $(V_{a_1}\cos\alpha_1 - V_{a2}\cos\alpha_2)$ is determined from the construction parameters α_1 and α_2 and the operating parameters V_{a1} and V_{a2}, so that the torque T_t must be controlled by means of the flow, i.e., by the pressure p_g in the generator chamber.